# THE MULTI-SCALE EFFECTS OF ENVIRONMENTAL VARIATION ON THE POPULATION DYNAMICS AND GENETIC STRUCTURE OF THE MOSQUITO VECTOR AEDES ALBOPICTUS ACROSS URBAN LANDSCAPES

by

#### PHILIP MICHAEL NEWBERRY

(Under the Direction of Courtney Murdock and Sonia Altizer)

#### **ABSTRACT**

Mosquito-vectored pathogens are globally significant sources of disease across equatorial areas and have expanded into temperate regions of the world. This dissertation examines heterogeneity in vector-borne disease (VBD) transmission across scales by investigating the invasive disease vector *Aedes albopictus* across an urban gradient in Atlanta, Georgia, USA. To begin with a broader perspective, I developed a synthetic review to critically evaluate different methods of modelling vector-borne disease systems across spatial scales. I offer perspectives regarding the importance of choosing the appropriate spatial scale to model transmission in response to environmental or biological processes. I also address both the relative strengths and limitations of statistical versus mechanistic representations of VBD systems and advances that can be made by integrating the two approaches. My empirical work focuses on larval and adult mosquito populations across a range of impervious surfaces to investigate the effects of human activity on *Ae. albopictus* populations. I identify and describe microclimatic and land use practices that impact vector abundance. This study shows a significant negative effect of minimum relative humidity and a positive effect of impervious surface coverage and daily

temperature range on adult *Ae. albopictus* abundance. Canopy cover strongly predicted greater larval habitat density. As these microclimate and landscape factors change in response to urbanization, findings here underscore the significance of human activity in determining fine-scale variation in vector populations. In other work, I measure the genetic population structure of *Ae. albopictus* populations across Atlanta using a SNP microarray for 95 mosquitoes collected across 16 locations. Analysis showed a mosquito population with small but significant genetic sub-structuring, suggesting a population shaped by a combination of human-mediation dispersal, natural dispersal, and landscape barriers. Reconstructions of the admixture history of these *Ae. albopictus* populations predict a single invasion event during the initial invasion of this species and population movement across the study area. This research highlights how anthropogenic landscapes produce fine-scale heterogeneities that drive variation in vector abundance while facilitating vector dispersal. This work also advises that integrated statistical and mechanistic models can advance understanding of how heterogeneities in biotic and abiotic factors drive pathogen transmission across spatial scales.

INDEX WORDS: Vector-borne disease, Microclimate, *Aedes albopictus*, Urbanization,
Population structure, Heterogeneity, Modelling

# THE MULTI-SCALE EFFECTS OF ENVIRONMENTAL VARIATION ON THE POPULATION DYNAMICS AND GENETIC STRUCTURE OF THE MOSQUITO VECTOR $AEDES\,ALBOPICTUS\,ACROSS\,URBAN\,LANDSCAPES$

by

#### PHILIP MICHAEL NEWBERRY

B.S., Emory University, 2010

A Dissertation Submitted to the Graduate Faculty of The University of Georgia in Partial

Fulfillment of the Requirements for the Degree

DOCTOR OF PHILOSOPHY

ATHENS, GEORGIA

2025

© 2025

Philip Michael Newberry

All Rights Reserved

# THE MULTI-SCALE EFFECTS OF ENVIRONMENTAL VARIATION ON THE POPULATION DYNAMICS AND GENETIC STRUCTURE OF THE MOSQUITO VECTOR $AEDES\,ALBOPICTUS\,ACROSS\,URBAN\,LANDSCAPES$

by

#### PHILIP MICHAEL NEWBERRY

Major Professors: Courtney Murdock

Sonia Altizer

Committee: Andrew W. Park

Kelly A. Dyer

Electronic Version Approved:

Vice Provost for Graduate Education and Dean of the Graduate School The University of Georgia May 2025

### **DEDICATION**

Dedicated to my Grandpa, David M. Newberry, whose career fighting smallpox and polio inspired me; to my Ranger buddy 2LT Travis A. Morgado, who I hope I have honored by my pursuit of life; and to my wife Dr. Megan Hopson, who has given me joy and endless support.

#### **ACKNOWLEDGEMENTS**

I am grateful for the many people who have supported me during my graduate studies. First of all, I would like to thank my advisors Dr. Courtney Murdock and Dr. Sonia Altizer for their wisdom, knowledge, and patience in guiding my development as a scientist. I would also like to thank my committee members, Dr. Andrew Park and Dr. Kelly Dyer, for their scientific expertise in guiding my research. I would also like to thank the many labmates that I have had the honor of working with over the years, including Nikki Solano, Dr. Michelle Evans, Dr. Blanka Tesla, Dr. Kerri Miazgowicz, Dr. Ash Pathak, Dr. Justine Shau, Dr. Christine Reitmayer, Juliana Hoyos, Dr. Cecilia Sanchez, Dr. Cali Wilson, Dr. Isabella Ragonese, Dr. Maria-Luisa Muller Theissen, Dr. Claire Teitelbaum, Julia Berliner, Charlotte Hovland, TJ Odum, Anna Willoughby, Lilith South, and many others. I am also thankful for Julie Gunby for her support as my Graduate Program Advisor and also for the wider Odum School of Ecology community. Additionally, thank you to my research assistants Valentina Suarez and Dina Constantinides who made my field work possible. I would like to thank my family, especially my mother Cheng-Suan Newberry Asbell and my stepfather David Asbell, for their years of support and encouragement during this period of my life. Most of all I would like to thank my wife Dr. Megan Hopson for believing in me even when I did not and for encouraging me to keep pursuing this dream.

### TABLE OF CONTENTS

		Page
ACKNO	WLEDGEMENTS	V
LIST OF	TABLES	ix
LIST OF	FIGURES	X
СНАРТЕ	ER	
1	INTRODUCTION AND LITERATURE REVEIW	1
2	THE CHALLENGES OF MODELING SPATIAL VECTOR-BORNE DISEASE	
	DYNAMICS	11
	Abstract	12
	Spatial Heterogeneity in Vector-Borne Disease Systems	12
	Drivers of Heterogeneity in VBD Across Scales	16
	Modelling VBD Heterogeneity: Approaches and Applications	19
	Mechanistic Models	20
	Statistical Models	23
	Moving the Field forward Conceptually and Practically	26
	Concluding Remarks	28
3	MICROGEOGRAPHIC VARIATION AND LAND COVER INFLUENCES ON	
	MOSQUITO VECTOR POPULATIONS INCLUDING THE MEDICALLY	
	SIGNIFICANT AEDES ALBOPICTUS ACROSS AN URBAN GRADIENT IN	
	ATLANTA GEODGIA	27

		Abstract	38
		Introduction	38
		Methods	42
		Results	48
		Discussion	53
		Conclusions	60
		Acknowledgements	61
		Funding	61
	4	POPULATION STRUCTURE OF THE ASIAN TIGER MOSQUITO AEDES	
		ALBOPICTUS IN AN URBAN ENVIRONMENT IN ATLANTA, GEORGIA	
		USING SNP CHIP GENOTYPING ARRAYS	76
		Abstract	77
		Introduction	77
		Methods	81
		Results	88
		Discussion	92
		Conclusions	96
		Acknowledgements	96
		Funding	96
	5	CONCLUSIONS	108
REFER	REN	NCES	115
APPEN	ND]	ICES	
	A	CHAPTER 3 SUPPLEMENTARY MATERIALS	158

В	CHAPTER 4 SUPPLEMENTARY MATERIALS	178
	DNA Extraction Checklist for Aedes albopictus	179

## LIST OF TABLES

Page
Table 3.1: . Study site names, locations, impervious surface percent coverage at a 500 m radius,
and canopy cover percent at 100 m radius.
Table 3.2. Principal component analysis quality of representation (cos2) values for PC1 in both
a) 7-day and b) 14-day lag datasets63
Table 3.3. GLMM models predicting Aedes albopictus adult abundance and larval habitat
density64
Table 4.1. Survey sites, site codes, coordinates, and landscape characteristics
Table 4.2. Fst values calculated by landscape characteristics: (a) canopy cover and (b)
impervious surface cover across study sites98
Supplementary Table A.1. All study site variable correlations for both 7-day lags and 14-day lags
with positive larval habitat characteristics and land cover traits
Supplementary Table A.2. Average study site temperature and relative humidity variables during
study period displayed with standard deviation
Supplementary Table A.3. Average monthly temperature and relative humidity variables across
site displayed with standard deviation.
Supplementary Table A.4. Adult Abundance Models Performance
Supplementary Table A.5. Larval Habitat Density Models Performance

### LIST OF FIGURES

Page
Figure 2.1. Vector and human host variables across spatial scales affecting the modelling of
vector-borne disease
Figure 2.2. Common human-made mosquito habitats in a heterogenous urban environment31
Figure 2.3. Applying mechanistic models of microclimate impacts on vector-borne disease
transmission
Figure 2.4. Recommended workflow for informing multi-scale models of VBD systems35
Figure 3.1. Map of impervious surface coverage of the study area
Figure 3.2. Mosquito community composition from across sites during the study period67
Figure 3.3. Larval habitats and Ae. albopictus abundances by site
Figure 3.4. Principal Component Analysis for biplots of 1 <sup>st</sup> and 2 <sup>nd</sup> PC loadings69
Figure 3.5. Adult Ae. albopictus abundances vs Month and Surface Imperviousness70
Figure 3.6. Adult Ae. albopictus abundances vs DTR and minimum RH
Figure 3.7. Larval habitat density vs Month and Canopy Cover
Figure 4.1. Survey Sites (x12) across Atlanta
Figure 4.2. Genotyping array workflow for SNP markers
Figure 4.3. Principal components 1 and 2 loading plots for sampled mosquitoes
Figure 4.4. Principal components 1 and 3 loading plots for sampled mosquitoes
Figure 4.5. Pairwise F <sub>ST</sub> values by site

Figure 4.6. Average F <sub>IS</sub> inbreeding coefficient for the individual <i>Aedes albopictus</i> sampled at
each study site
Figure 4.7. Genetic distance (Site-Site pairwise F <sub>ST</sub> ) vs geographic distance (km)105
Figure 4.8. Potential ancestral populations (k) and corresponding cross-entropy values106
Figure 4.9. Potential admixture history of <i>Aedes albopictus</i> populations across study sites107
Supplemental Figure A.1. Average daily values across the study sites by month. Monthly values
include both the 2021 and 2022 field season values averages
Supplemental Figure A.2. Average relative humidity values across the study sites by month.
Monthly values include both the 2021 and 2022 field season values averages173
Supplemental Figure A.3. Average maximum and minimum temperature values by month and
site imperviousness
Supplemental Figure A.4. 7-day lag variables scree plot
Supplemental Figure A.5. 7-day lag variables scree plot
Supplemental Figure A.6. 14-day lag variables scree plot

#### CHAPTER 1

#### INTRODUCTION AND LITERATURE REVIEW

#### Conceptual background

Natural populations often encounter diverse environmental conditions across different spatial scales. Heterogeneity in microclimate factors such as temperature and relative humidity can affect ecological processes, including the transmission of infectious diseases. For vectorborne diseases (VBD), the effect of environmental heterogeneity in temperature and rainfall is especially important given the poikilothermic nature of arthropod vectors and their often aquatic larval stages. Environmental variation has long been known to affect the distribution and abundance of organisms, and the consequences of this variation for population dynamics represent a fundamental question in ecology. At large spatial scales, environmental determinants are evident from spatial correlations between species distributions and abiotic and biotic variables (Stein et al. 2014). More recently, mechanistic models have directly incorporated links between physiological characteristics and environmental factors to predict species dynamics in response changing environments (Gotelli and Ellison 2006). This is especially important for forecasting shifts in species abundance and ranges in the face of climate change and habitat disruptions (Johnson et al. 2016). Environmental variation also occurs across fine spatial scales, manifesting as microclimatic heterogeneity and land cover variation across human land uses. In addition to affecting ecological dynamics of organisms, fine-scale variation can generate selection pressures through habitat selection, barriers to movement, isolation by distance, vector

control efforts, and human mediated gene flow (Paupy et al. 2004, Hemme et al. 2010, Hlaing et al. 2010, Richardson et al. 2014). Local adaptation to these selection pressures as well as genetic drift, founder effects due to invasion history, and mutation can generate ecologically relevant genetic variation across a landscape. An important open question involves how microgeographic adaptation and mechanisms that cause this variation will influence the ecological dynamics of species in nature.

Framework and considerations for modelling VBD systems

Incorporating spatial heterogeneity in environmental factors, socio-demographic factors, and genetic variation is important for understanding and mitigating VBD transmission. The R<sub>0</sub>, or basic reproductive ratio, of vector-borne pathogens is sensitive to temperature and other environmental variables, with both empirical measurements and computational models predicting significant relationships between temperature and variables that feed into VBD transmission (Murdock et al. 2012, 2014a, Mordecai et al. 2017a). At the same time, the microclimate that a species encounters in its ecological interactions is often mismatched with a larger spatial resolution for which environmental data are often available via remote sensing or weather stations (Potter et al. 2013, Murdock et al. 2017, Evans et al. 2019, Wimberly et al. 2020). Advances in the study of vector microclimate have improved scientific understanding of the appropriate scale at which climate affects mosquito ecology and arbovirus vectors more broadly (Cator et al. 2013, Evans et al. 2018, Wimberly et al. 2020, Valentine et al. 2020b). An important element in determining what variables and spatial scales are most important for a VBD system is accounting for the biological characteristics of the organisms in question, including their habitat preferences and dispersal capabilities. Importantly, cities can provide larval habitats for urban-affiliated mosquitoes, and urban heat islands can affect mosquito life history traits and

VBD dynamics at the scale that an individual vector samples its environment, typically a few hundred meters (Lacroix et al. 2009). As such, incorporating spatial heterogeneity in environmental factors, socio-demographic factors, and genetic variation is important for understanding and mitigating VBD transmission.

The Ross-Mcdonald model, first developed in the 1950s, is widely considered a cornerstone VBD theory (Smith et al. 2012). This model captures changes in the host and vector population density, the infection dynamics of both vector and host, disease-induced and background mortality, mosquito biting rates, and mosquito-human contacts. Many contemporary statistical and mathematical models focused on understanding the transmission dynamics of VBD, and on their prevention and control, rely to some extent on the Ross-Macdonald transmission model (Ruan et al. 2008, Reiner et al. 2013, Ruktanonchai et al. 2016). Mosquito life history-driven elements of the Ross-Macdonald model (survival, recruitment, biting rate, and the extrinsic incubation period, and  $R_0$ ) are especially sensitive to environmental conditions (Ahumada et al. 2004, Ruan et al. 2008, Tjaden et al. 2013, Ohm et al. 2018). Because of this environmental sensitivity, VBD risk can vary across heterogenous landscapes, as tracked by estimates for R<sub>0</sub>. Therefore, incorporating spatial heterogeneity into VBD models can help further scientific understanding of transmission by identifying refugia of disease or vector hotspots, and spatially explicit models can inform control efforts by determining where to focus interventions and what spatial coverage is needed to effectively lower transmission (Paupy et al. 2012, Eckhoff et al. 2015, Tokarz and Novak 2018). An understanding of a certain spatial coverage to achieve effective vector control goes back to the earliest models of VBD, with Roland Ross' original conception of a theoretical circle of control where mosquitoes could be eradicated at the center (Smith et al. 2012). Recent extensions of the Ross-Mcdonald model have

incorporated "patchiness" to model metapopulation dynamics of heterogenous disease risk (Auger et al. 2008, Gao et al. 2014, Wang et al. 2019), varying degrees of host and vector movement or mixing (Ruan et al. 2008, Reiner et al. 2013, Perkins et al. 2013, Eckhoff et al. 2015), and seasonal variations in vector abundance (Reiner et al. 2013).

Microclimate impacts on Aedes albopictus in VBD systems

The Asian tiger mosquito Ae. albopictus is a globally invasive vector of several medically and agriculturally significant VBD, including arboviruses like Dengue, Chikungunya, Zika, and Japanese Encephalitis, for which outbreaks are now common worldwide from the Americas to Africa and Southeast Asia (CDC 2024, "Chikungunya | CDC Yellow Book 2024" n.d.). While Ae. albopictus has spread globally in the last few decades, the earliest recognized introduction of the species to the continental United States occurred in the 1980's at the regional urban hubs of Houston, TX and Memphis, TN (Bonizzoni et al. 2013, Gloria-Soria et al. 2021). By 1994, all counties in the state of Georgia had reported the presence of Ae. albopictus (Womack et al. 1995), suggesting that the populations of this species in the metro-Atlanta area are at least in part descended from these original invasive populations. VBD, due to the nature of mosquito physiology, can be particularly sensitive to environmental variation due to the temperature dependent life cycles and often localized dispersal of arthropod vectors (Liew and Curtis 2004, Bellini et al. 2010, Wilke et al. 2017). At regional scales, climate factors such as the seasonal and latitudinal changes in rainfall, as well as socioeconomic and demographic trends that determine the contact rates with human hosts, can affect the distribution of suitable habitats and condition favoring pathogen transmission (Lambin et al. 2010). Fine-scale environmental variation can also alter vector development rates, reproduction and survival, body size, and overall abundance, especially in response to temperature and moisture (Murdock et al. 2017, Evans et al. 2019). For

example, mosquito development rates, adult lifespans, biting rates and egg production are sensitive to temperature, and microgeographic scale variations in temperature and relative humidity influence vectoral capacity and mosquito abundance (Murdock et al. 2017, Evans et al. 2019, Wimberly et al. 2020, Valentine et al. 2020b).

Fine scale variations in mosquito populations have been observed in many contexts and across diverse VBD systems. In the case of anthropophilic mosquito vectors, subpopulation variations may ultimately reflect in divergent urban adapted subpopulations and ancestral sylvatic populations. An example of this dynamic is seen in *Anopheles gambiae* genotypes that have varying tolerances to nitrogenous pollution and predation, allowing more anthropophilic populations to thrive in urban or agricultural larval environments(Gimonneau et al. 2010, Tene Fossog et al. 2013). Vector adaptation in response to evolutionary pressures and the anthropophilic niche of urban landscapes can influence biological characteristics (e.g., fecundity, biting rates, longevity) relevant to overall transmission potential (Louise et al. 2015). *Genetics of* Aedes albopictus

The genome of *Ae. albopictus* is the largest known for a mosquito species at 1,967 Mb with over half transposable elements and other repeat sequences; many of these repetitive elements include gene families involved with insecticide resistance and cold weather diapause (Chen et al. 2015). Understanding the invasion history of a mosquito vector can be informed by genetic analysis, which can help predict climate tolerance in the case of *Aedes albopictus*, where some subpopulations extend into cooler regions (Bosio et al. 2005, Kamgang et al. 2011, Tippelt et al. 2020). Phenotypic plasticity that allows for diapausing progeny when *Aedes albopictus* experiences reduced photoperiods has heritable genetic underpinnings, and there is evidence of the rapid evolution of this trait in expanding populations (Urbanski et al. 2012, Poelchau et al.

2013, Chen et al. 2015). The increased winter egg diapause survivability that some *Ae*. *albopictus* lineages exhibit can potentially shift northward the regions of the world at risk from the spread of this invasive vector beyond previous estimates, as some subpopulations exhibit more adaptive cold tolerance via female size and cold weather egg survival (Sherpa et al. 2022). Along the northern edge of the species distribution in the United States, genetic analysis has revealed a persistent diapausing population rather than seasonal reintroductions, demonstrating rapid establishment in relatively newer populations across a range of conditions (Gloria-Soria et al. 2022). Furthermore, the rise of insecticide resistance in some locations makes the identification of gene flow corridors important to vector control efforts (Vontas et al. 2012, Demok et al. 2019, Li et al. 2021). These inheritable traits make the identification of temperate or tropical phylogeographic origins essential for vector control efforts at the northern limits of *Ae. albopictus*' range.

Methodology for measuring genetic differentiation in *Ae. albopictus* populations has until recently included allozyme variation, microsatellite polymorphisms, and mtDNA haplotype analysis (Manni et al. 2015, Schmidt et al. 2017, Zhong et al. 2013, Chareonviriyaphap et al. 2004, Usmani-Brown et al. 2009). Using these tools, identification of population structure and lineages has been used to intuit the geographic origin of invasion events of *Ae. albopictus* (Black et al. 1988, Kambhampati et al. 1991, Urbanelli et al. 2000, Birungi and Munstermann 2002). The geographic origin of subpopulations of *Ae. albopictus* and its cousin *Aedes aegypti* are shown to impact vector competence at relatively close geographic distances (Failloux et al. 2002, Paupy et al. 2012, Gloria-Soria et al. 2021). Variability in susceptibility to infection is evident between *Ae. albopictus* subpopulations infected with Chikungunya virus and Dengue type 2 virus from identifiably distinct lineages, even when the population structure was not statistically

significant (Vazeille et al. 2001, Vega-Rúa et al. 2020). Similarly, both extrinsic incubation periods and vertical transmission rates of Zika virus in *Ae. albopictus* can vary between global populations, associating variability in infection susceptibility with distinct genetic lineages (Gutiérrez-López et al. 2019).

Another example of the importance of subpopulation characteristics is a hypothesized cryptic subspecies of *Ae. albopictus*, identified through mitochondrial *cox*1 haplotype divergence, that exhibits very low *Wolbachia* inoculation rates and possible *Wolbachia* resistance (Guo et al. 2018, Wei et al. 2019). Given the impact of *Wolbachia* in attenuating the transmission of Dengue virus in *Ae. albopictus* populations, identification of distinct lineages of this species would be informative to public health efforts (Mousson et al. 2012). Anthropophilic mosquito populations implicated in transmitting VBDs generally have limited innate dispersal capabilities, from 100-500 meters in the case of *Ae. aegypti* (Harrington et al. 2005) and often across similar ranges for *Ae. albopictus* (Bellini et al. 2010, Marini et al. 2010). In spite of these limited ranges, genetic structuring has been observed within relatively short distances (Hlaing et al. 2010, Olanratmanee et al. 2013). Gene flow across larger distances for mosquitoes with limited flight ranges can be through natural dispersal via host seeking and oviposition preferences, but it has also been be associated with human mediated movement (Huber et al. 2004, Rašić et al. 2015, Carvajal et al. 2020).

#### Dissertation overview

The goal of my dissertation is to examine vector-borne disease dynamics through the lens of vector ecology across spatial scales and in the context of human-altered landscapes. First, I present a synthetic review to evaluate modelling approaches for VBD transmission across spatial scales in Chapter 2. In this chapter, I demonstrate the utility and limitations of both mechanistic

and statistical approaches to modelling while advocating for the perspective of choosing the appropriate spatial scale to describe biological and environmental phenomena that determine VBD. Then, I demonstrate cases where an integrative approach of using quality fine-scale empirical field data, statistical models, and mechanistic models together to best represent potential VBD risk across a landscape. I use the insights from this chapter to inform what spatial scale to measure vector demographics and the environment variables, resulting in collecting data across spatial ranges based on knowledge of mosquito movement and life history. Affected vector characteristics include host-seeking behavior, oviposition preferences, habitat selection, and movement over the course of an individual vector's lifetime. This approach to scale then informs my empirical field work.

In Chapter 3, I conducted a field survey of mosquito populations across the city of Atlanta, GA to characterize how microclimatic and land cover characteristics associated with urbanization predict variation in *Aedes albopictus* populations and larval habitat density. This research surveyed both adults and larvae at sites across an urban gradient in the city, as determined by differing degrees of impervious surfaces surrounding each site. Mixed effects models were built and evaluated to identify and measure the effects of the most significant covariates predicting these demographic response variables. I found that minimum relative humidity (RH<sub>Min</sub>) had a significant negative effect on adult *Ae. albopictus* abundance, while impervious surface coverage and the magnitude of daily temperature range (DTR) had a significant positive effect on adult abundance. Canopy cover within each study site predicted greater larval habitat density. I conclude that urbanization, which alters microclimate and is often characterized by increasing surface imperviousness and heat island effects impacting RH and temperature, increases *Ae. albopictus* abundance. The study also suggests that human interaction

with the urban environment significantly drives vector populations through actions like preserving canopy cover in residential areas and providing larval habitats via landscaping containers and other cultural practices.

In Chapter 4, I measure the population genetic structure of Ae. albopictus across Atlanta, GA through the use of next-generation sequencing techniques and a newly developed SNP microarray. The genetic data showed a minimal degree of genetic differentiation between the subpopulations across the city, with F<sub>ST</sub> values only ranging up to 0.019. Although fixation indices between sites were small, these depressed fixation indices are expected to be lower than more traditional microsatellite analysis of genetic differentiation given the orders of magnitude larger number of polymorphism sites the SNP chip assessed. The pairwise genetic variation between most populations in the study was determined to be significant, with the exception being with one site near the center of the study area and those sites adjacent to it. Additionally, the ancestral history and admixture predictions of the population suggest a single introduction of Ae. albopictus into Atlanta, likely from the initial invasive population in the early 1990's. The models of possible admixture events demonstrate population movement across the study area, sometimes leap-frogging over the nearest sites. This dynamic, along with the high degree of gene flow, suggests a high degree of dispersal. This population movement is likely facilitated by human activity and enabled by limited landscape barriers to individual mosquito movement. This characterization of the genetic structure of Ae. albopictus demonstrates how this anthropophilic and urban adapted invasive species can rapidly invade and establish populations in a city due to

limited environmental barriers to dispersal and human mediated dispersal of individuals and eggs.

In a final conclusions section (Chapter 5), I integrate previously discussed findings towards developing a predictive framework and clearer understanding of vector ecology within human-altered environments. Overall, this research demonstrates the importance of incorporating the approaches of different disciplines (mathematical modelling, empirical measurements and collections of field samples, and genotyping using next-generation genetic tools) to describe a VBD system and to better understand the ecological interplay between vectors and anthropogenic changes to the environment

#### **CHAPTER 2**

# THE CHALLENGES OF MODELING SPATIAL VECTOR-BORNE DISEASE DYNAMICS: NEW APPROACHES GUIDED BY RECENT ADVANCES<sup>1</sup>

Author contributions; PMN: conceptualization, investigation, visualization, writing - original draft preparation, writing – review and editing; AWP: conceptualization, writing - review and editing; SMA: conceptualization, writing - review and editing; CCM: conceptualization, writing - review and editing. All authors agree that their contributions can be included in this dissertation.

<sup>&</sup>lt;sup>1</sup> Newberry PM, Park AW, Altizer SM, Murdock CC. To be submitted to the *Journal of Parasitology Research*.

#### **Abstract**

Over the past four decades, researchers have made significant progress incorporating vector and host dynamics into mathematical models describing vector-borne diseases (VBDs). Increasingly sophisticated modelling approaches used for predicting vector responses to environmental variations across space and time have propelled the field forward, with crucial importance for responding to health challenges posed by climate change, deforestation and urbanization. Environmental data on temperature, rainfall, and vector habitats is typically available across large areas at lower resolutions than the scale at which actual transmission occurs. Determining how fine-scale heterogeneities in vectors, microclimates, and hosts should be quantified, analyzed and modeled is a persistent challenge in describing and predicting VBD. Here we review the scale of processes that influence VBDs and propose that integrating the relative strengths of mechanistic and statistical models offers a powerful strategy for predicting and mitigating the global burden of VBDs.

#### Spatial Heterogeneity in Vector-Borne Disease Systems

Vector-borne pathogens are important biological enemies of humans, animals, and plants and are transmitted by arthropods within and between host species. In humans, despite significant resources committed to controlling these pathogens, vector-borne diseases (VBD) account for 17% of all infectious diseases and cause upwards of 700,000 deaths annually (World Health Organization and UNICEF/UNDP/World Bank/WHO Special Programme for Research and Training in Tropical Diseases 2017). Vector-borne pathogens impose heavy burdens on agricultural systems, threatening livestock and crops (Jones et al. 2023), and can also be devastating for natural ecosystems. This is exemplified by avian malaria-caused extinctions of Hawaiian Honeycreepers (Samuel et al. 2015) and the widespread declines of crows, jays, and

other corvids following the introduction of West Nile Virus into North America (LaDeau et al. 2011). To predict and respond to the negative consequences of vector-borne diseases, scientists have developed mathematical models to explore underlying transmission process, to assess the efficacy of interventions, and to forecast VBD transmission seasonally, geographically, and in response to future climate and land use change.

Mathematical models are often limited by the necessity of simplifying assumptions, the aggregation of data used to fit the models, and the need to choose what spatial and temporal scale to use when investigating relevant variables. A major simplifying assumption of most mathematical models is that host and vector populations mix randomly and contact each other according to mass action principles. However, real-world patterns of VBD incidence (Chaves et al. 2011, Perkins et al. 2013) instead show that incidence can vary sharply across space (Lambin et al. 2010), with some areas highly suitable for transmission serving as persistent reservoirs or sources of infection (Yoon et al. 2012, Salje et al. 2017). Spatial heterogeneity in VBD incidence could occur due to geographic variation in abiotic (Murdock et al. 2014a, Evans et al. 2018, Wimberly et al. 2020) and biotic (Murdock et al. 2014a, Russell et al. 2022) factors and socioeconomic variables that determine people's risk of exposure to disease. Human-driven environmental changes in turn influence vector densities, environmental suitability for vector and pathogen development, and risk for pathogen transmission (Becker et al. 2014, Tesla et al. 2018, Evans et al. 2018). Incongruence between model assumptions and vector biology was recognized by Smith et al 2012 (Smith et al. 2012), where they conclude "fluctuations in mosquito populations are extremely difficult to predict over time and space, and important sources of heterogeneity and the spatial and temporal scales of transmission remain poorly characterized".

As ectotherms, arthropod vectors like mosquitoes, sandflies, and ticks are subject to a diversity of environmental factors that can interact to affect their fitness, distributions, abundance and behavior. The include abiotic factors of temperature (Murdock et al. 2014a, Mordecai et al. 2019, Evans et al. 2019, Wimberly et al. 2020), relative humidity (Murdock et al. 2017, Mordecai et al. 2019, Evans et al. 2019), and precipitation (Mordecai et al. 2019); and biotic factors like intra- and interspecific competition (Armistead et al. 2008, Evans et al. 2019), biological enemies (Russell et al. 2022), and the quality/quantity of habitat and resources (Murdock et al. 2014a, Mordecai et al. 2019, Evans et al. 2019). Environmental determinants of vector and pathogen distributions occur at different spatial scales, with biotic factors showing greater heterogeneity at local spatial scales (Murdock et al. 2017, Evans et al. 2019) and climate factors varying at more regional spatial scales (Tesla et al. 2018, Khan et al. 2020) (Figure 2.1). Additionally, socioeconomic variables can shape people's exposure to arthropod vectors in the case of housing structure, water storage practices, use of outdoor spaces, and access to public health resources like bed nets and vaccines (Morgan et al. 2021). These social factors vary both within and between neighborhoods and communities (Figure 2.1). Finally, vectors and the pathogens they carry can disperse at limited local (natural dispersal or within a community) (Harrington et al. 2005) or longer-distances (human-mediated) (Hlaing et al. 2010). Inferences based on drivers of infection dynamics at only a single scale could generate misleading predictions of pathogen transmission, spatial distribution, and incidence. Thus, a crucial need remains for mathematical theory and tools that allow scientists to integrate biological processes that vary across multiple scales into a unified framework to predict the distribution and abundance of VBDs.

Another challenge of incorporating spatial variation into mathematical models of vector-borne disease transmission involves the methods by which both infection data and environmental metrics are collected and aggregated. The spatial resolution of available data might not match well with the spatial scale at which key variables have the largest effects on the transmission process. For example, macroclimate or socioeconomic data aggregated at coarse spatial scales could cause researchers to underestimate habitat suitability for pathogen transmission or vector persistence (Irvine et al. 2018) or to overlook small-scale clusters of VBD transmission (Salje et al. 2017). Alternatively, if pathogens and vectors are dispersed at larger spatial scales due to human mobility (Hlaing et al. 2010), then hosts can encounter pathogens from outside the hotspots predicted by finer-scale data on natural processes.

In this article, we begin by exploring the underlying factors that shape the distribution and dynamics of VBD transmission and the spatial scales across which these effects are likely important. We present several modeling frameworks characterizing the spatial risk of VBD transmission and the merits of approaches at different spatial scales. We also explore the VBD forecasting implications of mismatches between the relevant spatial scale for a given process and the spatial scale across which data are collected and aggregated. Finally, we end with a broader discussion of the future theory and research that is required to move this field forward. These efforts have the potential to better predict how the geographic distribution and abundance of VBD will change with climate change and increasing urbanization. Throughout, we focus mainly on mosquito-borne diseases owing to their public health impacts and economic global burden. In particular, malaria remains a leading cause of human mortality and morbidity, with approximately 263 million cases and 597,000 deaths in 2023 alone, primarily in children in sub-Saharan Africa (World Health Organization n.d.). Further, 2023 saw the highest number of

dengue cases in history, with over 6.5 million cases and 7,300 deaths. Other mosquito-borne pathogens of human health concern include chikungunya virus, Zika virus, yellow fever virus, West Nile virus, and Japanese encephalitis. Collectively, the global cost of treating these and other mosquito-transmitted diseases exceeds \$9 billion per year (Halstead 2007, Packierisamy et al. 2015, Shepard et al. 2016).

#### **Drivers of Heterogeneity in VBD Across Scales**

The risk of mosquito-borne disease varies spatially owing to variation in multiple processes that affect the distribution and dynamics of both vectors and the pathogens they transmit. These include environmental variables that affect mosquito fitness, behavior, population dynamics, and within-host pathogen development as well as processes that affect vector and pathogen movement (e.g., mosquito dispersal ability, human-mediated dispersal, environmental barriers and corridors). If significant spatial variation results in barriers to pathogen movement, genetic variation can also manifest spatially across mosquito populations that in turn influence their ability to become infected and to transmit pathogens. Finally, variation in socio-economic factors that influence human exposure to biting mosquitoes and access to public health resources also exhibit spatial structure. Overall, the combined effects of the various processes determine patterns of transmission risk and disease incidence. The fact that these processes exhibit variation at different spatial scales and are measured with different spatial resolutions makes prediction of these effects on the transmission process challenging (Figure 2.1).

It has long been understood in the field of spatial ecology that three processes generally determine the distribution of organisms. These are biotic factors (e.g., inter- and intra-specific competition and trophic-level interactions), abiotic factors that lead to environmental filtering (e.g., temperature, precipitation, relative humidity, pH and salinity), and the amount of the

environment an organism can sample (e.g., dispersal range and movement). While substantial spatial variation exists in both biotic and abiotic environmental variables, this variation does not necessarily occur at similar spatial scales. For example, climate variables typically vary at regional spatial resolutions (IPCC 2023), with relatively minor variation at smaller, local scales. Thus, it has been hypothesized that environmental suitability or filtering will occur at scales >10<sup>4</sup> km² in the absence of major elevational changes or landscape disturbances. In contrast, biotic factors (including species interactions, habitats and resources) often vary at smaller spatial scales, which is reflected by finer-scale spatial resolution in species composition data. Evidence for rapid turnover in species composition and biotic interactions is supported across several wildlife disease systems (e.g., chytrid fungus in frogs, West Nile virus in birds, and Lyme disease in mammals) (Cohen et al. 2016). This would suggest that the effects of climate variation on mosquito population and pathogen dynamics will occur across regional scales and that biotic factors affecting the distribution and carrying capacity of local mosquito populations (largely unaccounted for in predictive models) likely influence spatial structure at finer spatial scales.

The spatial scale that is relevant for a given biological process will not only depend on the level of heterogeneity in underlying variables across space, but also on an organism's dispersal and ability to sample the environmental space. Variation that might be physiologically relevant for an organism that has constrained dispersal capabilities can appear as environmental noise for an organism that can sample wider geographic areas. Interestingly, mosquito-borne pathogens can be transported via both mosquito movement and human movement. Mosquitoes vary in their natural capability to disperse, with extreme examples including *Aedes aegypti* that exhibit very limited mean dispersal (<100-200m) versus *Culex annulirostris* with high dispersal (6200m) capabilities (Verdonschot and Besse-Lototskaya 2014). As a result, mosquito species

with more limited dispersal can show a high degree of genetic and phenotypic variation across space, which is amplified by the presence of environmental barriers (e.g., roads or forests (Hemme et al. 2010)). Host-mediated movement of pathogens or mosquitoes across a landscape also can also drive the spatial dynamics of pathogen transmission as has been observed for a multitude of mosquito-borne disease systems of humans (dengue (Hlaing et al. 2010, Araujo et al. 2015), West Nile virus (Brownstein et al. 2002), malaria (Marshall et al. 2016) and wildlife systems acting as sylvatic reservoirs or potential targets of novel introductions of VBD (Valentine et al. 2019, 2020a, Hanley et al. 2024). The connectivity of humans and animal hosts will determine how individual hosts move across space and if local mosquito populations and environmental conditions vary in suitability geographically. Meta-populations can arise in these VBD systems with source (highly suitable conditions) - sink (unsuitable conditions) transmission dynamics. An example of a host-mediated source population connecting to increased VBD is the observed amplification of Dengue in rural Thailand that is driven by a relatively small subset of houses in the community (Yoon et al. 2012).

For human transmitted vector-borne pathogens, socio-economic and demographic changes across space will further influence the risk human populations experience in acquiring mosquito-borne pathogens (Dowling et al. 2013). These include variation in housing structure, permeability to mosquitoes (e.g., presence of screens, curtains, and enclosed spaces), water storage practices, access to public health resources, and public sanitation (Caprara et al. 2009). In urban environments, this heterogeneity can arise across relatively small spatial scales (Figure 2.2) and interact with environmental variables such as urban heat island effects (Araujo et al. 2015) and create human-provided larval habitats in the case of water storage, potted plants, and discarded household items (Wilke et al. 2019). Construction sites, although temporary, provide

ample habitat for multiple mosquito populations due to high amounts of standing water, resting habitat, and often unprotected human laborers to feed on (Wilke et al. 2018). Further, these sites do not necessarily receive the same level of entomological and epidemiological surveillance as permanent populations in cities. Importantly, human populations of lower socio-economic standing tend to exhibit the highest burden of acquiring and transmitting mosquito-borne pathogens (Dowling et al. 2013, Little et al. 2017, Goodman et al. 2018).

Overall, it is the combined effects of a multitude of environmental parameters, pathogen dispersal, and social-ecological processes that result in the spatial patterns of transmission risk and disease incidence (Figure 2.1). To accurately predict the spatial and temporal epidemiology of a given vector-borne disease, incorporating data describing each process at the appropriate spatial resolution for transmission and control is critical. Current challenges that constrain the ability of mathematical models to predict spatial patterns of disease incidence arise because these processes exhibit variation at different spatial scales. Data collected on these processes can be aggregated at inappropriate spatial resolutions, and determining the relative importance of various mechanisms of pathogen dispersal (e.g., vector or host-mediated) is a non-trivial undertaking.

#### Modelling VBD Heterogeneity: Approaches and Applications

Mathematical models of pathogen transmission are simplified explicit expressions of a given system, and when paired with appropriate validation, are an important tool in identifying the key sources of variation that drive host-pathogen dynamics. The need to model VBDs accurately across varied landscapes, host patterns, and vector ecologies is partly motivated by the severe detrimental impacts VBDs have on people, domestic animals, and wildlife. Modeling a VBD system allows researchers to identify links between mechanisms and patterns. Models are

also crucial for exploring potential vulnerabilities in transmission that can be targeted in disease or vector control efforts - ranging from pesticide applications and genetically modified vectors to larval habitat elimination, indoor residual spraying, and the provisioning of bed nets to affected communities. Thus, mathematical models are critically important for predicting the elements in a system that can be leveraged for control or management or used in forecasting the effects of certain control measures on disease cases (Figure 2.3) (Colón-González et al. 2021). Approaches to modelling these systems broadly separate into (i) mechanistic or (ii) statistical models that use different, but complimentary, approaches to better understand the factors driving spatial and temporal disease dynamics.

#### **Mechanistic Models**

Mechanistic models mathematically describe how different variables interact to determine VBD transmission. Identifying links between individual-level components of the VBD system and population-level effects, such as the prevalence of infection, make these models informative for vector control efforts. The historic Ross-Macdonald model is an excellent example of the development and application of mechanistic models in understanding malaria dynamics and control (Reiner et al. 2013). The development of this simple yet powerful model helped identify key elements of the transmission cycle on which to focus disease control measures. The Ross-Macdonald model showed that reducing mosquito longevity yielded the largest decreases in the basic reproductive number, R<sub>0</sub>, due to fewer mosquitoes surviving each day, which decreases the mosquito-human population ratio and density of mosquitoes living long enough to become fully infectious. The basic reproductive number (R<sub>0</sub>) describes the number of secondary infections resulting from one initially infected vector given a susceptible host population; the Ross-Macdonald model helped derive epidemiological expressions describing

VBD systems like the entomological inoculation rate and vectorial capacity (Figure 2.3). The model's estimations have informed many of the interventions against mosquito-borne disease used today such as indoor residual spraying and insecticide treated bed nets targeting the adult stages of mosquito vectors (Reiner et al. 2013, Smith et al. 2021).

To date, mechanistic modeling approaches have incorporated environmental variables governing mosquito population dynamics that vary spatially and temporally. To do this, laboratory experiments quantify relationships between key processes that determine transmission and an environmental factor of interest, such as temperature. Field studies are also useful for quantifying how temperature (Mordecai et al. 2017a, Ryan et al. 2021), rainfall (Auger et al. 2008, Fukui et al. 2022), and relative humidity (Brown et al. 2023) predict changes in mosquito densities. These relationships can be incorporated into process-based mathematical models using functional relationships to couple a rate to an underlying environmental variable (Figure 2.3). These models can then be used to predict how environmental suitability for the mosquito or the pathogen, disease incidence, or disease prevalence varies at fine (within city (Wimberly et al. 2020)), regional (within country), or global scales, as well as temporally with season, interannually (Shutt et al. 2022), or in response to future climate change (Tesla et al. 2018, Colón-González et al. 2021).

Another approach to modeling spatial heterogeneity builds on multi-patch models. Multi-patch models formalize spatial variation more explicitly by simulating the dynamics of different host and vector populations that exist in distinct demographic or environmental conditions (Nipa and Allen 2020, Wu et al. 2023). These models can then explore how variation in patch characteristics and host connectivity across patches influences transmission dynamics (Auger et al. 2008, Vyhmeister et al. 2020). In VBD systems, multi-patch models have led to insights

regarding the importance of human movement and residence time on VBD infection rates(Lee and Castillo-Chavez 2015, Barrios et al. 2018). These insights include understanding how occupational commutes between human populations can amplifying VBD case incidence across a region or even whether the directionality or residence time of inter-patch movement varies the resulting epidemic size (Lee and Castillo-Chavez 2015, Barrios et al. 2018). Similarly, spatially explicit models of vector elimination efforts can predict the competing effectiveness of different methods (i.e. aerial spraying vs. door to door reduction of larval breeding habitats) (Demers et al. 2020).

Individual and agent-based models simulate the encounter rates of individual hosts and vectors through different decision and encounter probabilities as they move through heterogenous environments (Wu et al. 2020). Such approaches capture some of the stochasticity evident in real life systems, especially in low density transmission situations where individual vector or host actors can have major impacts on the persistence of pathogens (Smith et al. 2018). Understanding the behavior of an individual mosquito moving through a heterogenous microclimate as it encounters resources, seeks hosts, oviposits, and encounters vector control measures has been simulated in some cases (Menach et al. 2005, Gu and Novak 2009). Still these approaches rely on assumptions of scale and the parameterizations of the vector's interactions with its environment, including obstacles, mortality, and host quality. Agent-based models can also account for variation in host population density, movement patterns, and medical interventions such as potential vaccines (Carter 2002, Reiner et al. 2014). Decisions on relevant heterogeneities require knowledge of a VBD system, such as household clustering and vector dispersal ranges (Wu et al. 2023), as well as the particular human or environmental context that the vector exists within.

Mechanistic models, whether they describe individual vector and host actions or the categorical states of populations interacting with a VBD, are particularly useful for predicting transmission in novel conditions for which observations are limited or do not exist. However, one of the constraints mechanistic models face is that parameterization can be data intensive, requiring detailed experimental work. It can also be difficult connecting experimental results to field observations in natural settings, making model validation challenging. For example, spatial variation in the application and effectiveness of vector control measures, can have unexpected consequences on the sporozoite development rate and the mosquito biting rate (Auger et al. 2008, Perkins et al. 2013, Gao et al. 2014, Smith et al. 2021). Thus, it is critical to determine key environmental factors that determine transmission and the spatial scale across which they vary most.

#### **Statistical Models**

Statistical models make inferences using observed relationships between mosquito densities or disease incidence and different environmental or socio-economic metrics that vary spatially and are hypothesized to affect transmission (Dowling et al. 2013, Little et al. 2017, Morgan et al. 2021). Statistical models characterizing patterns over space and time can also explore lagged or non-linear relationships. Additionally, statistical inference from observational field data relates closely to real-world transmission (Heersink et al. 2016, Fairbanks et al. 2024). Statistical methods are particularly useful in forecasting and require less a priori knowledge of the mechanisms governing variation in mosquito densities or disease transmission, so may be more appropriate than a purely mechanistic approach when the ecology of a vector, for example is not well-known (Williams et al. 2008, Bondo et al. 2023, Whittaker et al. n.d.). This approach can also reveal what combinations of covariates (e.g., environmental, socio-economic,

connectivity) are important for predicting the spatial patterns of disease cases (Becker et al. 2014, Shutt et al. 2022, Bondo et al. 2023).

The most commonly used families of statistical models include ecological niche and species distribution models. Correlative species distribution models (SDMs) use multiple regression approaches to infer how the observed distribution of a species or a pathogen varies as a function of geographically referenced climatic predictor variables (e.g., temperature, rainfall, relative humidity). In mosquito-borne disease systems, SDMs can generate maps of environmental suitability for a given mosquito species or for pathogen transmission across regional (Cianci et al. 2015, Barker and MacIsaac 2022) and continental areas (Rogers et al. 2014, Khan et al. 2020), such as has been demonstrated for Zika and Dengue virus (Messina et al. 2016, Colón-González et al. 2018). These approaches allow researchers to examine how well different combinations of covariates, and their relationships, match the data using model-fit metrics like the Akaike Information Criterion (AIC). Choosing the most important elements that describe a VBD system can be complemented with data reduction methods such as Principal Component Analysis (PCA), while more general checks for collinearity can help reduce the number of factors needed to understand transmission. Another family of statistical models includes machine learning algorithms, which are mathematical methods (e.g., linear regression, decision trees, random forest, etc.) that find patterns in a set of data. Machine learning algorithms are trained on a particular set of data and consider various covariates of interest. After training, the resulting function with rules and data structures is called the trained machine learning model. The trained, optimized model can then be used to predict these patterns in a previously unseen dataset. These models perform very well at near-term forecasting of temporal and spatial patterns in mosquito abundance or disease cases, and can be updated easily as new data become available (Laureano-Rosario et al. 2018, Zhao et al. 2020).

While statistical models can make inference with less knowledge of the vector and pathogen biology and can be operationalized faster, it is important to couple statistical inference with biological knowledge, especially if non-linear or more complex processes are at play. For example, strong correlations between different environmental covariates over time could hide true causal relationships and challenge the ability to identify the biologically meaningful drivers of VBD dynamics. Further, species distribution models require data not only on species presences, but also of absences - and for many systems, records of species absences are not commonly present in the literature. Finally, a general assumption of statistical models is that the species of interest is at equilibrium with their environment and that the environmental variables have been adequately sampled. Thus, applying statistical models to novel scenarios, such as in response to land use change, future climate change, or pathogen emergence can be problematic (Hay et al. 2009, Lessler and Cummings 2016).

Selecting the best modeling approach for understanding how spatial heterogeneity in relevant factors influence VBD dynamics often depends on the specific question and system of interest (Madzokere et al. 2020). Short-term forecasts in focused areas can be managed highly effectively with statistical approaches that do not require much mechanistic information about a system if sufficient entomological or epidemiological data are available. In fact, Johnson et al. 2018 (Johnson et al. 2018) demonstrates that mechanistic models performed well at predicting the seasonality of dengue cases but failed to predict large outbreaks because of error being introduced in anomalous years. Statistical models performed much better at predicting multi-year outbreaks because they phenomenologically matched the patterns from disease data alone.

Further, weighted averages of forecasts from super ensembles (e.g., multiple statistical models) can reduce model error by smoothing over variation across individual forecast scenarios. In contrast, mechanistic models are essential for understanding the biological drivers of VBD dynamics in novel scenarios and for anticipating the effects of vector control or other interventions on the VBD system (Kearney and Porter 2009, Cator et al. 2020, Ezanno et al. 2020). Ultimately, both modeling frameworks are useful and provide complimentary insights that can inform and augment each other.

# Moving the Field forward Conceptually and Practically

The union of mechanistic and statistical approaches for species distribution modelling is becoming more prevalent in characterizing vector borne disease risk, leveraging broadly available remote sensing and temperature/humidity data with empirically identified steps in the ecology of VBD transmission involving the vector, the host, and the pathogen (Madzokere et al. 2020). This provides more precise predictions of potential/realized ranges of VBD due to thermal responses (key for arthropod vectors) that will result from climactic shifts (Tesla et al. 2018, Ryan et al. 2021). Mindful application of mechanistic tools accounting for environmental and vector/host heterogeneity and of statistical models informed and parameterized by empirical examination of disease processes can overcome the pitfalls sometimes associated with these approaches on their own (Figure 2.4).

Key to this approach is obtaining data appropriate to the spatial or temporal scale relevant to the ecology of a particular VBD system. Often fine-scale resolution data are lacking due to limited resources and the logistical challenges of widescale microclimate and vector monitoring. Scale mismatches between the processes driving transmission and the data used to validate the model can make it difficult to gain inference at a desired spatial scale or can obscure patterns that

arise at fine spatial scales. For example, modeling VBD transmission in urban environments predicts significant variation at very fine scales - within tens of meters - largely owing to thermal variability (Romeo-Aznar et al. 2024) and patterns of host population density (Romeo-Aznar et al. 2022). Further, fine scale temporal modelling of vector systems, such as the *Culicoides*-spread hemorrhagic disease in whitetail deer, explains otherwise cryptic larger-scale patterns of VBD dynamics (Park et al. 2016). Insights gained from more complex mechanistic models of multi-vector or multi-host systems can then be used in conjunction with statistical models incorporating environmental variables to both predict and explain relevant levels of VBD risk regionally (Cleveland et al. 2023).

Future modeling approaches should identify transmission parameters that are most tightly coupled to environmental variables in an established workflow (Figure 2.4) (Wimberly et al. 2020). Furthermore, understanding heterogeneity in environmental processes that drive transmission, as well as determining vector and pathogen dispersal, will be critical for targeting surveillance and vector control strategies. If variation in vector-host contact rates occurs across a landscape, and if vector control measures such as larval source management (Smith et al. 2013) or adult control measures are applied unevenly or at inappropriate spatial scales, this can result in ineffective control (Rochlin et al. 2022, Romeo-Aznar et al. 2024). Alternately, identifying the most important elements of a patchy environment allows for more effective targeting of vector and host populations for emerging vaccines, vector sterilization, and broad insecticide spraying. Genetic tools can be very useful for determining the spatial scales at which population structure is evident. Advances in single nucleotide polymorphism (SNP) microarrays, affordable whole-genome sequencing, and microsatellite markers allow for very precise characterization of a vector species' admixture history(Bosio et al. 2005, Palatini et al. 2020, Carvajal et al. 2020,

Wei et al. 2022, Cosme et al. 2024), telling a story of invasions and introductions across heterogenous landscapes including potential barriers to dispersal (Hemme et al. 2010, Wilke et al. 2017, Regilme et al. 2021).

# **Concluding Remarks**

Significant computational and methodological advances have been made in recent years harnessing computing power and the wide collection of empirical data, allowing researchers and public health professionals to craft increasingly sophisticated models of vector-host-pathogen systems. Key to maintaining this momentum is continuing to collect data on the relevant drivers and variables in a complex system to characterize the transmission process, but with more mindfulness of the spatial scale across which these processes are relevant. Recent advances in data collection instruments, include the use of embedded sensors, wearable devices, sophisticated survey tools, and cloud-based platforms now allow for real-time data capture of spatial and temporal heterogeneities and deeper insights from diverse sources Systems with increased human dispersal may alternatively approach panmixia as people can sample more environmental space with modern travel, creating VBD corridors of spread following societal movement patterns (Marshall et al. 2016, Saucedo and Tien 2022). Studies that synthesize both mechanistic approaches and statistical techniques are crucial for future predictive models of VBD systems. Finally, improved mathematical and statistical models of VBD as well as AI-powered machine learning techniques and big-data analytics can indicate fundamental pitfalls such as scale mismatches and overlooking important ecological phenomena underpinning VBD transmission.

# **Figures**

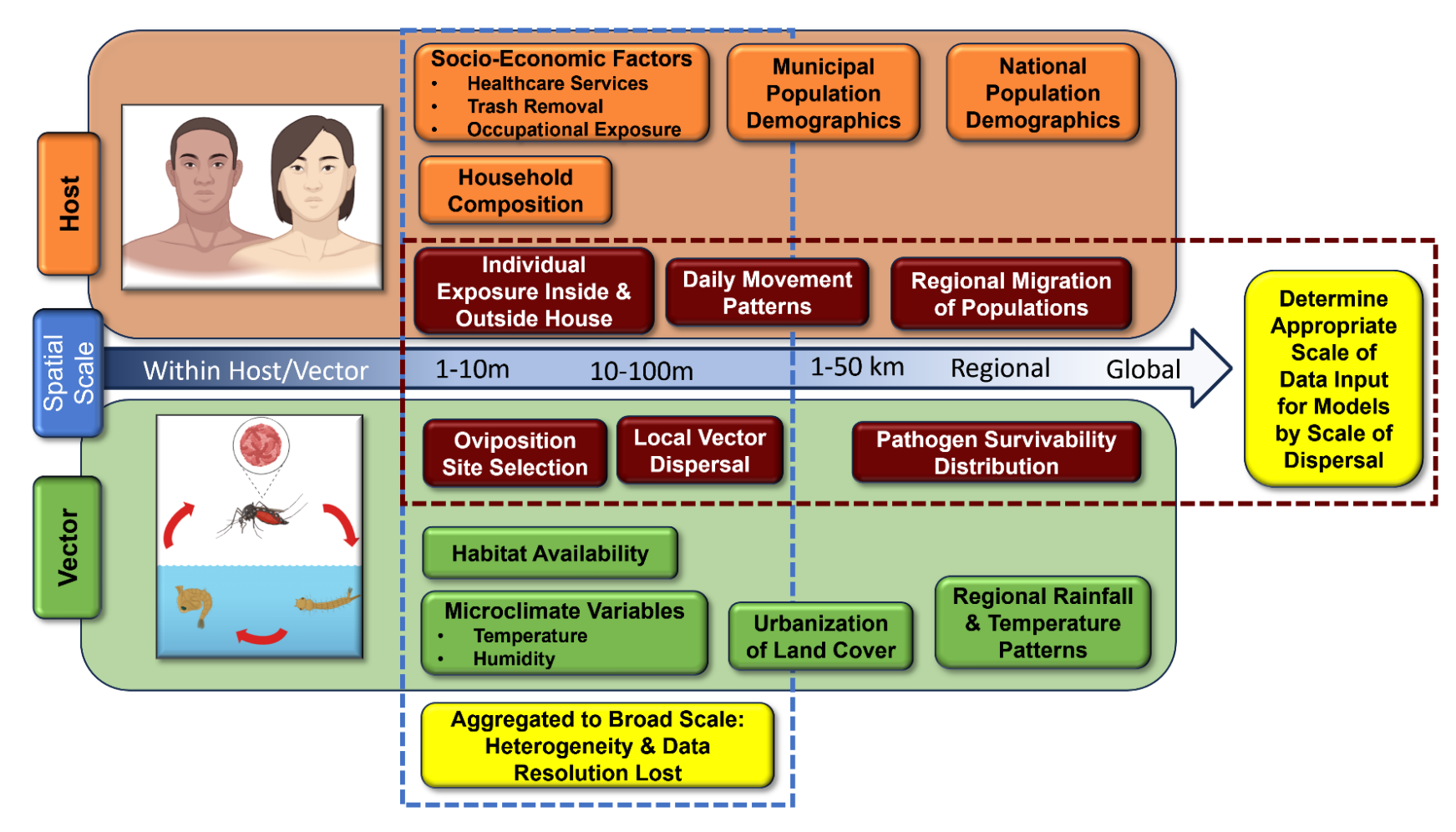


Figure 2.1. Vector and human host variables across spatial scales affecting the modelling of vector-borne disease.

Human host and vector variables that determine vector dispersal and pathogen transmission are highlighted in dark red boxes. Factors that determine the relevant scale for describing a VBD system often depend on the scale at which the vector disperses and interacts

with the host, which in turn depends on vector life history and the movement of infected persons. In human VBD systems, human movements as well as trade and transport of goods can cause the introduction of vectors to novel locations (variables boxed in red). Key variables for the mosquito vector and for human hosts that are heterogenous at finer spatial scales are boxed in blue.



**Figure 2.2.** Common human-made mosquito habitats in a heterogenous urban environment. (A) Urban landscape in the island nation of St Kitts and Nevis, a location with multiple endemic vector-borne diseases spread by mosquito populations such as Dengue virus

and Chikungunya virus. Larval mosquito habitats vary dramatically at fine spatial scales and are exposed to significantly different microclimates: (**B**) rainwater storage barrel, (**C**) discarded used tire, and (**D**) drainage along urban street. Agricultural rain barrels offer more persistent water for larval habitats than roadside drainage in urban areas, increasing vector abundance in rural regions. However, a more ephemeral used tire larval habitat may produce fewer mosquito vectors but be closer to population centers, increasing contact rates between vectors and hosts.

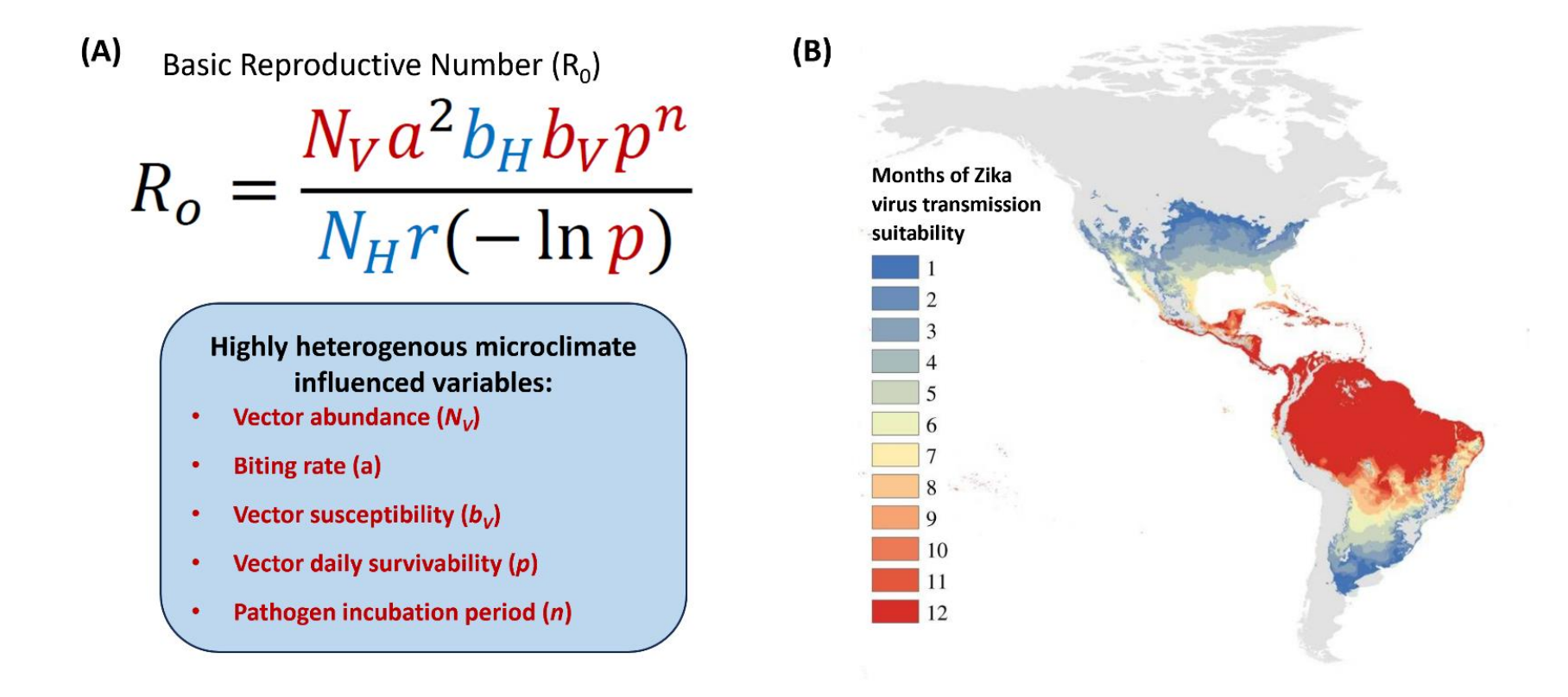
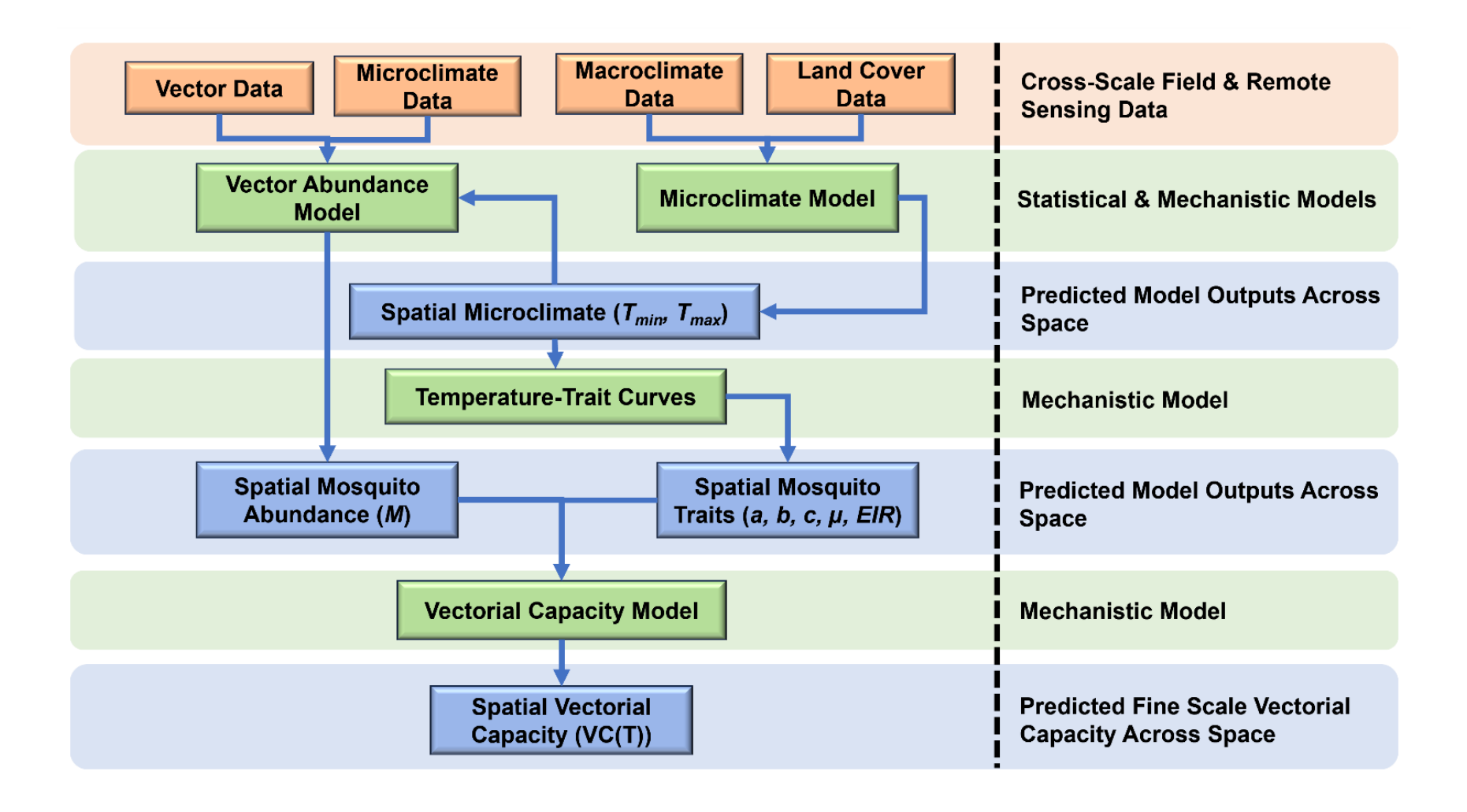


Figure 2.3. Applying mechanistic models of microclimate impacts on vector-borne disease transmission. (A) The Ross-MacDonald Model describes the basic reproductive number of a VBD system, derived from and traditionally applied to mosquito vector-borne disease systems. Variables expected to be significantly heterogenous in space and time are displayed in red: vector abundance ( $N_V$ ), biting rate (a), vector susceptibility ( $b_V$ ), vector daily survivability (p), and pathogen incubation period (n). These variables can be informed by empirical field collected microclimate data. Model variables not expected to vary greatly due to

heterogenous microclimates are displayed in blue: host abundance ( $N_H$ ), host susceptibility ( $b_H$ ), and host recovery rate (r). (**B**) Map representing months of Zika transmission suitability informed by empirical organismal level thermal response data derived from laboratory experiments. The resulting risk map represents a more accurate expression of months of Zika virus susceptibility than a purely statistical model portrays. Reproduced and adapted from Tesla et. al. (2018), represented here in accordance with the Creative Commons Attribution License.



**Figure 2.4. Recommended workflow for informing multi-scale models of VBD systems.** The demonstrated workflow pictured here elegantly incorporates field-derived parameters into a spatially informed model of vectorial capacity. It also represents the synthesis of both statistical approaches. Data inputs are displayed in orange boxes, models are displayed in green boxes, and model outputs are

displayed in blue boxes. Adapted from Wimberly et. al. (2020), represented here in accordance with the Creative Commons Attribution License.

# **CHAPTER 3**

MICROGEOGRAPHIC VARIATION AND LAND COVER INFLUENCES ON MOSQUITO VECTOR POPULATIONS INCLUDING THE MEDICALLY SIGNIFICANT AEDES ALBOPICTUS ACROSS AN URBAN GRADIENT IN ATLANTA, GEORGIA<sup>2</sup>

\_

Author contributions; PMN: conceptualization, investigation, software, visualization, writing - original draft preparation, writing – review and editing, project administration, formal analysis, data curation; VS: investigation; DC: investigation; SMA: conceptualization, writing - review and editing, supervision, resources, methodology, funding acquisition; CCM: conceptualization, writing - review and editing, supervision, resources, methodology, funding acquisition. All authors agree that their contributions can be included in this dissertation.

<sup>&</sup>lt;sup>2</sup> Newberry PM, Suarez V, Constantinides D, Altizer SA, Murdock CC. To be submitted to *PLOS Neglected Tropical Diseases*.

### **Abstract**

Empirical evidence in recent years has emphasized the importance of microclimate in influencing the urban adapted and anthropophilic mosquito species Aedes albopictus, a significant vector of disease worldwide. Environmental variables like temperature, humidity, canopy cover, and impervious surface cover change as landscapes urbanize, and these factors are heterogenous within the geographic scale that Ae. albopictus experiences its environment. This study examines microclimate variables predicted to influence vector-borne disease risk as modulated through impacts on mosquito abundance. We distributed temperature and relative humidity data loggers across 12 sites in Atlanta, GA, USA, covering a range of impervious surface coverage. Microclimate measures were matched with monthly adult mosquito trapping and larval habitat surveys from Jun-Oct for two consecutive years. Principal component analysis and mixed-effects models were used to identify the most significant environmental variables and their respective influences on adult *Aedes albopictus* abundance and larval habitat density. Results showed that impervious surface cover and daily temperature ranges with 14-day lags predicted greater adult Ae. albopictus abundance, whereas mosquito abundance decreased with greater minimum relative humidity. Larval habitat density increased with canopy cover across sites. Collectively, our findings predict that Ae. albopictus in urbanizing landscapes are supported by a mosaic of residential, commercial, and forested areas. We speculated that adult mosquitoes are attracted to residential and commercial areas with higher human host abundance, whereas larval development depends on greater forest cover.

#### Introduction

Human alteration of landscapes can affect the abundance, distribution and characteristics of aquatic larval habitats and the development of container breeding mosquitoes of medical

significance, including the globally invasive Asian-tiger mosquito *Aedes albopictus*. This species was first identified in the United States in 1985 following an invasion facilitated by the used tire trade from Asia, and by 1994 all counties in the state of Georgia had reported the presence of *Ae. albopictus* (Womack et al. 1995). *Ae. albopictus* is a competent vector for many arboviruses including the Dengue, Chikungunya, and Zika viruses. From its ancestral origins in Southeast Asia, this species has spread globally to all continents except Antarctica. Species distribution models predict global climate change shifting the range of *Ae. albopictus* northwards (Rochlin et al. 2013, Kraemer et al. 2015, Laporta et al. 2023) while also moving the transmission risk of various arbovirus into regions not accustomed to these arboviruses (Tesla et al. 2018, Leta et al. 2018, Ryan et al. 2021, Gloria-Soria et al. 2021, Bohers et al. 2024). *Ae. albopictus* is also known to prefer both general mammalian and specifically human hosts across sylvatic/rural, residential/suburban, and urban environments, potentially with evidence of different feeding preferences depending on the physical environment and host community composition (Richards et al. 2006, Valerio et al. 2010, Faraji et al. 2014).

Given the importance of *Ae. albopictus*, it is critical to understand the factors that affect its distribution and abundance to inform surveillance and control efforts as well as to anticipate future spread. The distribution and abundance of *Ae. albopictus* depends on abiotic and biotic variables that determine their development rates, population growth, and daily survival (Alto and Juliano 2001, Delatte et al. 2009, Brady et al. 2013). These variables directly affect mosquito life history traits, and effects on juvenile stages can carry-over to affect adult traits (e.g., body size (Gunathilaka et al. 2019, van Schoor et al. 2020), reproduction (Christiansen-Jucht et al. 2015, Ezeakacha and Yee 2019, Salim et al. 2023), as well as pathogen susceptibility (Westbrook et al. 2010, Alto and Bettinardi 2013, Moller-Jacobs et al. 2014, Murdock et al. 2014b, Evans et al.

2018, 2020)). Specifically, temperature and relative humidity are critical determinants of Ae. albopictus population dynamics (Murdock et al. 2017, Wimberly et al. 2020). Temperature variation has non-linear and unimodal effects on mosquito life history traits with intermediate optima (Murdock et al. 2017, Evans et al. 2018, Mordecai et al. 2019). While relatively understudied, relative humidity is also important (Murdock et al. 2017, Brown et al. 2023). Daily fluctuations in these two environmental variables have added effects not necessarily captured in current experimental work (Evans et al. 2018, 2019, Wimberly et al. 2020). These effects, in turn, influence how mosquito population dynamics vary across space with land use and season (Richardson et al. 2011, Mordecai et al. 2017a, Evans et al. 2019, Wimberly et al. 2020). Urbanization, and the heterogeneity in land use associated with the urban environment, results in temperature and relative humidity variation across urban landscapes at spatial scales not reflected by local weather station data. The built up environment is often associated with increases in temperature and decreases in relative humidity through heat island effects resulting from the thermal properties of urban structures (Arnfield 2003, Mohajerani et al. 2017), reduced air flow, waste heat, and reduction in vegetation and evaporative cooling (Tan et al. 2018). Some investigations into VBD in cities also directly implicate expanding urban heat island effects in increasing Dengue virus or malaria incidence (Araujo et al. 2015, Akhtar et al. 2016, Misslin et al. 2016, Santos-Vega et al. 2023). The relationship between mosquitoes, urban temperature effects, and resulting impacts on VBD has been shown to be both significant and heterogenous at scales of 100m to several km (Nagao et al. 2003, Murdock et al. 2017, Evans et al. 2018, 2019).

In addition to abiotic variation, the quality and quantity of larval habitats is another key driver of *Ae. albopictus* population dynamics (Evans et al. 2019). For mosquitoes that thrive in containers, human activity can directly increase available larval habitats via the increase in the

prevalence of artificial container habitats that often accompanies human habitation, thus facilitating mosquito population growth (Li et al. 2014, McClure et al. 2018), and this can vary with socio-economic status. For example, lower socioeconomic levels may involve a lack of indoor plumbing and necessitating the household storage of water in containers, while decreased garbage collection leads to more larval habitats (Nagao et al. 2003). Alternatively, higher socioeconomic status could increase gardening activities and potted plants prevalence, increase local vegetation and aquatic container habitat. Additionally, higher humidity levels may be seen in austere housing more open to the outdoor surrounding, facilitating mosquito vector exposure to the inhabitants (Baruah and Rai 2000).

In this study, we examine microgeographic variables and land cover changes that facilitate *Ae. albopictus* populations in urban environments, using measures of mosquito abundance and larval habitat density as indicators. We accomplish this by investigating sites with varying impervious surface and forest cover in Atlanta, GA, USA. We placed multiple temperature and RH loggers across each site to capture microgeographic variation at the scale an individual mosquito experiences environmental heterogeneity. Paired with adult and larval mosquito surveys, we investigated the relationships between fine scale microclimate variables and land cover characteristics with *Ae. albopictus* abundance and distribution as well as positive larval habitat density. We predicted that larval mosquitoes would be more common in areas with higher canopy cover owing to more potential breeding siters, and that adult abundance would increase in residential and commercial areas with greater human activity and density.

#### **Materials and Methods**

Study site selection:

We collected data between Jun-Oct in 2021 and 2022 in Atlanta, Georgia, USA, between the city center and the eastern perimeter covering a 15x15km area. The study area contained diverse urban land uses including commercial centers, forested parks, and suburban residential zones (Figure 3.1). Twelve survey sites were selected to capture the full spectrum of impervious surface coverage, maintaining at least 1600 meters between them. Previous research supports that impervious surface coverage strongly impacts microclimate in urbanized area, so this was the primary selection metric (Evans et al. 2018, Wimberly et al. 2020). The National Land Cover Database 2016 dataset was used to generate an impervious surface map with ArcGIS ArcMap 10.7.1 (ESRI) with each site's impervious surface calculated as the average impervious coverage within a 500-meter radius of the site center. Each site was also characterized by canopy cover over a 100-meter radius from the center of the site. The different radii for these landscape characteristics were informed by previous work in Athens, GA (Murdock et al. 2017, Wimberly et al. 2020) indicating microclimate effects between 1km to capture urban heat island effects down to 150m to ensure sensitivity to microhabitat variation. We chose a 500m radius moving focal window to avoid excessive homogenization of site characteristics and to capture any effects of heat islands. Sites ranged from 5% to 71.8% impervious surface cover and 0.4% to 95.2% canopy cover (Table 3.1). An initial set of potential sites covering the range of impervious surface values was initially chosen across the gridded area, with final site selection informed by accessibility, ability to gain site permissions, and to ensure sites were independent of each other (minimum distance between sites was 1670 m). Each of these were delineated by 100-meter radius from a central point in accordance with previous studies showing most female Aedes

albopictus dispersal occurs within that range (Figure 3.1)(Bellini et al. 2010, Marini et al. 2010). See Table 3.1 for the full list of survey sites, site codes, coordinates, and associated land cover measures. Bounds of the entire study area were approximately 12x12 kilometers, covering predominantly the eastern half of metro Atlanta across varying levels of urban development from paved commercial centers and parking lots to forested parks and suburban neighborhoods.

Access and sampling in municipal areas was authorized by local Dekalb County officials. Other site permissions in residential or commercial areas were granted by homeowners, local business owners, and private park managers.

# Aquatic larval surveys:

We surveyed each site for aquatic larval habitats monthly, with surveys for the 12 sites separated 30 days and avoiding extreme rainfall events. Each month, we visually inspected every site for standing water or potential container habitats using a walking survey. We recorded the long axis, short axis, depth GPS coordinates, canopy cover and description of all larval habitats noted per site. We estimated canopy cover with a spherical crown forester densitometer with values rounded to the nearest 10%. If we identified larvae or pupae in a particular habitat, we used a 1.5 cm volume transfer pipette to collect the mosquito larvae/pupae. Each habitat for a sampling month/site had a 50 mL Falcon tube with a thin mesh cover and a cotton ball stopper. We collected a subset of up to 25 larvae/pupae from each habitat to avoid destructive sampling and to preserve the site population size in subsequent sampling months. Sampled larval tubes contained the original habitat's water (20-40 mL) along with 5 mg of dry flake fish food (Tetra Cichlid) to support development. We added deionized water as needed to prevent evaporation of water within the larval tube. Larvae were reared in tubes specific to a particular larval habitat and placed in a Percival Scientific incubator at 28.0°C +/- 0.5°C and 80% +/- 5% RH with a diurnal

program (14:10 day/night). We checked tubes daily for adult emergence, which were immediately placed in a -20 °C freezer. Sex and species was determined after freezing following Darsie and Ward prior to long term storage at -80°C (Darsie and Ward 2005).

# Adult trapping:

We sampled Adult mosquito monthly from June to October in both 2021 and 2022 field seasons in conjunction with larval surveys to measure abundance and community composition of mosquitoes at each study site. We deployed Biogents Sentinel 2 traps (BGS) (Biogents AG, Regensburg, Germany) for adult trapping and placed in the center of each site for a 24-hour period in each sampling month. We baited the traps with octanol lures (Biogents AG, Germany) and 1000g of dry ice placed in an open insulated water bottle to generate a CO<sub>2</sub> plume. The traps were powered by 12V 1400 mAh batteries, which we ran continuously for each 24-hour period to reduce the risk of escape. At the end of each sampling period, we sealed the catch bag with captured mosquitoes within a zippered plastic bag and immediately stored in a cooler of dry ice until storage in a -20 °C freezer for later identification. Sexing and identification to species was performed following Darsie and Ward prior to long term storage at -80°C (Darsie and Ward 2005). We recorded the date of each collection as the day the trap was set. Occasionally traps in public places were stolen, tampered with, or destroyed, necessitating a subsequent adult sampling period as close to the larval survey date as possible.

# Microclimate measurement:

Because weather station data do not accurately reflect the climate conditions mosquitoes experience (Cator et al. 2013, Paaijmans et al. 2014, Murdock et al. 2017, Wimberly et al. 2020) due to variation in land cover and surrounding land use, we deployed six data loggers at each site (n=72 total) to record daily variation in temperature (T) and relative humidity (RH). At each site,

four RFID Track-It loggers by Monarch Instruments (Amherst, NH) were deployed along with two MX2300 loggers and solar radiation shields by HOBO (Onset). Logger models were mixed due to the limited availability of the MX2300 models, which had enhanced data download capabilities and measurement accuracy/resolution (T accuracy of 0.2°C vs 1.6°C and RH accuracy 2.5% vs 3%; T resolution of 0.01°C vs 0.5°C and RH resolution of 0.01% vs 0.5%). Loggers were placed in full shade at 1m high affixed with zip ties to vegetation and with solar shields for loggers exposed to direct sunlight. The loggers recorded T and RH readings every 15 minutes continuously. Some loggers were lost due to removal by the public or otherwise destroyed during the sampling period. Loggers would be replaced as soon as the loss was identified, and all sites had coverage of at least 5 loggers for each day. For each logger on each day, the average, maximum, and minimum Ts as well as the DTR were calculated. Additionally, the daily average, maximum, and minimum RHs were calculated along with the daily RH fluctuation. These daily temperature and RH values were then averaged over the preceding 7 and 14-days from the last survey data to account for different lags associated with mosquito development times for each site. Intra-site variation between loggers was small for temperature (0.576 °C) and larger for RH (12.934%).

# Data analysis:

To determine the effect of different microclimate variables on *Ae. albopictus* abundance, a principal component analysis (PCA) was performed alternatively using 7-day and 14-day lags for the RH (minimum, maximum, average, and fluctuation) and temperature (minimum, maximum, average, and DTR) variables after normalization. This PCA identified the strongest microclimate and landscape predictors of site variation with which to test in downstream models of adult *Ae. albopictus* abundance and larval habitat density. Larval habitat density specifically

refers to a larval habitat that was positive for mosquito larvae, and a larval habitat was considered positive for larvae if there were any mosquito species identified. This was because almost all larval habitats that had non-Ae. albopictus mosquito larvae also had Ae. albopictus larvae present.

The variables explaining the most variation for the 7- and 14-day lags, using a cos2 quality of representation cutoff of 0.2, were then used to test different generalized linear mixed effects models predicting adult *Ae. albopictus* abundance and larval habitat density for immature mosquitoes. Adult abundance of *Ae. albopictus* was chosen as the primary response variable representing population size, while larval habitat density at a particular site was used as a proxy for site suitability for mosquito populations. The distribution of the adult count data followed a negative binomial pattern (mean = 28.6, variance = 3727.1). Larval habitat density was likewise determined to follow a negative binomial distribution, although with a less extreme mean/variance ratio (mean = 1.3, variance = vs. 3.4). Models predicting for these response variables fitted to a negative binomial distribution outperformed those fitted to a poison distribution.

The glmmTMB package (version 1.1.10) in R was used to build different mixed effect models, and model performance was assessed by comparing AIC values, degrees of freedom, convergence, and the significance of difference from a null model with only random effects tested with likelihood ratio tests. Site and Month/Year were the random effects for each model tested, with Month nested within Year. Microclimate temperature and RH variables exhibited non-linear relationships with adult abundance and larval habitat density, so these variables transformed using a basis spline (b-spline) function for fitting into a linear model. After normalization or microclimate variables, basis-spline fitting using the "s()" function in the

"splines" R package (version 3.6.2) (R Core Team 2024) was performed on each temperature and RH variable in order to improve model convergence. Canopy cover and impervious surface coverage also showed a nonlinear effect with larval habitat density and was also transformed with a b-spline for the larval habitat density models, while the relationship was more linear versus adult abundance. Model fit was tested in the univariate models with and without b-splines assigned to the microclimate variables to ensure AIC values and model convergence improved. Dispersion and uniformity for each model was tested with the DHARMa R package (version 0.4.7) (Hartig 2024). The fixed effects tested as predictive of adult abundance and larval habitat density were chosen according to the most important elements of the first loading of the PCA. Mixed-effects models with these different microclimate variables and combinations of microclimate variables were then used to investigate the most important predictors of Ae. albopictus abundance. Predictor variables that were highly positively or negatively correlated were typically not placed in the same model to avoid the confounding effects of extreme covariance between effects. Although RH terms were correlated with DTRs for both 7-day and 14-day lags (negatively for minimum/average/maximum RH with DTR, positively for RH fluctuation and DTR), models with both RH and DTR were tested due to the likely importance of both RH and DTR in this system. Adding a term in the mixed effects model to account for the interaction between RH and DTR typically improved model fit, but the interactions were not significant. Larval habitat density was also added as a fixed effect for the adult abundance model to account for the biological importance of larval habitat availability in driving population size.

For predicting both adult abundance and larval habitat density, a total of 34 mixed effects models were tested to evaluate what combinations of fixed effects that best predicted their respective response variable. The seven best performing adult abundance models and the three

best performing larval habitat density models are displayed in Table 3.3. The 10 other temperature and RH microclimate variables (maximum, average, and minimum temperature; maximum and average RH) with both 7-day and 14-day lags were also tested for performance against the multivariate models for both adult abundance and larval habitat density for a total of an additional 20 models. However, none of these univariate models outranked the multivariate models for predicting adult abundance. Larval habitat density was then tested as a univariate predictor of larval population density independent of adult abundance, and the univariate models here performed better relative to other larval habitat models. See Supplementary Table A.4 for the full list of adult abundance model performance and Supplementary Table A.5 for the full list of larval habitat density model performance.

### **Results**

Specimen and site overview:

Over the two field seasons, a total of 17 species of mosquito and 4985 mosquito specimens were collected, and adult abundance by month peaked from August to September. Species richness at the site level ranged from 2 to 10, with an average value of 5.75 and a median value of 5.5 species per site. Across all sites, *Ae. albopictus* was the species that was the most prevalent, making up 91.84% of the specimens collected (n=867 larvae and n= 4578 adults) (Figure 3.2). A total of 133 unique larval habitats were identified, with 83 positive for mosquito larvae (44.8%). Of these larval habitats, 25 were classified as natural (ephemeral drainage ditches, stagnant pools, and tree holes) with 20 of these natural habitats being positive for mosquito larvae (79.9%). The remaining larval habitats (n=108) were classified as artificial, meaning they were directly tied to human activities (e.g., trash containers, buckets, flowerpots, planters, stagnant fountains, and water storage tanks). Out of these artificial larval habitats, 63

were positive for mosquito larvae (58.3%). The average number of larval habitats for the sites was 11.1 with an average of 6.9 of these larval habitats positive for immature mosquitoes. Site FR had the most larval habitats (n=34) and site PPR had the second highest (n=26) larval habitats, with a correspondingly habitat positivity rate (occupied/total larval habitats) (FR=82.4% and PPR=76.9%). Sites FR and PPR also had the most *Ae. albopictus* larvae collected from them (FR: n=250 and PPR: n=214) (Figure 3.3a). Interestingly, despite the low habitat abundance and number of larvae collected from sites DD and NDS, these sites had the highest numbers of adult *Ae. albopictus* collected from them (DD: n=1301 and NDS: n=628) (Figure 3.3b). *Ae. albopictus* abundance increased through both seasons, peaking in August and decreasing through October (Figure 3.5). Similarly, larval habitat density increased through both seasons, peaking in August and decreasing through October (Figure 3.7a).

Over the field seasons, the minimum, average, and maximum temperature values across all sites increased together until July before decreasing together until October (Supplementary Table A.3 and Supplementary Figure A.1). Minimum, average, and maximum RH values over the field seasons likewise tracked together, peaking in August and decreasing until October (Supplementary Table A.3, and Supplementary Figure A.2). Averages for each site across the field seasons show site MD as having the highest average temperatures and site DD having the lowest average temperatures. The highest average RH were at site WG and lowest average RH at site DD (Supplementary Table A.2). Classifying the sites by degree of site imperviousness as low (<25%), medium (25-45%), and high (45-72%), high impervious sites showed a large degree of variation compared to medium and low, corresponding to higher DTR values. All levels of imperviousness had similar minimum average temperatures across the seasons (Supplementary

Figure A.3). Low impervious sites showed the highest minimum RH values and high impervious sites showed the most variation in maximum RH values (Supplemental Figure A.4).

Principal component analysis:

Using 7-day lags, the first and second principal components captured 72% and 18.5% of the variability in the dataset, respectively. Using the cos2 quality of representation measures for PC1, the most important variables were the minimum RH, fluctuation in RH, average RH, DTR, canopy cover (Can100m: 0.263), and impervious surface (Imp500m: 0.228) (Table 3.2a). The average of daily RH<sub>MIN</sub> and RH<sub>MEAN</sub> were strongly positively correlated (0.8879679), so only RH<sub>MIN</sub> was used to capture the effect of RH in the microclimate models since it outranked average RH in cos2. With the 14-day lags, the first principal component captured 77.2% and the second principal component 16% of the variability in the dataset. Using the cos2 quality of representation measures for PC1, the same measures as 7-day lags were the most important except with 14-day lags: fluctuation in RH, minimum RH, average RH, DTR, canopy cover (Can100m), and impervious surface (Imp500m) (Table 3.2b). Likewise, the mean daily RH<sub>MIN</sub> and RH<sub>MEAN</sub> were strongly positively correlated (0.8511583), so only RH<sub>MIN</sub> was used as the higher quality variable according to cos2 rank. See Supplementary Table 3.1 for a complete list of variable correlations and Supplementary Figures A.5 and A.6 for 7-day and 14-day lag variable scree plots, respectively.

Generalized linear mixed effects models

The temperature and RH variables were tested in univariate models to isolate any potentially strong indicators of adult abundance or positive larval habitats that existed independent of other variable interactions. None of these univariate models for predicting adult abundance outperformed the multivariate models for predicting adult abundance, suggesting the

importance of accounting for the effects of T, RH, and land cover variables together. Also, all models for adult abundance were tested with larval habitat abundance as a predictor, as this is biologically an important limiting factor for population sustainment. While larval habitat density was not a significant effect in the adult abundance models, it did however significantly predict the actual larval population size of each site in a separate model with just larval habitat density as a fixed effect. The close relationship between larval habitat density and actual number of larvae is expected given the reliance of identifying a positive larval habitat prior to sampling its larvae for the larval specimen count. While this is a less effective measure of population size than adult abundance since the larval habitats were not destructively sampled in order to minimize the month-to-month influence of sampling, it is potentially informative when accounted for in addition to more precise measures of adult abundance. For all models, Site and Month: Year (nested) were included as random effects.

One interesting phenomenon is the disparity regarding high larval populations and larval habitat density vs adult population. This may suggest some movement of larval populations once they emerge as adults, especially considering mismatch between the sites with the greatest abundance of adults and the sites with the most larvae collected (Figure 3.3b). Alternatively, the imbalance between larval and adult abundance may be a consequence of whether a study site population was sampled immediately after a mass adult emergence somewhat synchronized by a rainfall event some days earlier. Additionally, larval abundance in of itself was not necessarily a direct representation of every larvae at a site, as larval habitats were not destructively sampled in order to mitigate potential month to month influences caused by local extirpation of larvae during the preceding sampling event. Larval habitat density as a response variable was most strongly predicted by the model just using canopy cover as a fixed effect. Testing other fixed

effects both alone and in combinations of T, RH, and landscape variables did not perform as well, judged by AIC values and significance of difference from the null model of larval habitat density.

The best performing model predicting adult abundance was a 14-day lag model (AIC = 946.2) that incorporated the following fixed effects: daily RH<sub>MIN</sub> (p= 4.35e-06 \*\*\*), DTR (p = 0.000175 \*\*\*), and impervious surface (spatial resolution 500m; p = 0.007734 \*\*). The secondbest performing model (AIC = 947.8) included the same fixed effects, but with the interaction between RH<sub>MIN</sub> and DTR incorporated in the model: daily RH<sub>Min</sub> (p= 0.00106 \*\*), DTR (p = 0.02188 \*), impervious surface (spatial resolution 500m; p = 0.00912 \*\*), and RH<sub>Min</sub>: DTR (p = 0.51422 ). For this model, the RH<sub>Min</sub> and DTR interaction was not significant. For both of these models, the effects of Site, Month: Year were included as random effects (Table 3.3). Additionally, both of these models were significantly different from the null model of adult abundance (p = 0.005856 \*\* without the interaction term RH<sub>MIN</sub>: DTR and p= 0.009611 \*\* with the interaction term RH<sub>MIN</sub>: DTR). Adult mosquito abundance increased positively with impervious surface coverage (Figure 3.5b) and 14-day DTR (Figure 3.6a), while increases in the daily RH<sub>Min</sub> had a negative effect on adult abundance (Figure 3.6b). The best performing model for predicting larval habitat density was a univariate model (AIC = 292.7) with canopy cover (100m resolution) as a fixed effect (p = 0.0194\*) and Site and Month: Year sampled as random effects (Figure 3.7b).

# Time Lag Performance

The superior performance of 14-day lags for predicting adult abundance may be due to longer larval development times at the varying temperatures at the sites. Previous studies into development times for *Ae. albopictus* found egg to adult emergence times at 32°C to be 9-10

days but as long as 35-40 days at 12°C in controlled lab environments with constant temperatures (Briegel and Timmermann 2001). While this lower range of minimum temperatures was not seen until the end of each season in October when very few mosquitoes were caught, the average minimum temperatures did range from 20.5°C to 16.57°C in June through September, supporting that 14-day temperature lags may better capture the biological effects of temperature on larval development in this system.

# **Discussion**

Mosquito Communities and Larval Habitats

The high proportion of Ae. albopictus in all mosquito communities in the study sites supports that this species is urban adapted and highly successful in the habitats tied to anthropogenic alteration of the landscape. Most larval habitats were artificial and associated with human activity, creating ideal habitats for an urban adapted container breeding species like Ae. albopictus. The most productive sites for Ae. albopictus were DD, NDS, GPR, and WG. Many of the larval habitats at these sites constituted flowerpots, small garden fountains, fishponds, and landscaping water containers. Regarding the most predictive microclimate variables, the best performing model of adult abundance incorporated impervious surface coverage at 500m, RH<sub>MIN</sub> with a 14-day lag, and DTR with a 14-day lag. The best performing model of larval habitat density only included canopy cover as a fixed effect. While this may be a result of more vegetation providing more standing water or more refugia for ovipositing adults. But there may also be an interesting socio-environmental interaction along with landscape effects for predicting larval habitat density. A possible explanation would be that sites representing higher income residences or maintained parks may also have increased canopy cover actively cultivated by the community, along with landscaping and decorative sources of larval habitat via flower pots and

sculptures. Additionally, larval habitat density was a significant predictor of larval specimens counts, but not of adult abundance, This suggests a degree of dynamic population movement across the urban landscape between immature and adult life stages.

Variance of microclimate across land cover and over seasons:

Temperature values increased over each season, peaking in July before decreasing through October (Supplemental Figure A.1). Similarly, RH values increased during each season, peaking in July and decreasing through October (Supplemental Figure A.2). The relationship between microclimate variables and land cover measures tended to be opposite in their directional effects on impervious surfaces and canopy cover. For instance, T<sub>Avg</sub> correlated positively with impervious surfaces but negatively with canopy cover, while RH<sub>Avg</sub> negatively correlated with impervious surfaces but positively with canopy cover. These relationships between microclimate variables and associated land cover types led to interesting effects such as impervious surfaces with RH<sub>Min</sub> and DTR variables predicting adult abundance, while canopy cover best predicting larval habitat density. Potentially different sites alternatively provided better habitat for adult or immature stages.

Determinants of larval habitat density:

As canopy cover was the strongest predictor of larval habitat density, the correlations of canopy cover with other microclimate variables is informative. Canopy cover had the strongest negative correlations with impervious surface coverage and RH fluctuation, while the strongest positive correlations were with RH<sub>Min</sub> and RH<sub>Avg</sub>. However, these microclimate variables were not significant predictors of larval habitat density, suggesting that the association of human activity with the cultivation of canopy cover in this urban environment may be a stronger determinant of larval habitat density than microclimate variables alone. Studies of *Ae. albopictus* 

and *Ae. aegypti* populations in the US state of Florida found significant contribution of human supplied container habitats like cemetery flower vases, demonstrating how seemingly minor culturally driven alterations in an urban environment can have outsized roles in vector abundance (Leisnham and Juliano 2009, Leisnham et al. 2014).

Determinants of Ae. albopictus abundance:

The significance of impervious surfaces, RH<sub>Min</sub>, and DTR in predicting adult abundance supports the theory that urbanization increases the abundance of *Ae. albopictus*, with impervious surfaces having a strong positive relationship in the model. This land cover variable likely reflects a combination of urban heat island effects supporting faster development of mosquito populations and the physical construction of an environment suitable to an urban adapted species like *Ae. albopictus*. Additionally, impervious surface coverage did positively correlate with maximum temperature values (0.226), supporting urban heat island theory. The RH<sub>Min</sub> with a 14-day lag had a negative relationship with adult abundance in the model, indicating lower relative humidity was associated with greater adult *Ae. albopictus* abundance and higher relative humidity correlated with less adult abundance.

Empirical investigations have previously shown that increases in RH<sub>Min</sub> and RH<sub>Avg</sub> significantly decrease the probability of adult emergence from larval habitats (Murdock et al. 2017). This effect suggests a role of RH influencing the physical characteristics of the aquatic larval habitats. The atmospheric physics of relative humidity interacting with liquid water makes reductions in surface tension a potential reason, as immature mosquito life stages rely on a minimum level of surface tension to properly feed, develop, and eclose. This is important enough to larval development that the mechanism of action for some larvicides is lowering surface tension of larval habitats (Nayar and Ali 2003, Dawood et al. 2020). As RH values increase,

surface tension tends to decrease (Pérez-Díaz et al. 2012). Furthermore, RH will decrease as temperature increases given a set amount of water vapor (US Department of Commerce 2025); this interaction with temperature makes teasing out the relative impact of each microclimate variable difficult, especially since an increase in RH coincide with rainfall events which may also flush out larval habitats (DeGaetano 2005, Dieng et al. 2012).

The Ae. albopictus populations in this study positively increased with the magnitude of DTR values, but the thermal optimums for mosquito vector systems likely play a concurrent role in affecting population size. There is previous evidence of the magnitude of temperature fluctuations being important, with DTRs around 18°C shown to reduce larval survival and adult fecundity (Carrington et al. 2013b) while also reducing Dengue virus infection rates (Lambrechts et al. 2011, Carrington et al. 2013a) in Ae. aegypti. The average DTR values in our study were above 18°C at sites DD (18.2°C), GPR (19.2°C), and NDS (18.9°C), all of which ranked high in adult Ae. albopictus abundance. This positive relationship may be explained by any negative impacts on immature mosquito survivability from large temperature fluctuations being offset by the positive demographic effects of faster generation times at warmer temperatures. Larger DTR values occurred in sites with higher average maximum temperatures at GPR (36.8°C) and NDS (37.1°C) when compared to the average maximum temperature across all of the sites (32.9°C). The association of greater DTR values coinciding with larger mosquito abundances may be caused by the temperature regime that an individual mosquito experiences shifting into optimum metabolic ranges. This is seen in the increasing DTR values occurring later each sampling season coinciding with lower average temperatures in the fall, suggesting a thermal rescue effect in sites whose land cover characteristics theoretically enabled more time an individual has near its thermal optimum (Dee et al. 2020). DTR values positively correlated with impervious surface

coverage (0.462) and negatively with canopy cover (-0.482). Urban heat island effects are often partially ameliorated by planting vegetation (Soltani and Sharifi 2017), with canopy cover blocking the absorption of solar radiation that would otherwise be absorbed by low albedo paved areas and also allowing for more evaporative cooling (Howe et al. 2017). Parts of a city that are more urban are also observed to have greater diurnal peaks as they absorb solar radiation(Chang et al. 2021). Urban heat islands in growing municipalities have been associated with truncated diurnal variation, with minimum daily temperatures increasing faster than daily maximums (Merkin 2004). In the case of our study, however, temperature fluctuations actually were limited by increased vegetation and amplified by increased paved areas (Yan et al. 2023). The explanation of the disparity may have to due with varying size of urban heat islands between cities and the varying effects of vegetation on lowering daily maximum temperatures.

The actual mechanisms by environmental temperature impacts *Ae. albopictus* populations are tied to the thermal physiology of this ectothermic system, which has well-documented thermal optimums regarding life history traits. For instance, in the *Ae. albopictus* system, higher eclosion rates have been observed under modest temperature fluctuations of 25°C to 29°C with a corresponding drop off in larval survival at 35°C, indicating developmental benefits up until a thermal limit (Monteiro et al. 2007). This may also indicate higher potential vectorial capacity at sites with larger temperature fluctuations if they move into predictively modelled (Mordecai et al. 2017a, 2019, Huber et al. 2018, Shocket et al. 2020) or empirically validated (Shah et al. 2019, Miazgowicz et al. 2020) pathogen thermal optimums resulting in the unimodal temperature-pathogen response curves expected in many vector-borne pathogen systems (Mordecai et al. 2017b, Brown et al. 2023). Overall, the dynamic nature of the urban

temperatures the mosquito populations in this study experienced show the important interplays of urbanization and vector population dynamics.

The sites had a higher variation in RH with an average standard deviation of 6.07 vs 3.24 in a similarly designed field study in a nearby, but smaller, Georgia city also using temperature/humidity loggers (Evans et al. 2019). This observation may be explained by site DD pulling the average variance up due to the high imperviousness of the site matched with a high canopy cover unusual for highly impervious locations in this study, as DD contained both an urban park alongside retail and municipal administration spaces. Site DD additionally had a much higher standard deviation of 18.2 in average RH fluctuations. Without site DD, the average standard deviation in average RH with 14-day lags was still 4.97, which may be a result of more RH variation in the larger urban landscape of Atlanta.

A synthesis of the RH literature described in Brown et. al. (Brown et al. 2023) suggests greater longevity with higher RH, seemingly making the negative role of minimum RH on adult mosquito populations paradoxical. However, positive effects of RH on mosquito longevity are generally in regard to the adult life stage (Buckner et al. 2011, Asigau and Parker 2018), while negative effects seem to be limited to the larval and pupation life stages. The relative magnitude of RH on the different life stages, as well as any interactions between life stages via carry-over effects, would be informative future directions of research. The average minimum RH at the study sites ranged from 41.6% to 70% with an overall site average of 51.0%, and the average maximum RH for the sites was 98.4%. Although the body of research into the effects of RH on mosquitoes frequently implicates lower RH values with higher mortality at extreme RH measures (Schmidt et al. 2018, Brown et al. 2023), the *Ae. albopictus* in this field study with dynamic RH values likely only experienced RH levels outside their optimum range

intermittently. This may result in behavioral modification regarding timing of host seeking, preferred oviposition locations, and resting spot choice being shifted, causing potentially positive or negative impacts on abundance depending on other variables.

# Limitations:

While the variables tested in the mixed effects models were chosen according to the principal component loadings describing the most variation between sites, they were often correlated to some degree with other variables. These correlations are important in that they may also describe the underlying mechanistic phenomenon driving positive larval habitat prevalence and adult Ae. albopictus abundance. For instance, impervious surfaces predicted adult abundance in the best mixed effects model, while canopy cover alone was the strongest indicator of larval habitat density. Still, canopy cover and impervious surface measures strongly negatively covaried (-0.848), suggesting that understanding canopy cover values of a location may may still inform our predictions of adult abundance while impervious surfaces may help predict larval habitat density. Furthermore, some of these correlations are likely tied to the relationships between relative humidity, temperature, and precipitation. The precipitation variable was not extensively evaluated in this study. Although most of the artificial larval habitats were consistently occupied by larvae to some degree throughout each field season, it is possible that sites with higher canopy facilitated the persistence of more larval habitats by virtue of retaining precipitation more than high impervious sites.

*Ae. albopictus* is generally considered a weak flyer, with the average flight ranges largely be within 100 meters in some mark-recapture studies (Lacroix et al. 2009, Verdonschot and Besse-Lototskaya 2014). Still, some field trials have found dispersing *Ae. albopictus* recaptured at ranges from 200-300 meters (Bellini et al. 2010, Marini et al. 2010, Vavassori et al. 2019).

One study from Brazil showed female *Ae. albopictus* traveling over 1000m when released in a sylvatic habitat; these females were subsequently caught near human habitations, while females released near homes dispersed little (Maciel-de-freitas et al. 2006). This suggests that female *Ae. albopictus* are capable of moving distances of several hundred meters from their original larval habitats as they quest for preferred host feeding and oviposition areas. Future investigation is warranted into potential corridors of vegetative refugia (Lacroix et al. 2009) that may connect disparate mosquito populations. Future research may also include expanding the 100m radius search area to identify if there are any source populations near these sites with great differences in adult abundance and larval habitat density.

#### **Conclusions**

This study confirms the importance of land cover and microclimate heterogeneities in temperature and humidity concerning the prediction of adult abundance and the larval habitat density for the medically significant *Ae. albopictus*. Collecting climactic data at the scale of mosquito ecology can be used to identify likely variations in *Ae. albopictus* habitat suitability, although this approach is more resource intensive than using distant weather stations and remotely sensing imagery. The significance of microclimate variables as well as measures of human alteration of the landscape demonstrate the importance of continued environmental surveillance to identify the relative risk posed by disease vectors. Whether the apparent mismatch between larval habitat density and larval abundance vs adult abundance at some sites is actually caused by movement as opposed to pulsed emergence events tied to precipitation or other variables also poses a further avenue of study. To identify whether larger adult abundances are actually showing a recent mass emergence of larvae, more frequent sampling events within each month can be performed. Testing the relationships between precipitation data vs larval or

adult abundance may also be informative as well. Movement from ideal larval habitats to habitats favored by adults for reasons of refugia or host availability can be tested by tracking population dispersal through urban environments via mark-recapture methodologies. This may show potential source-sink dynamics associated with human activities and the urban landscape where resources like hosts, larval habitats, and vegetative refugia are varied. Increasing urbanization worldwide, along with global climate change, makes understanding the implications of these fine-scale environmental variables essential for targeted vector control and public health policy making.

## Acknowledgements

Thank you to the many homeowners in the communities across Atlanta who graciously allowed me to sample and place traps on their property and to Dekalb County and the City of Decatur for access permissions to multiple parks and municipal areas.

## **Funding**

This work was supported by the National Science Foundation [Graduate Research Fellowship # #1842396] and by National Science Foundation Research Traineeship: Interdisciplinary Disease Ecology Across Scales [Grant no: 1545433]

# **Tables**

**Table 3.1**. Study site names, locations, impervious surface percent coverage at a 500 m radius, and canopy cover percent at 100 m radius. Sites are ordered from lowest to greatest canopy cover.

Site Name	ID	Latitude	Longitude	Imp500m	Can100m
Deepdene Park	DP	33.77222	-84.3197	5.0	95.2
Fernbank Residential	FR	33.78627	-84.3188	14.1	73.9
Callanwolde Center	CC	33.78175	-84.3458	17.1	49.0
Woodlands Garden	WG	33.78621	-84.3037	24.6	89.4
Grant Park East	GPE	33.73627	-84.3527	25.8	69.0
Grant Park Residential	GPR	33.72621	-84.3685	34.0	14.3
Piedmont Park Residential	PPR	33.78156	-84.3642	37.5	33.4
North Druid Hills	NDH	33.81758	-84.3111	40.2	0.8
Memorial Drive	MD	33.77908	-84.2407	47.6	0.9
Briarcliff	ВС	33.8272	-84.3321	58.0	0.4
North Decatur Station	NDS	33.79242	-84.2849	61.7	4.7
Downtown Decatur	DD	33.77524	-84.2965	71.8	3.4

**Table 3.2.** Principal component analysis quality of representation (cos2) values for PC1 in both a) 7-day and b) 14-day lag datasets.

a.	7 Day Lag	cos2	b.	14 Day Lag	cos2
	RH7Min	0.402		RH14Flux	0.429
	RH7Flux	0.394		RH14Min	0.410
	RH7Avg	0.333		RH14Avg	0.373
	Temp7DTR	0.325		Temp14DTR	0.370
	Can100m	0.263		Can100m	0.288
	Imp500m	0.228		Imp500m	0.283
	Temp7Avg	0.169		Temp14Avg	0.198
	RH7Max	0.056		RH14Max	0.191
	Temp7Min	0.199		Temp14Min	0.139
	Temp7Max	0.192		Temp14Max	0.124
	LarvalHabitats	0.087		LarvalHabitats	0.088

**Table 3.3.** GLMM models predicting *Aedes albopictus* adult abundance and larval habitat density. Green cells represent models predicting adult abundance and blue cells represent the larval habitat density model. All models displayed converged, passed dispersion and uniformity tests, and were significantly different from the null model with only random effects tested via likelihood ratio tests. The model best describing adult abundance incorporated. Significance thresholds: p < 0.001 (\*\*\*), p < 0.01 (\*\*), p < 0.05 (\*).

Fixed Effects	Fixed Effect Interactions	Random Effects	AIC	Resid (df)	Different from Null Model?	Significant Effects	Direction and Magnitude of Significant Relationships
RH14Min + Temp14DTR + Imp500m + LarvalHabitats	na	Site Month/Year	946.2	109	Yes (p = 0.005856 ***	Imp500m: 0.007734 ** RH14Min: 4.35e-06 *** Temp14DTR: 0.000175 ***	Imp500m: +1.5674 +/- 0.5885 RH14Min: -1.5638 +/- 0.3404 Temp14DTR: +1.0860 +/- 0.2894
RH14Min + Temp14DTR + Imp500m + LarvalHabitats	RH14Min: Temp14DTR	Site Month/Year	947.8	108	Yes (p= 0.009611 **)	Imp500m: 0.00912 ** RH14Min: 0.00106 ** Temp14DTR: 0.02188 *	Imp500m: +1.5619 +/- 0.5990 RH14Min: -1.3944 +/- 0.4260 Temp14DTR: +0.9069 +/- 0.3956
RH7Flux + Temp7DTR + Imp500m + LarvalHabitats	RH7Min: Temp7DTR	Site Month/Year	948.6	108	Yes (p = 0.01309 *	RH7Flux:Temp7DTR: 0.03674 * Temp7DTR: 0.00652 **	RH7Flux:Temp7DTR: -4.3960 +/- 2.1047 Temp7DTR: +2.0822 +/- 0.7654
RH14Min + Temp14DTR + Can100m + LarvalHabitats	na	Site Month/Year	950.2	109	Yes (p = 0.0281 *)	Temp14DTR: 0.000745 ***	Temp14DTR: +1.0679+/-0.3167
RH7Flux + Temp7DTR + Imp500m + + LarvalHabitats	na	Site Month/Year	950.3	109	Yes (p = 0.02901*)	RH7Flux: 0.0121 * Temp7DTR: 0.0171 *	RH7Flux: -1.1327+/-0.4516 Temp7DTR: 0.7678+/-0.3219
RH14Min + Temp14DTR + Can100m + LarvalHabitats	na	Site Month/Year	951.2	109	Yes (p = 0.0345 *)	RH7Flux: 0.01213 * Temp7DTR:0.01705 *	RH7Flux: -1.1327+/- 0.4516 Temp7DTR: 0.7678 +/- 0.3219
Can100m	na	Site Month/Year	292.7	113	Yes (p = 0.02804 *)	Can100m: 0.0194*	Can100m: +1.552 +/- 0.6637

# **Figures**

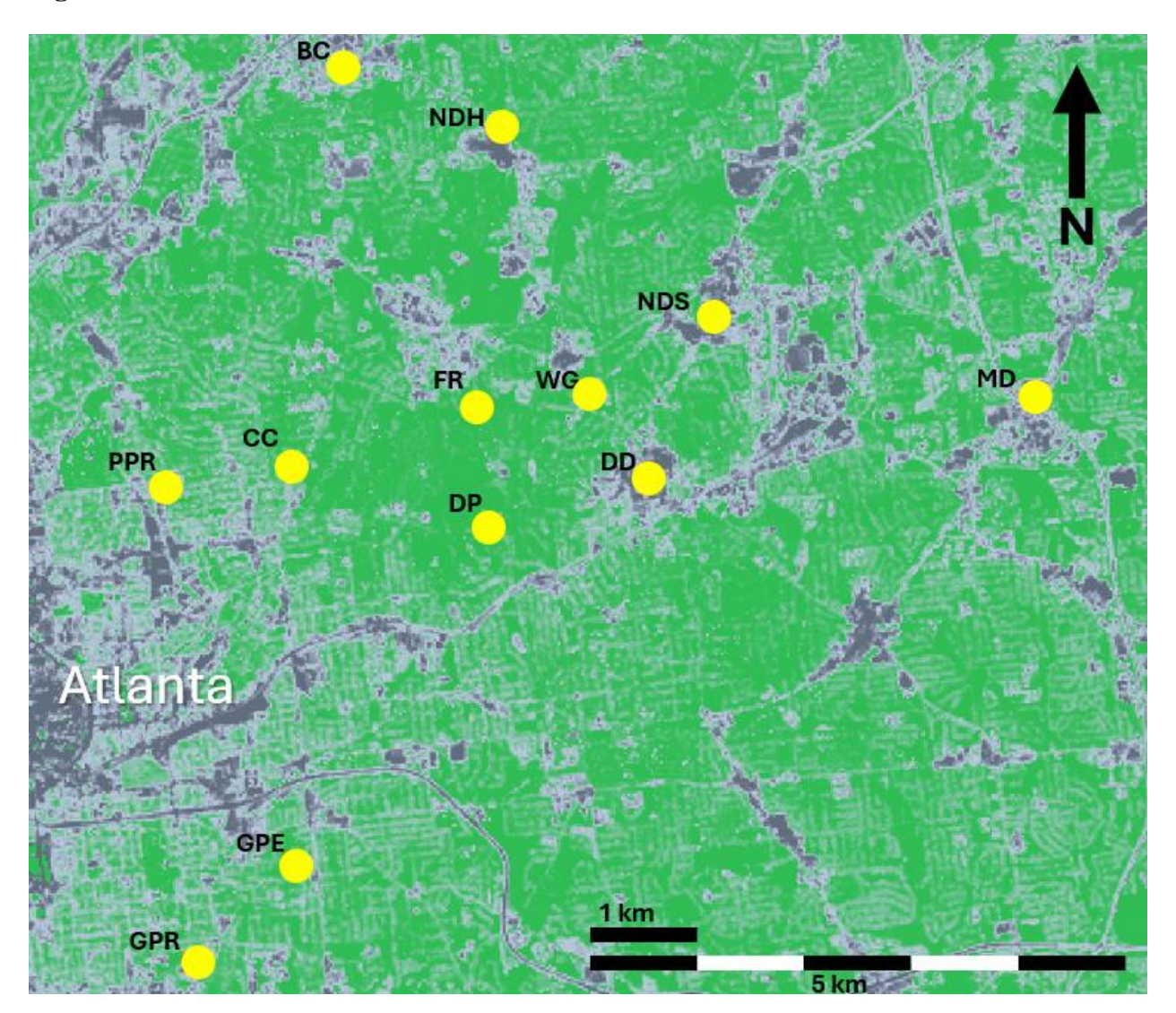


**Figure 3.1.** Map of impervious surface coverage of the study area. Grey representing impervious surfaces derived from the National Land Cover Database (2019). Study site locations identified with Site ID and the 500m radius impervious surface area circumscribed in red.

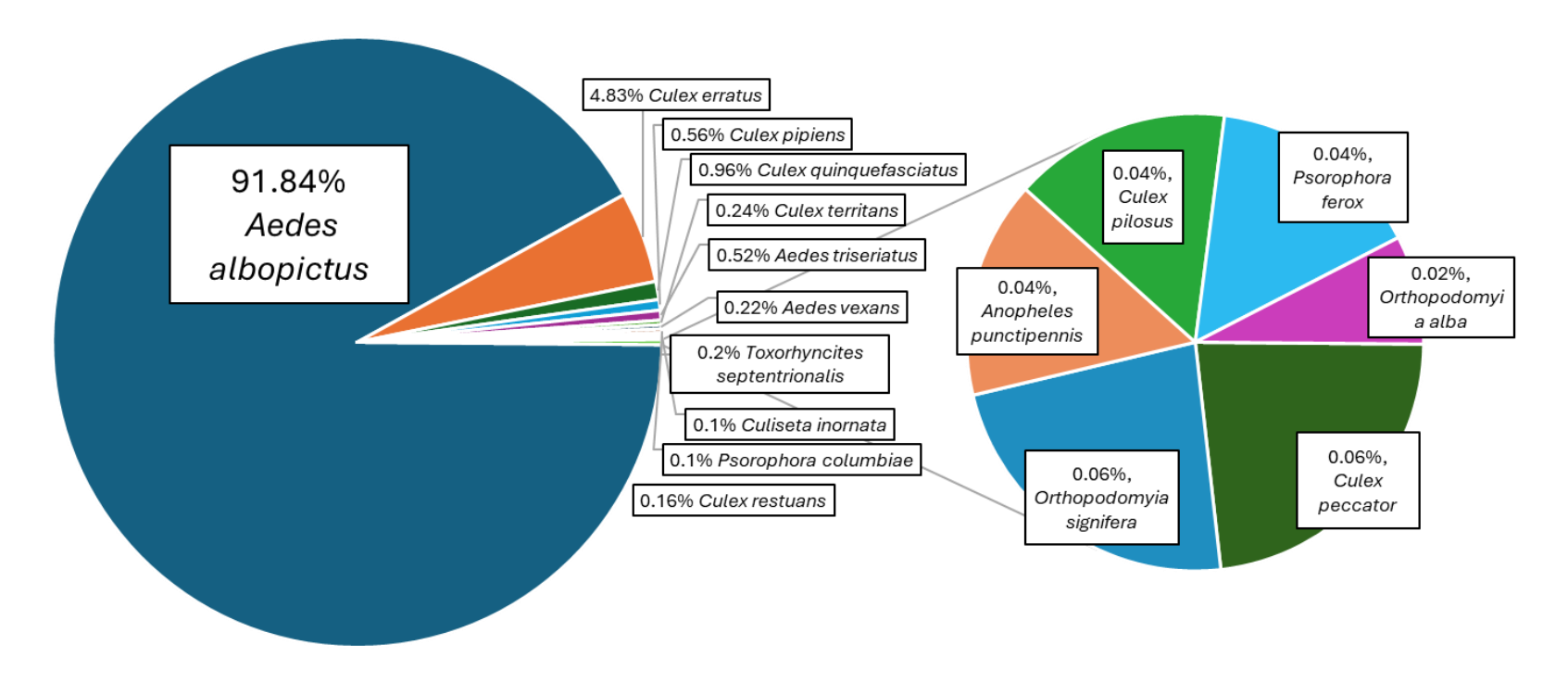


**Figure 3.2.** Mosquito community composition from across sites during the study period. Represents the total adult and larvae specimens identified from each species, and the percent of the total number of specimens is displayed. The smallest populations found are represented in the inset circle graph. *Aedes albopictus* (dark blue) dominated mosquito communities at all sites in this study, constituting 91.8% of all mosquito specimens.

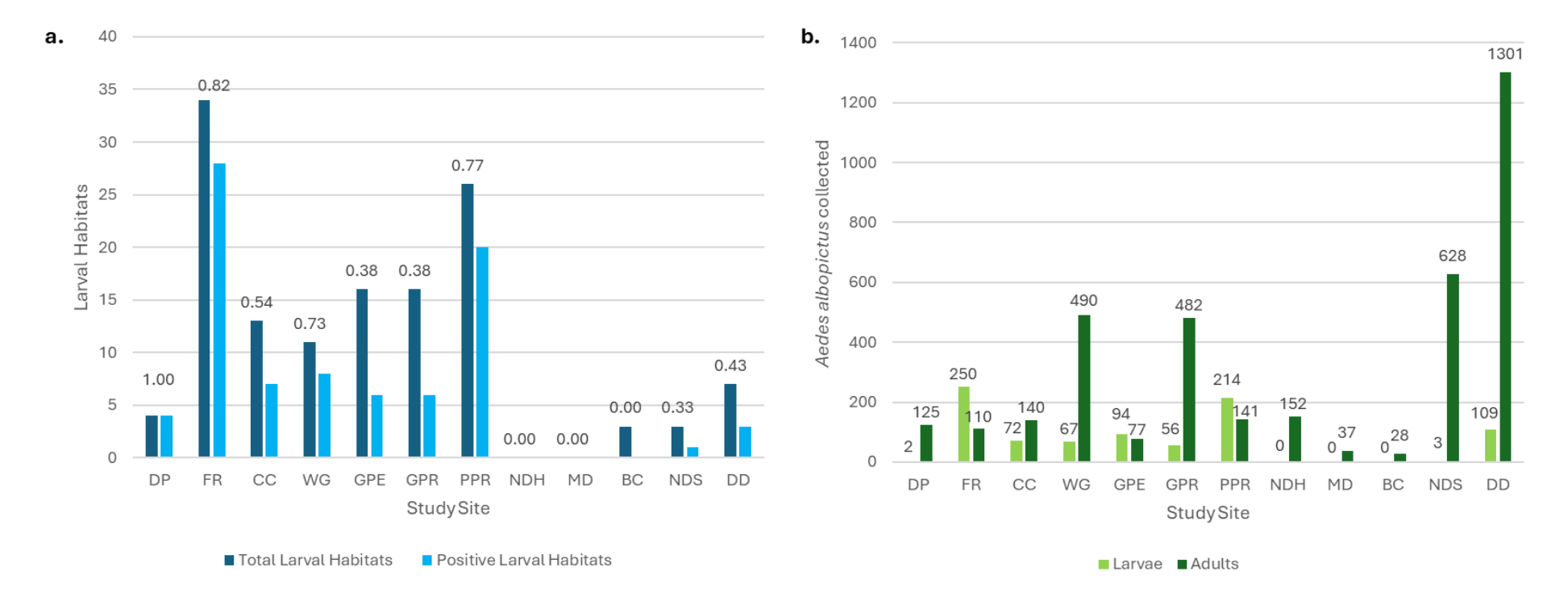


**Figure 3.3.** Larval habitats and *Ae. albopictus* abundances by site. (a) Total number of unique larval habitats and larval habitats positive for mosquito larvae across the sites. Dark blue represents total habitats, while light blue represents habitats occupies by mosquito larvae. (b) Total number of adult and larval *Aedes albopictus* specimens collected across sites. Larval counts are represented in light green, and adult counts are represented in dark green.

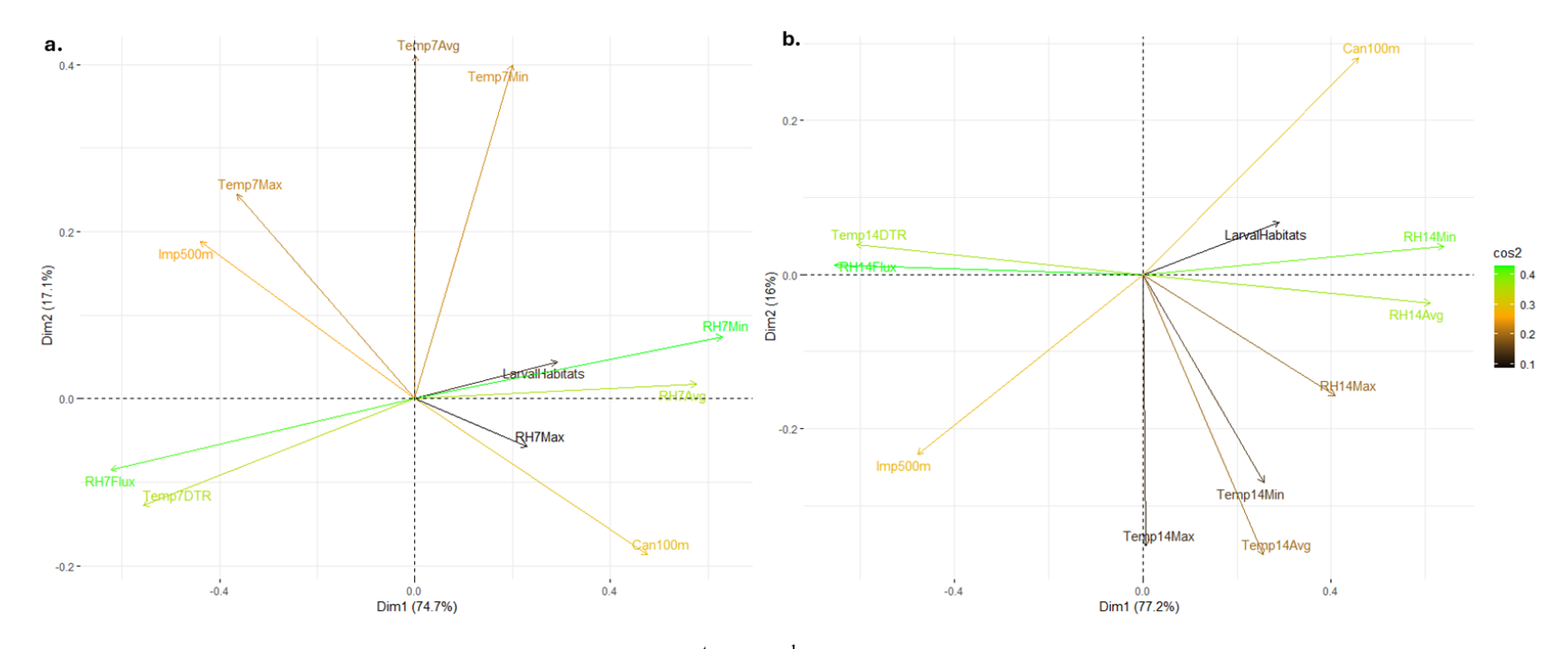


**Figure 3.4.** Principal Component Analysis for biplots of 1<sup>st</sup> and 2<sup>nd</sup> PC loadings. **(a)** 7-day lag variables and **(b)** 14-day lag variables. Quality of representation (cos2) values colored with the strongest predictors of variation in green, intermediate predictors (representing a 0.2 cos2 cutoff) in orange, and the weakest predictors in dark brown and black.

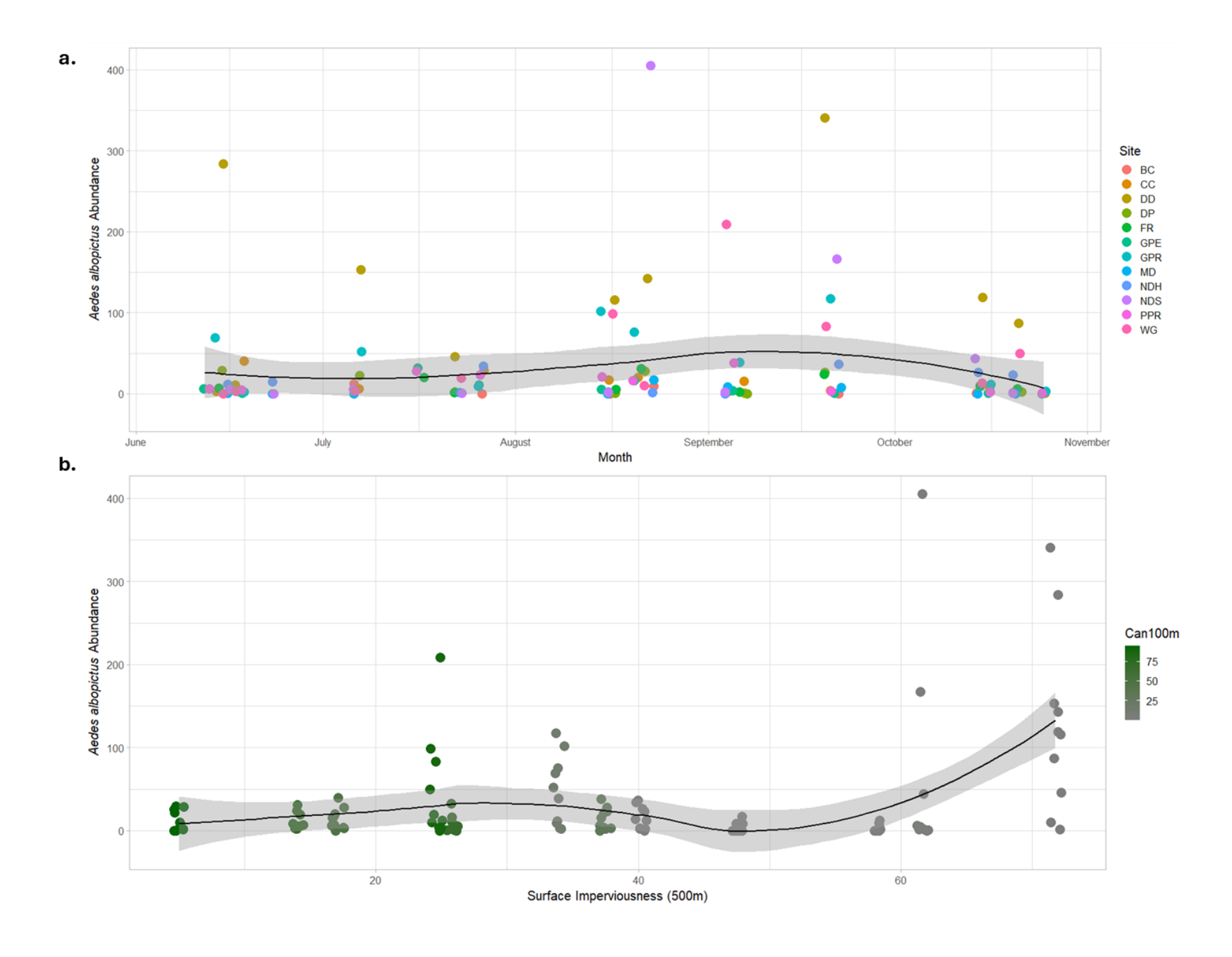


**Figure 3.5.** Adult *Ae. albopictus* abundances vs Month and Surface Imperviousness. **(a)** Adult *Ae. albopictus* abundances vs Month, **(b)** Adult *Ae. albopictus* abundances vs percent impervious surfaces at a 500m radius (Imp500). Timepoints are displayed according to Julian date and labelled by Month. Regression lines displayed with 95% confidence interval and fit with the "loess" method of localized regression in (a) and the "loess" method in (b) using the gglot2 R package.

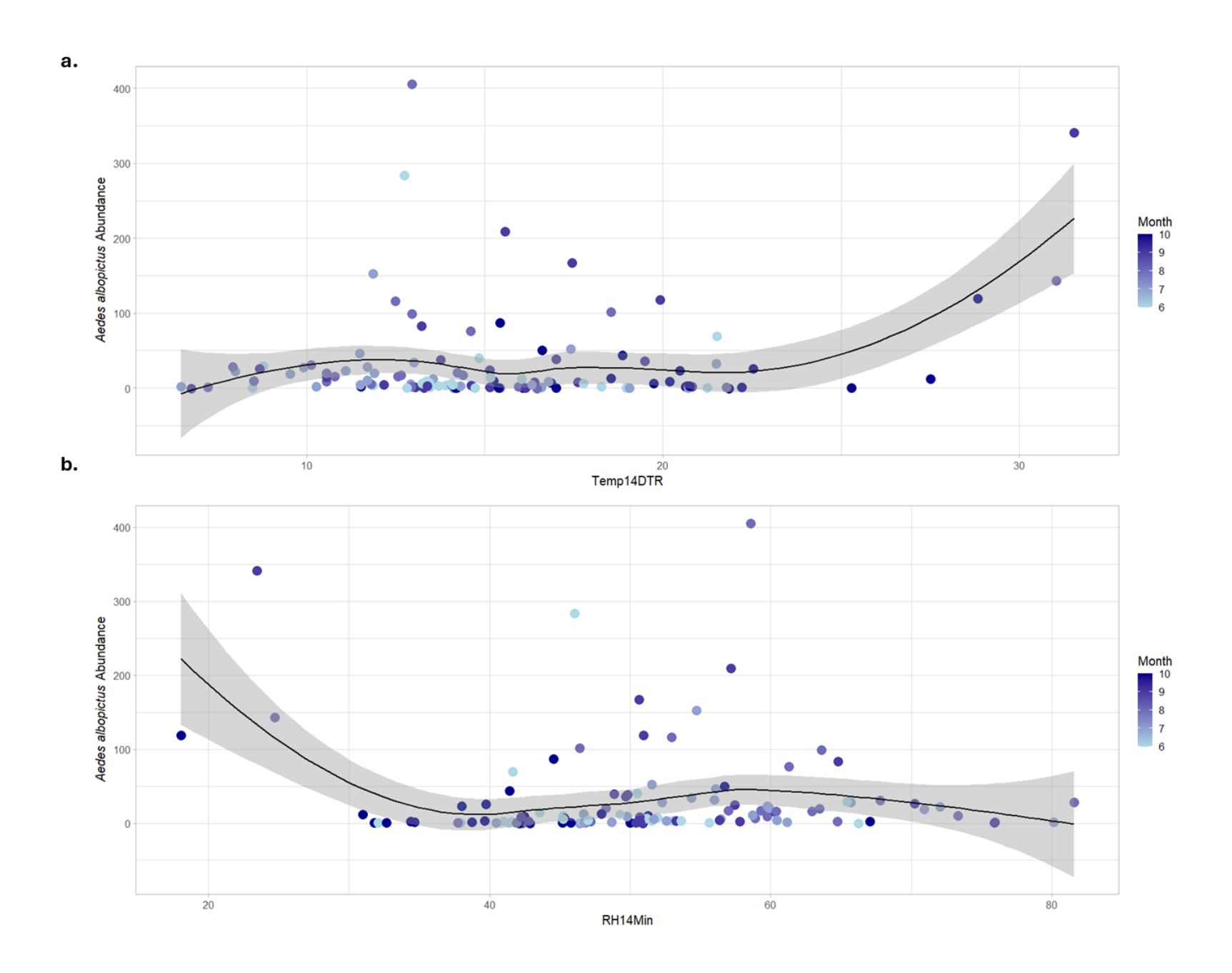


**Figure 3.6.** Adult *Ae. albopictus* abundances vs DTR and minimum RH. **(a)** Adult *Ae. albopictus* abundances vs DTR with a 14-day lag (Temp14DTR), and **(b)** Adult *Ae. albopictus* abundances vs minimum relative humidity with a 14-day lag (RH14Min). Timepoints are displayed according to Julian date and labelled by Month. Regression lines displayed with 95% confidence interval and fit with the "loess" method using the gglot2 R package.

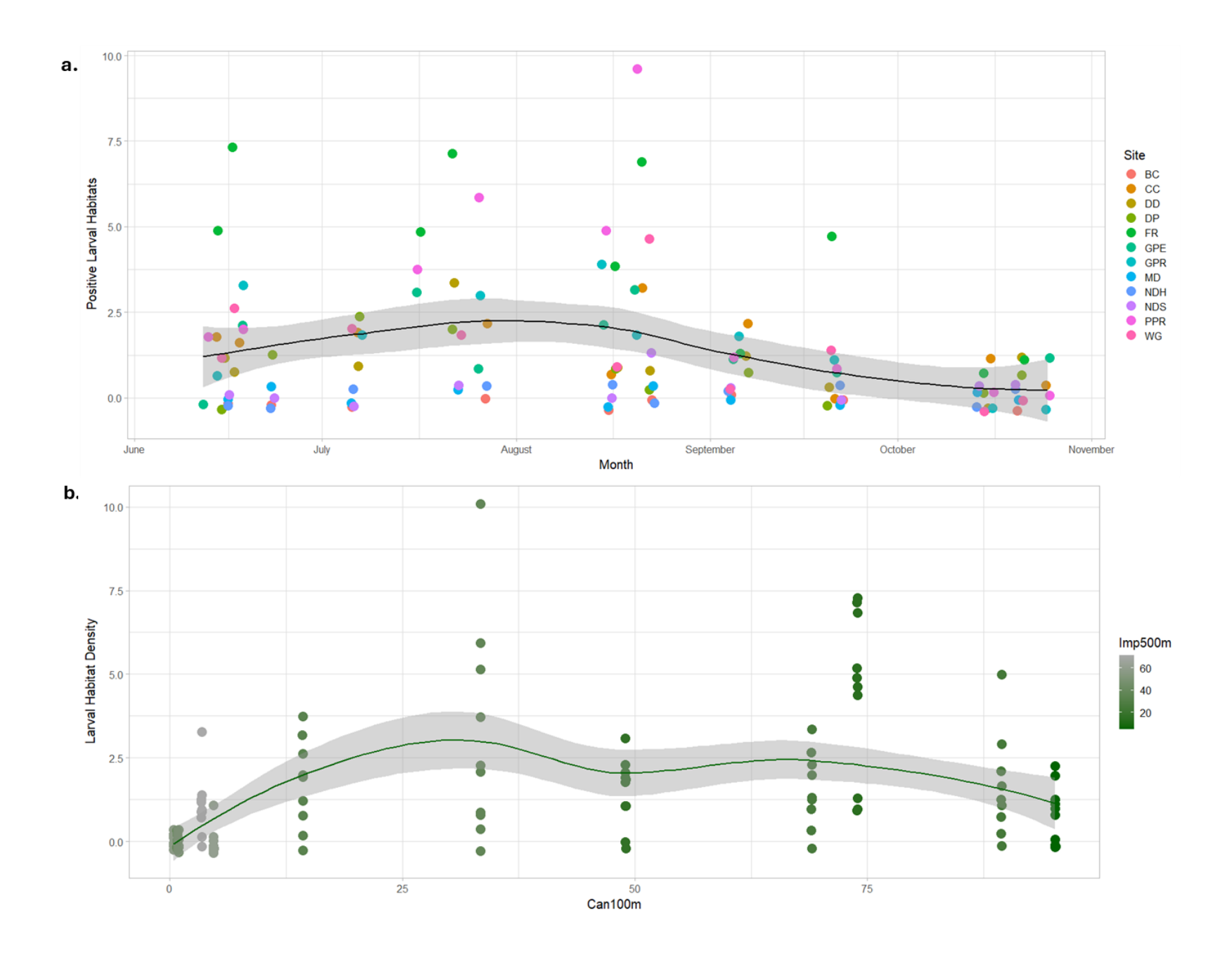


**Figure 3.7.** Larval habitat density vs Month and Canopy Cover. **(a)** Larval habitat density vs Month and **(b)** Larval habitat density vs canopy cover at a 100m radius (Can100m). Timepoints are displayed according to Julian date and labelled by Month. Regression lines displayed with 95% confidence interval and fit with the "loess" method of localized regression in (a) and the "lm" method in (b) using the gglot2 R package.

## **CHAPTER 4**

<sup>3</sup> Newberry PM, Dyer KA, Altizer SA, Murdock CC. To be submitted to *Parasites & Vectors*. Author contributions; PMN: conceptualization, investigation, software, visualization, writing – original draft preparation, writing – review and editing, project administration, formal analysis, data curation; KAD: conceptualization, methodology, writing – review and editing; SMA: conceptualization, writing – review and editing, supervision, resources, methodology, funding acquisition; CCM: conceptualization, writing – review and editing, supervision, resources, methodology, funding acquisition. All authors agree that their contributions can be included in this dissertation.

## **Abstract:**

Aedes albopictus is a long-established invasive mosquito in the Southeastern United States and is a competent vector for many arboviruses such as Dengue, Chikungunya, and Zika. Genetic studies regarding the population structure of this species across regions and within urban areas vary in the degrees and patterns of relatedness observed, and Ae. albopictus's reliance on human mediated dispersal is frequently implicated in shaping patterns of dispersal. This study uses a recently developed SNP microarray to observe population structure and patterns of gene flow in Ae. albopictus specimens collected at 12 sites across an urban landscape in Atlanta, GA. This study found significant but small F<sub>st</sub> values between subpopulations within the city as well as limited association clustering by study site, surface imperviousness, or canopy cover. While isolation by distance was not significant, there was still a positive correlation between genetic and geographic distance. Ancestry analysis suggests that the study specimens likely all derived from a single ancestral population and that multiple subsequent local admixture events occurred. This study shows a high degree of relatedness and gene flow in the Ae. albopictus populations in the city, and this panmictic population dynamic shows the suitability in this urban environment for vector control efforts relying on the dispersal of adult Ae. albopictus.

## Introduction

Aedes albopictus, or the Asian Tiger Mosquito, is a an aggressively invasive and anthropophilic species that serves as a vector for many medically significant arboviruses, including Dengue, Chikungunya, Zika, Japanese Encephalitis, and Yellow Fever. The expansion of this species from its original range in Asia makes understanding the history of invasion, patterns of population connectivity, and variation in population characteristics important avenues of investigation when developing vector control measures. Genotyping of Ae. albopictus

populations likewise reflect this ecological history of rapid expansion, with admixture events showing both repeat and continuing long distance introductions of the species (Kamgang et al. 2011, Schmidt et al. 2020, Lucati et al. 2022, Cosme et al. 2024). These invasion histories are constructed from genetic comparisons of populations, and they can indicate whether new introductions are happening, identify barriers or factors that facilitate invasion of new territories, and highlight vulnerable transportation centers (Zhong et al. 2013, Beebe et al. 2013, Kamgang et al. 2013, Schmidt et al. 2017).

Understanding the population structure of disease vectors is key to elucidating the projected patterns of vector-borne disease (VBD) along corridors of population connectivity and also to revealing the ecological history of this disease system. In the case of *Ae. albopictus* in the greater Atlanta region, the population has been present since the early 1990's, and it remains to be seen if this is the same long-established population or one admixed with or replaced by repeated introductions from key ground transportation routes or global air travel through the Hartsfield-Jackson Atlanta International airport. The prevalence of interstate highways could predict isolation of populations due to creating impassible areas locally while also facilitating long range dispersal into or out of the city (Moore and Mitchell 1997). Additionally, rapid global transportation and shipping may allow repeat invasions of *Ae. albopictus* (Boukraa et al. 2013, Willoughby et al. 2024). This vector globally and historically is most notorious for its rapid global maritime dispersal via used tires and bamboo exports from East Asia, and shipping ports are likely continuing important sources of introduction (Reiter 1998, Garcia-Rejon et al. 2021, Swan et al. 2022).

Identifying population structure at spatial scales relevant for mosquito population biology and control would reveal barriers to movement and facilitators to diuspersal. The often better

described cousin to Ae. albopictus regarding movement ranges, Aedes aegypti, is often limited in individual dispersal range while also showing adaptations to human-mediated dispersal corridors or urban centers (Huber et al. 2004, Costa-da-Silva et al. 2005, Hemme et al. 2010, Vadivalagan et al. 2016, Joyce et al. 2018, Hopperstad et al. 2019). Long distance dispersal of Ae. albopictus specifically has directly been observed via car transportation of adults as suggested by evidence of increased gene flow between population centers and in simulations of Ae. albopictus dispersal networks (Vazeille et al. 2001, Medley et al. 2015, Eritja et al. 2017, Lucati et al. 2022, Yeo et al. 2023). Parsing out the connectivity and movement among mosquito vector populations is crucial for 1) anticipating the rate of spread of insecticide resistance alleles, and 2) planning vector control measures, especially in the case of emerging vector control technologies (e.g., SIT, Wolbachia infection, genetically modification) that rely on gene-drive technologies and mosquito movement to deliver these control measures to suppress or replace mosquito populations (Lees et al. 2015, Oliva et al. 2021, Wang et al. 2022). While targeting central source populations may be ideal for spreading an intervention through a population, identifying genetically isolated sites may also be desired to better measure effectiveness of a SIT strategy in testing phases; this strategy also limits any dilution of the demographic effects of a new control measure due to outside migration of unreachable vector populations (Olanratmanee et al. 2013, Iyaloo et al. 2014, Gouagna et al. 2020). In this way, identifying genetically isolated vector populations would also be useful.

Studies of *Ae. albopictus* populations using microsatellite markers and mitochondrial haplotypes have shown limited genetic diversity and mostly non-significant fixation index values (F<sub>st</sub>) values (Beebe et al. 2013, Goubert et al. 2016, Md. Naim et al. 2020), while some other studies do indicate significant F<sub>st</sub> values and isolation by distance (Paupy et al. 2001, Kamgang

et al. 2011, Multini et al. 2019, Wei et al. 2019). The spatial distances in previous studies of *Ae. albopictus* genetic structure range from subpopulations within hundreds of meters on an island (Md. Naim et al. 2020) to hundreds of kilometers across oceans and over international borders (Kamgang et al. 2011, Wei et al. 2019). However, even distant sties separated by water bodies impassable to individual mosquitoes can have genetically similar *Ae. albopictus* populations due to the species' invasive capacity via international shipping (Beebe et al. 2013). Advances in next generation sequencing has enabled characterizing polymorphisms at a greater number of marker sites (Dritsou et al. 2015, Chen et al. 2015), and improving reference genomes of *Ae. albopictus* are allowing the measurement of population differences with more precision and at more marker sites than the traditionally lower cost microsatellite analysis (Chen et al. 2015, Miller et al. 2018, Palatini et al. 2020, Zimmerman et al. 2020, Cosme et al. 2024). These next-generation techniques have been increasingly used to identify gene flow across urban areas and major transportation routes, producing well informed descriptions of *Ae. albopictus* subpopulations in human environments (Schmidt et al. 2017, Wei et al. 2022).

The population structure of *Ae. albopictus* within human impacted landscapes appears to be affected by the potentially opposing forces of repeat introductions of different subpopulations from afar and the homogenizing effects gene flow via the natural dispersal of ovipositing females occurring at much shorter distances of typically less than a few hundred meters in both *Ae. albopictus* and *Ae. aegypti* (Harrington et al. 2005, Bellini et al. 2010, Marini et al. 2010). These countervailing effects could result in some neighboring populations being less related due to new migrations through human mediated introductions while other proximal populations show a high degree interbreeding via natural dispersal (Ismail et al. 2015, Md. Naim et al. 2020). The extension of the importance of human mediated migration is that geographically distant

populations of *Ae. albopictus* may be closely related, resulting in counterintuitive genetic differentiation patterns of a city exhibiting more genetically distant subpopulations within it than with subpopulations outside the city (Oliveira et al. 2003, Sherpa et al. 2018). Given the dynamic nature of the Atlanta metro area with frequent travel and shipping, either a pattern of homogeneity or genetic differentiation may be expected given the likely presence of both natural dispersal and human mediated spread within a long-established vector population. The relative importance of either mechanism of population spread is ecologically informative.

This study of populations of *Ae. albopictus* in Atlanta makes use of a recently developed SNP microarray developed for *Ae. albopictus* by the authors of Cosme et. al. 2024 to investigate the population structure of *Ae. albopictus* across an urban landscape (Cosme et al. 2024). This approach will grow the current body of knowledge of factors influencing *Ae. albopictus* population structure by exploring many more polymorphism sites than traditional microsatellite methods and with potentially more accuracy than other next generation methods as demonstrated in Cosme et. al. 2024. With this new technique, we will have the capacity to identify patterns of gene flow with greater resolution and statistical power. The anthropophilic nature of this species and its exploitation of human-mediated dispersal will help explain what features of the urban environment impede or facilitate gene flow at spatial scales relevant for control, providing useful insights for control efforts and public health in the city of Atlanta.

## Methods

Study Design:

To examine the effects of spatial variation in land cover on the population structure of urban *Ae. albopictus*, 12 study sites were selected randomly across Atlanta, GA to reflect relevant variation in impervious surface and percent canopy cover (Figure 4.1). We used a

spatially gridded map with 10m impervious surface and vegetation cover resolution taken from the National Land Cover Database 2016 dataset. ArcGIS ArcMap 10.7.1 published by ESRI was used to calculate land cover percentage. Previous research from nearby Athens, GA indicated the significance of impervious surface and vegetation coverage at ranges up to 1000 meters on Ae. albopictus populations, so site impervious surface coverage averaged at a distance a radius of 500 meters as a compromise distance to allow for landscape heterogeneity to still be observed (Wimberly et al. 2020). Each point was the center of a study site and the surface imperviousness percent coverage within a 500-meter radius was chosen as the distinguishing metric for site selection. An initial set of potential sites covering the range of impervious surface values were initially chosen across the gridded area, whereupon final site selection was informed by accessibility, ability to gain site permissions in the case municipal land and private parks, and the requirement to keep sites were independent of each other (minimum distance between sites was 1670 m). Each of these were delineated by 100-meter radius from a central point in accordance with previous studies showing most female Ae. albopictus dispersal occurs within that range (Figure 4.1)(Bellini et al. 2010, Marini et al. 2010). See Table 4.1 for the full list of survey sites, site codes, coordinates, and associated land cover measures. Bounds of the entire study area were approximately 15x15 kilometers, covering predominantly the eastern half of metro Atlanta across varying levels of urban development from paved commercial centers and parking lots to forested parks and suburban neighborhoods.

## Sampling design:

Ae. albopictus specimens were selected from August 2022 as part of a wider survey of Ae. albopictus from 2021 to 2022. A single timepoint was chosen to remove any effects of temporal variation between the populations and individuals genotyped. The month of August

was chosen because Ae. albopictus populations are generally peaking during the late summer in this environment, allowing for the maximum number of sites that could provide the goal of at least 8 individuals for sequencing. Both adults and larvae were sampled across our sites. Adult Ae. albopictus were sampled using BG-2 Sentinel Traps set for a 24-hour period near the center of each study site, and each trap was baited with BG-Lures from Biogen and 1000g of dry ice in an opened insulated container (Cello brand, 900 mL capacity model: 1000g dry ice broken up occupied approximately 2/3 of bottle at a volume of 641 cubic cm) as described previously (Evans et al. 2019). At collection, adults in a catch bag were transferred to a sealed plastic bag and immediately placed in a cooler with dry ice, moved to the lab, and placed in -25°C storage. Ae. albopictus larvae were collected from any pools of standing water present at each site. Collected larvae were brought back to the laboratory and maintained in a 50 mL falcon tube in their original habitat water with 5 mg of finely ground Tetrafin brand flake fish food. Larvae tubes were then housed in a Percival incubator (36-VL, Percival Scientific) at a 28.0°C (+0.1°C), 80% (+5%) relative humidity with a 14:10 hour day:night diurnal cycle, and sampled larvae were allowed to develop and emerge as adults for species identification and sexing. A subset of all captured adults for a site were selected for downstream genotyping, while only one larvae per aquatic habitat was selected to reduce the likelihood of genotyping siblings from a single oviposition site in accordance with best practices in other studies (Delatte et al. 2013). DNA Extraction and SNP Chip Methods:

DNA extraction was performed with the DNEasy (Qiagen) kit following methodology adapted from the manufacturer's directions using Dr. Andrea Gloria-Soria (CT-Yale Agricultural Extension) protocols (see Appendix B: Supplementary Information "DNA Extraction Checklist for *Aedes albopictus*" and informed by Cosme 2024 (Cosme et al. 2024)). Key details include

each mosquito being broken down with a sterile microcentrifuge tube pestle attached to an electric homogenizer. Proteinase K incubation was in a hot water bath at 56°C for 2 hours, and 4 uL of RNAse A was used. TE solution with low EDTA (0.1 mM) was used for the final DNA elution. Following DNA extraction, samples with a DNA concentration below 10 ng/uL were concentrated using an Amicon Ultra 0.5 mL -30k centrifugal unit. All samples were then normalized to 10 ng/uL and confirmed via Qubit fluorometer using the dsDNA HS Assay Kit (Invitrogen). 20 uL of each of the 95x sample solutions was then pipetted into a Beckman Coulter deep well plate (96x well), leaving the last well empty for the Axiom control reference. The samples were then sent to the UNC Genomics Core to be genotyped using the "Aealbo" SNP Axiom Plate genotyping array developed by the team in Cosme et. al. (2024) and manufactured by Affymetrix (Cosme et al. 2024). The SNP chip contains probes for 175,396 polymorphic sites covering all three Ae. albopictus chromosomes, and genotype calls were made using library files developed by Affymetrix for use with the Axiom Analysis Suite 5.4.0.23 software. The resulting SNP data set was exported from Axiom Analysis Suite in .ped and .map file formats readable by the open-source genetic analysis software PLINK 1.7. The data were further converted into binary .bed format as well as associated .bim and .fam files. Further genetic analysis was performed using PLINK 1.7 and RStudio 24.09.0 with R version 4.3.2. *Selection of Single Nucleotide Polymorphisms:* 

The dataset of 113,841 SNPs exported from Axiom Analysis Suite as "Best and Recommended" was checked for individuals missing more than 10% of SNPs and for SNPs missing in more than 10% of the population. All 95 individual mosquito specimens passed. A minor allele frequency significance cutoff of p=0.1 was then used to removed 19,867 SNPs, and filtering for SNPs out of Hardy-Weinberg Equilibrium with the significance cutoff of p<0.1

0.000001 removed an additional 5,975 SNPs. The remaining 87,999 SNPs were then screened for linkage disequilibrium (LD), selecting only for SNPs with the r2 association statistic below 0.1 to ensure independent assortment between retained markers. The LD screen window was 5KB with a moving window of 1 SNP. The r2 < 0.1 value selection was informed by the findings of Cosme et.al. 2024 comparing r2 values of 0.1 and 0.01. The cutoff of 0.1 balances the need for maximum retention of any population structure signal while still removing the most correlated polymorphic markers; the suspected homogeneity between specimens at such fine spatial scales weighs more towards the need for retaining as many markers as possible for what are likely closely related specimens. The retained pruned selection of SNPs after the LD filter contained 40,441 SNPs, which were then screened for siblings with the kinship coefficient or relatedness set to 0.5 (corresponding to parent-offspring and sibling levels of relation). Specimens were then screened for being heterozygosity outliers (falling > 4sd from the mean heterozygosity). The specimen FR5 was flagged as > 4sd below average heterozygosity and was removed from  $F_{st}$  analysis as an excessively homozygous outlier.

To select SNPs as close to neutral as feasibly possible for population structure analysis, the OutFLANK package developed by Whitlock and Lotterhos (2015) was used to was used to infer neutral F<sub>st</sub> SNP markers and remove outlier markers that may be under selection (Whitlock and Lotterhos 2015). This step removed a further 2,808 SNPs as F<sub>st</sub> outliers, leaving a neutral set of 37,633 SNPs for population structure analysis. See Figure 4.2 "SNP Filtering Workflow" for a graphical representation of the SNP marker filtering used in this investigation.

## Population Genetic Analyses:

Principal component analysis was used to identify any potential genetically distinct subpopulations either within or between sites across the study area. PLINK was used to generate

a 94x94 distance matrix of the remaining specimens using the filtered 37,634 SNPs as input. A principal component analysis (PCA) of this data set was performed using the cmdscale() function from the R package "stats" version 4.3.2 to generate the first 5x principal components from the distance matrix. Cluster plots were generated with the first 2 principal components, accounting for 4.85% and 3.24% of the variance in the dataset, respectively. Individual mosquito specimens identified alternatively by site, impervious surface, canopy cover, and geographic region in the city to visually check for subpopulation clustering. Sites were binned by landscape characteristics, with impervious surfaces classified as low (5-25%), medium (25-45%), and high (45-72%). Canopy cover was likewise binned with Low (0-5%), Medium (5-50%), and High (50-96%).

Population structure was investigated through generating fixation index (F<sub>st</sub>) scores for each study site out of the total study area. F<sub>st</sub> describe the amount of genetic variation within a subpopulation out of the total population. Similarly, the inbreeding coefficient (F<sub>is</sub>) describes the amount of genetic variation in a subpopulation that is present within an individual. F<sub>st</sub> is often employed to make pairwise comparisons between two populations, while F<sub>is</sub> best describes the degree of inbreeding at site. In both cases, lower values indicate less genetic differentiation with the scales varying by species and the markers chosen. The fixation index F<sub>st</sub> between each site was found using the R package "StAMPP" version 1.6.3. The SNP dataset was converted into a genlight object using stamppConvert(), and the pairwise F<sub>st</sub> values were calculated using the function stamppFst() with a 95% confidence interval and 1000x bootstraps to allow for significance testing. Mean pairwise F<sub>st</sub> values for each site were calculated to characterize the overall degree of genetic differentiation at each site. For comparing average site F<sub>st</sub> values, the site NDH was excluded as a family due to only having 2x samples compared to the 8-9x samples

in each of the other populations. The average pairwise Fst values comparing each site were then averaged for each land cover class (impervious surface and canopy cover) to identify potential trends of the degree of population differentiation according to landscape.

F<sub>st</sub> values were also calculated treating the sites as belonging to geographic regions in the study area: North (containing sites BC and NDH), South (containing sites GPR and GPE), East (containing site MD), West (containing sites PPR and CC), and Center (containing sites WG, DD, FR, DP, and NDS). In the case of generating subpopulation fixation indices using land cover bins or geographic regions, samples from NDH were included as they were instead treated as members of a larger subpopulation, reducing potential errors in the F<sub>st</sub> characterizations from a low specimen count. Regions inside the study area were determined such that all sites in a particular region were within 2.25 km of each other (with the exception of NDS in the center region, where NDS was assigned the Center region due to its greater proximity to the Center than the other regions; see Figure 4.1). F<sub>IS</sub> coefficients of inbreeding were calculated for each individual within each site, and the F<sub>is</sub> values of the individual mosquitoes were then averaged for each study site.

Isolation by distance was tested for using the Mantel test to see if the spatial distance between the subpopulations significantly correlated with the genetic distance. The dataset was converted into the genlight format using R package "adegenet" version 2.1.10. After importing the latitude and longitude coordinates for each site matched to each sampled mosquito, the R package "dartR" version 2.9.7 was used to calculate isolation by distance using the gl.ibd() function. This function was used to perform a Mantel Test incorporating the F<sub>st</sub> values from the genlight object and geographic distances of the site coordinates Mercator projected into meters and using 999 permutations.

Reconstructing potential ancestral histories of the Atlanta Ae. albopictus was done to investigate if multiple invasion events occurred, to map out the possible order of colonization at the study sites, and to see if there was evidence for discrete admixture events between subpopulations. Potential numbers of ancestral populations of Aedes albopictus were assessed using the R package "LEA" version 3.19.1 through sparse non-negative matrix factorization algorithms via the snmf() function and the genotype data inputted in .geno format. This process simulates different hypothetical ancestral populations (k) and the corresponding average cross entropy values to determine the most likely number of ancestral populations (value of k with the lowest cross entropy). The R package ADMIXTOOLS 2 version 2.04 described in Maier et. al. 2023 was used to calculate f-statistics for the genotyped mosquitoes and to simulate different potential admixture events by minimizing associated f-statistic residuals(Maier et al. 2023). The f-statistics utilized by this program describe systematic comparisons of alternate pairings of subpopulations and the resulting allele similarity to build likely sequences of population migrations and admixture events (Lipson 2020). Potential admixture graphs were simulated with an estimated 300 generations corresponding to the approximately 30 years since the introduction of Aedes albopictus to Atlanta, GA and assuming 10 generations per year. Several admixture graphs were simulated with different numbers of admixture events. The admixture graphs with the best correlation to the observed allele frequencies between the populations were selected as possible representations of a true admixture history of Ae. albopictus populations dispersing through different sites across Atlanta.

## **Results**

From the PCA on the pruned SNP dataset, the first, second, and third principal components captured 3.49%, 2.81%, and 2.66% of the genetic variation, respectively. While

these PC loading values were low compared to other methodologies, they are similar to a study using the same SNP microarray (Cosme et al. 2024). Using the first and second principal component (PC) loadings, there was little distinct clustering in the 95 *Ae. albopictus* specimens (Figure 4.3). However, there does appear to be some limited association of some specimens sharing the same site or landcover. This potential association between individuals by site or landcover characteristics occurred with a high degree of overlap, suggesting some limited and weak associations. Site MD (Figure 4.3.a) did show a degree of clustering, but other sites also occupied the same area on the ordination plot suggesting the genetic profile of site MD was widespread, but other genotypes at other sites were not. This effect was weak, however, with no strongly evident clusters of genotypic characterizations.

Dividing the sites into geographic regions, the East region appears as a cluster that also overlaps with the Center, North, and West regions (Figure 4.3.b). When classifying sites by canopy cover (Figure 4.3.c), there was no clustering observed. However, when classifying specimens by the imperviousness of their respective sites (Figure 4.3.d), high imperviousness sites occupied a tighter portion of the plot although with extensive overlap with specimens from low and medium impervious sites. Observing the first and third PCs, there are two weak potential clusters evident (Figure 4.4). When classifying specimens by site (Figure 4.4.a), site MD specimens clustered together while also overlapping with sites DD and BC. Looking at specimens classified by the geographic region of their sites, the East region specimens all clustered on the rightmost plot also with a lot of overlap. Similar to the first and second PC plots, the first and third loading plots showed no clustering according to the canopy cover of the sites (Figure 4.4.c). The specimens associated with high imperviousness predominantly plotted on the right cluster (Figure 4.4.d), but also with the same overlap seen before. The lack of tight

clustering and the presence of overlap in potential clusters shows very little genetic differentiation using PC1 vs PC2 and PC1 vs PC3.

The pairwise F<sub>st</sub> values between the study sites were low, ranging from -0.003 to 0.019 (Figure 4.5.a). The negative F<sub>st</sub> values between sites WG:BC and WG:CC were -0.003 and -0.001, respectively. These values were interpreted as zeroes, with no meaningful genetic variation between the populations. The highest F<sub>st</sub> value of 0.019 between sites MD:DP is in the general range of very low subpopulation fixation indices, indicating very little genetic distance between these populations. Averaging the pairwise F<sub>st</sub> values for each study site yielded similar values, ranging from 0.0023 for WG to 0.012 for MD (Figure 4.5.b). Even though the pairwise F<sub>st</sub> values between sites were low, most sites were found to be significantly different from each other using 1000 bootstraps to generate significance results. All sites were significantly genetically distinct in pairwise comparisons except for site WG versus BC, CC, and PPR.

Averaging the  $F_{st}$  values according to impervious Surface Cover and Canopy Cover also provided low  $F_{st}$  values (Table 4.2). Average  $F_{st}$  values by Impervious Surface Cover were 0.0083, 0.0074, and 0.0076 for Low, Medium, and High, and average  $F_{st}$  values by Canopy Cover were 0.0088, 0.0073, and 0.007 for Low, Medium, and High. The inbreeding coefficients  $F_{is}$  for the *Ae. albopictus* specimens within each study site yielded values between 0.21 and 0.01, excluding site NDH due to the low sample size of 2x mosquitoes resulting in elevated  $F_{is}$  values (0.52 and 0.53). The average  $F_{is}$  values by site likewise excluding NDH ranged from 0.063 to 0.092 (Figure 4.6). A single-factor ANOVA for the inbreeding coefficients of each mosquito did not show significant differences between the sites (p = 0.904).

Relatedness between individual mosquitoes at each site was investigated to determine any patterns of generational dispersal, but these familial connections were found to be limited.

This validated the decision to only sample 1x specimen from each larval habitat to prevent sampling siblings. At site MD, there were 2x mosquitoes that were 2<sup>nd</sup> order relations. At DP, CC, WG, and NDS, each site had 2x mosquitoes that were 3<sup>rd</sup> order relations. Due to the lifespan of *Ae. albopictus* in the wild rarely exceeding a month (Maimusa et al. 2016, Cui et al. 2021, Blanco-Sierra et al. 2023) and the egg/larval development times often around 5-15 days (Evans et al. 2018, Yang et al. 2020), 2<sup>nd</sup> order and 3<sup>rd</sup> order relations are not likely. However, some generational overlap is reasonable to expect in a system containing multiple generations not dispersing far and not necessarily reproducing synchronously. Sites FR, GPE, GPR, NDH, and BC did not show any 1<sup>st</sup> through 3<sup>rd</sup> order relations between the sampled mosquitoes.

Testing for the significance of isolation by distance with the Mantel Test did identify a positive correlation between genetic distance (measured as inter-site  $F_{st}$  values) and geographic distance (Euclidean) with a Mantel statistic of 0.3307. While the relationship was not significant (p = 0.068), given the large number of polymorphism tested in this methodology, the positive relationship between geographic and genetic distance is still meaningful (Figure 4.7). This positive relationship indicates that the urban environment does create some important barriers to geneflow for *Ae. albopictus*, even if population movement due to human activities are also likely characteristic of this system.

The *Ae. albopictus* ancestral population analysis for the study specimens showed that they all most likely derived from one ancestral population (k = 1), as measured by minimizing the cross-entropy measure of error. However, the cross-entropy values for two ancestral populations (k=2) were also low and show that 2 introductions could be possible, if less likely, than 1 introduction (Figure 4.8). The simulations for the number of admixture events between the sites after the initial colonization of the area with *Ae. albopictus* shows that at least 2 admixture

events likely occurred between the study populations after the initial colonization. The admixture chart shown in Figure 4.9 demonstrates one possible scenario for how movement of the mosquito populations may have occurred across the city. This one hypothetical model fits the SNP dataset the best when comparing F-statistic residuals between simulated admixture histories. Still, even when simulating other less well performing models of admixture, ADMIXTOOLS 2 consistently identified 2 admixture events as the likeliest scenario. Notably, the populations shown as descending from each other do not consistently correlate to geographic proximity. For instance, site MD is projected to be between FR and DD in genetic lineage even though MD is not physically between these two sites. This may be a result of human mediated population dispersal or other stochastic events. Other portions of this admixture history graph do map genetic descent according to geographic proximity, showing the continued importance of gradual and sequential dispersal.

## **Discussion**

While the specimens show a degree of positive association for some sites and land cover characteristics, these clusters were not distinct from other sites or site characteristics due to high degrees of overlap. This may be a result of near-panmictic conditions where related lineages can rapidly disperse across the study area. Additionally, given the dense human population density and similarly high degree of vehicle movement in the study area, human-mediated transportation likely plays a role in facilitating rapid gene flow. The stochastic nature of container habitats being deposited by human activity via discarded containers holding either *Ae. albopictus* larvae or eggs would likely have a homogenizing effect on genetic variation. The slow natural dispersal of ovipositing female mosquitoes probably still plays an important role considering the admixture simulations showing many sites being colonized by neighboring sites. The decades

since the initial colonization event in Atlanta further supports the effect of population dispersal, given the time populations have had to gradually spread. Natural dispersal of this nature would likely be represented by isolation by distance. The Mantel test did show a positive relationship between physical and genetic distance, albeit not significant, but these results are still informative. This may indicate that random human mediated movement of eggs or larvae has a nearly as important or even stronger effect on population dynamics than gradual dispersal.

The highest pairwise F<sub>st</sub> values for the sites did not quite reach 0.02 for the most genetically distant site comparison (MD:DP), with the other pairwise F<sub>st</sub> values between sites often much less. However, these low pairwise F<sub>st</sub> values are consistent with what was seen between Ae. albopictus populations from adjacent or nearby countries covering hundreds of kilometers, as seen in the Cosme et. al. 2024 study using the same SNP chip (Cosme et al. 2024). Given the much smaller spatial scale of this study across Atlanta, low F<sub>st</sub> values can be expected. Additionally, the high number of SNPs incorporated into the F<sub>st</sub> analysis likely lower the magnitude of the fixation indices relative to methods more prevalent in the literature such as microsatellite techniques. The meaningfulness of genetic variation between most sites is supported by the pairwise F<sub>st</sub> comparisons showing significant differences between all sites except for the pairwise comparisons with WG versus BC, CC, and PPR. Furthermore, studies of closely related Ae. albopictus populations with low F<sub>st</sub> values show significant differences after a similar significance determination in an island environment (Md. Naim et al. 2020). Such low F<sub>st</sub> values have also been seen to be significant regarding Ae. albopictus populations in China hundreds of kilometers apart on the Yangtze River, albeit not using genome wide SNPs to characterize population structure (Ma et al. 2023). Further, another study of Ae. albopictus population structure in Nanjing, China did find significant pairwise F<sub>st</sub> values between sites

characterized as urban, urban fringe, and rural but no significant isolation by distance (Zhang et al. 2022b), while similar studies in Chinese cities found no significant population structure between ports less than 200 km apart (Zhao et al. 2024). This lack of a consistent signal both in the literature and in this study between distance and population structure suggests a population dynamic shaped by two drivers: natural dispersal as measured by isolation-by-distance and human mediated dispersal reflected in non-proximal spread in reconstructed admixture histories. The upshot is that these mosquito populations depend greatly on the human-vector relationship in a particular environment; for instance, distant port cities may be closely related due to invasion dynamics, while nearby subpopulations may be less related due to the same stochastic dynamic of human aided colonization events.

The central location of the WG site may play a role in its less significant differentiation from other sites. Again, the close association of human activity with the successful dispersal of this anthropophilic species, human-mediated transportation is very likely a major force behind population mixing as well as dispersal of populations that may be closely related (Manni et al. 2017). The close geographic distances between the study sites in this investigation, however, also allow natural dispersal to also be a significant driver of genetic mixing between subpopulations. Additional analysis across months and years could potentially reveal relatedness and if offspring are moving between these sites as well as the time it takes for the dispersal. Very fine scale (10 km radius) surveys of population structure in the related species *Aedes aegypti* likewise identified significant population structure across both time and distance, with temporal structure suggesting outsized contributions of just a few key source populations producing seasonal waves of closely related adults (Olanratmanee et al. 2013). The difference here with the ecologically similar *Ae. albopictus* showing very little population structure within a city may have to do with

the recentness of its invasion of the region. While *Ae. aegypti* invaded many regions globally hundreds of years ago, many *Ae. albopictus* populations outside of Asia are only a few decades old. Some studies posit that repeated invasion events in a short period of time allow multiple distinct lineages of *Ae. albopictus* to persist and counter-balance genetic bottleneck effects (Maia et al. 2009, Eskildsen et al. 2018, Kamgang et al. 2018, Motoki et al. 2019), but other investigations show rapid human-mediated transportation having a homogenizing effect in some heavily urbanized areas (Zhang et al. 2022a). The case of Atlanta's *Ae. albopictus* populations seem to reflect the latter phenomenon of rapid colonization followed by likely human-mediated panmictic dispersal conditions, resulting in little population structure.

The average fixation indices in this study were lower than values found in other investigations of *Ae. albopictus* populations sampled from the northern edge of the species' expanding range in the United States (Gloria-Soria et al. 2022). This may be a result of different genotyping techniques, or perhaps the lower F<sub>st</sub> measures in Atlanta are a result of sequencing within a city population versus across multiple states. The number of ancestral populations, most likely only k=1, supports the scenario where a single invasion event occurred. The invasion event predicted in the admixture model was likely the seminal observation of *Ae. albopictus* spreading across all counties in the state of Georgia by 1994 (Womack et al. 1995).

The early invasion of *Ae. albopictus* followed interstate highway corridors (Moore and Mitchell 1997), showing that rapid human-mediated dispersal played an important early and likely continuing role in the establishment of this vector across the region. Another study comparing *Ae. albopictus* populations worldwide using a similarly large set of SNP markers identified multiple invasion events reflected in the admixture reconstructions of invasive populations (Kotsakiozi et al. 2017). The admixture simulations in our study show that, most

likely, two admixture events occurred between the *Ae. albopictus* subpopulations in the city. It shows largely unimpeded dispersal of individuals to new sites, as many sites most close in admixture genealogical and admixture history are adjacent geographically. However, as some of these hypothesized population admixtures occurred between sites non-adjacent to each other, human facilitated dispersal is also indicated.

#### **Conclusions**

The ecological history and the current genetic characterization of *Ae. albopictus* in Atlanta is important to understand as a model of invasion and establishment of a medically significant vector species. The high level of population movement and gene flow indicates that sterile insect technique, *Wolbachia* inoculation, or the release of genetically modified mosquitoes resistant to pathogens would require less population coverage than if significant population structure was present. However, insecticide resistance or other inheritable adaptations introduced to the population may also likewise spread quickly and impede control measures. This research provides valuable insight into the invasion ecology, dispersal dynamics, population structure, and vector control options regarding this invasive and damaging species.

## Acknowledgements

Thank you to Dr. Andrea Gloria-Soria for guidance in developing the DNA extraction and Affymetrix SNP-chip preparation methodology and to Dr. Margaret K. Corley for guidance in handling the SNP chip data and providing the library files used for Axiom Analysis Suites.

### **Funding**

This work was supported by the National Science Foundation [Graduate Research Fellowship # #1842396], the National Science Foundation Research Traineeship: Interdisciplinary Disease Ecology Across Scales [Grant no: 1545433], and the Cornell University Seed Grant.

# **Tables**

 Table 4.1. Survey sites, site codes, coordinates, and landscape characteristics.

Site Code	Site Name	Canopy Cover (100m)	Canopy Classification	Impervious Surface Cover (500m)	Imperviousness Classification	Latitude	Longitude
DP	Deepdene Park	95.2	high	5	low	33.77222	84.31966
FR	Fernbank Residential	73.9	high	14.1	low	33.78627	84.31875
CC	Callanwolde Center	49	med	17.1	low	33.78175	84.34579
WG	Woodlands Garden	89.4	high	24.6	low	33.78621	84.30366
GPE	Grant Park East	69	high	25.8	med	33.73627	84.35269
GPR	Grant Park Residential	14.3	med	34	med	33.72621	84.36847
PPR	Piedmont Park Residential	33.4	med	37.5	med	33.78156	84.36424
NDH	North Druid Hills	0.8	low	40.2	med	33.81758	84.3111
MD	Memorial Drive	0.9	low	47.6	high	33.77908	84.24073
BC	Briarcliff	0.4	low	58	high	33.8272	84.33205
NDS	North Decatur Station	4.7	low	61.7	high	33.79242	84.28486
DD	Decatur Downtown	3.4	low	71.8	high	33.77524	84.29651

**Table 4.2.** Fst values calculated by landscape characteristics: (a) canopy cover and (b) impervious surface cover across study sites.

Impervious Surface Cover	Mean F <sub>st</sub>		
Low (5-25%)	0.0083		
Med (25-45%)	0.0074		
High (45-72%)	0.0076		
Canopy Cover	Mean F <sub>st</sub>		
Low (0-5%)	0.0088		
Low (0-5%) Med (5-50%)	0.0088 0.0073		

# **Figures**

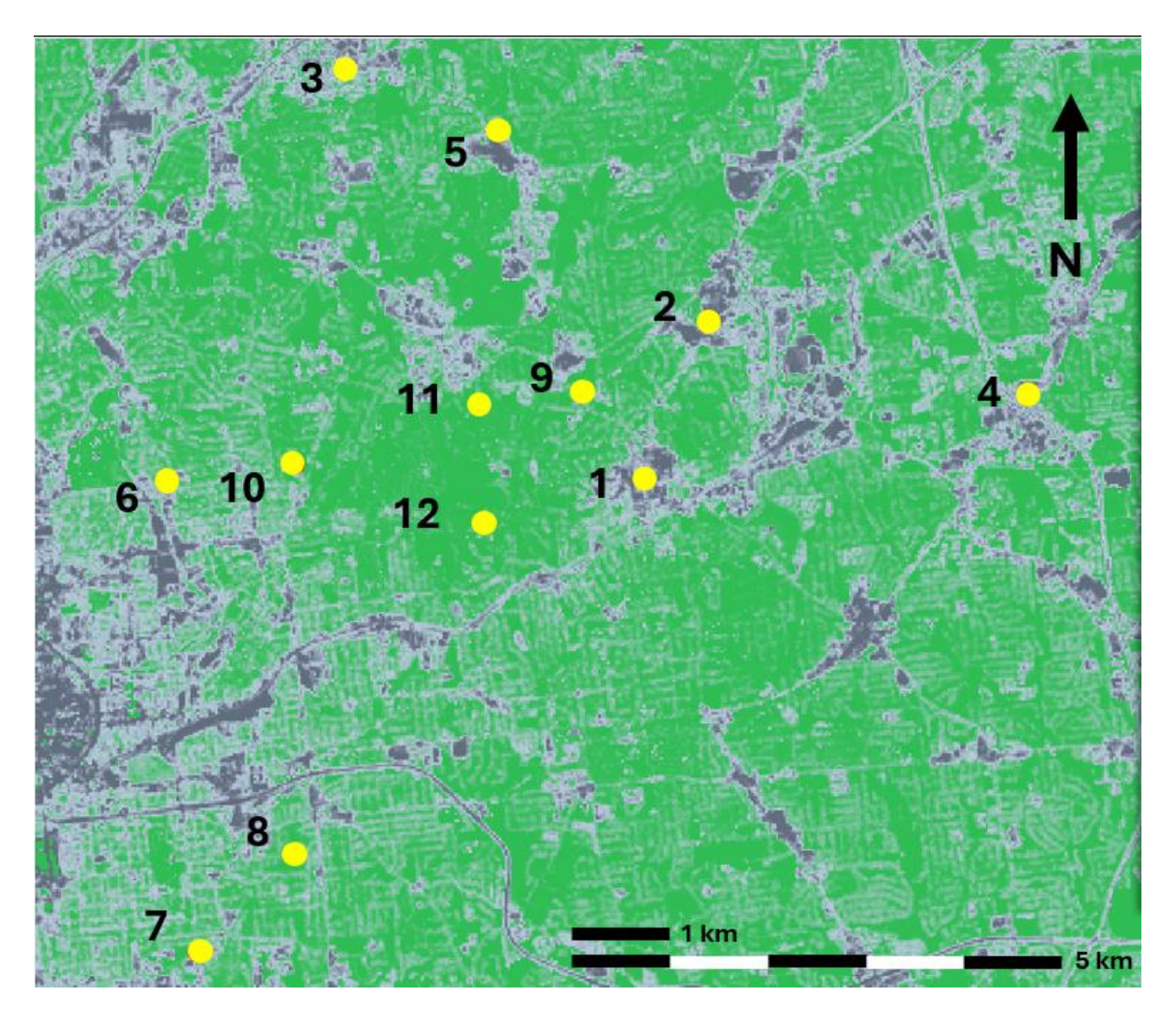


**Figure 4.1.** Survey Sites (x12) across Atlanta. GA: DP, FR, CC, WG, GPE, GPR, PPR, NDH, MD, BC, NDS, and DD. Distance scale and North indicated.

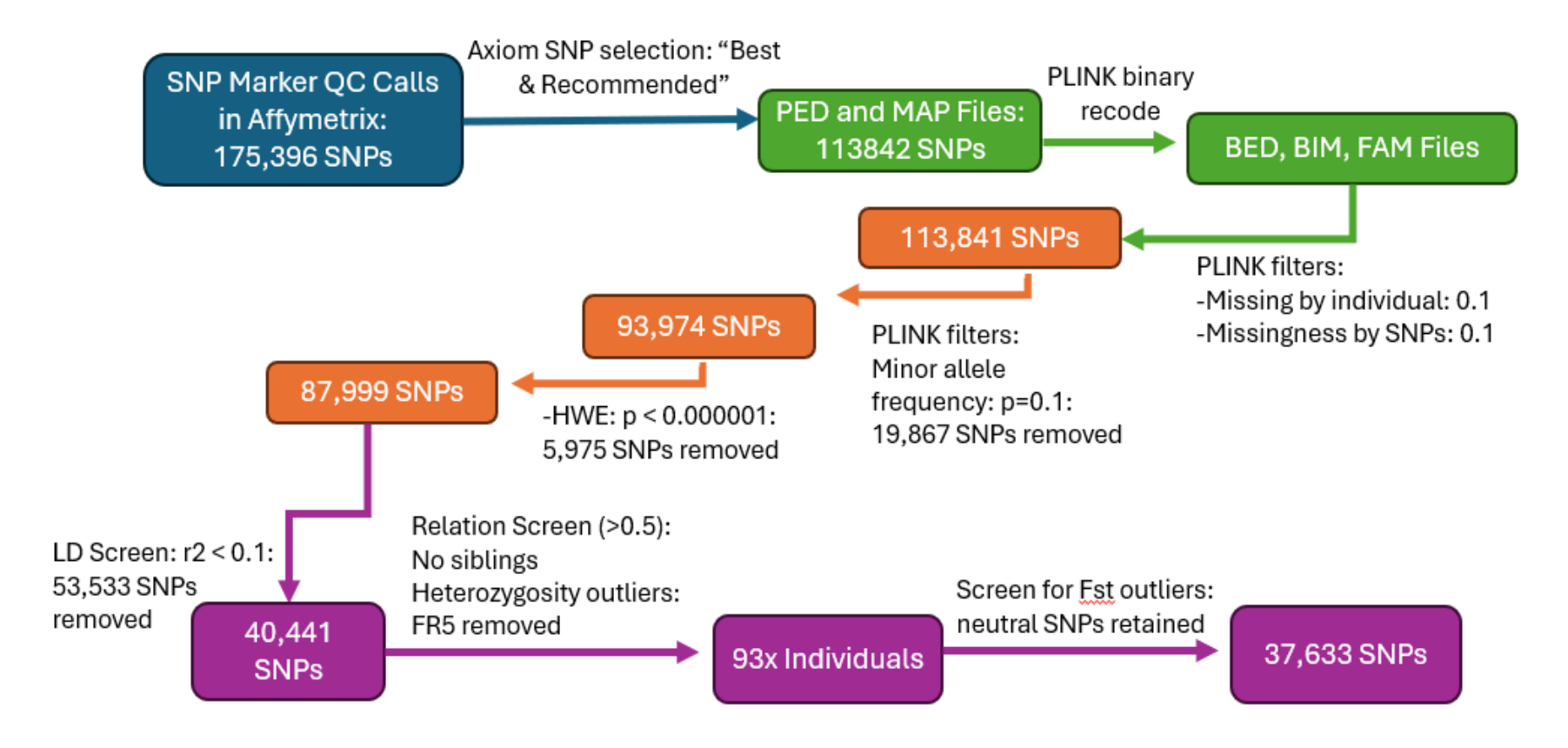


**Figure 4.2.** Genotyping array workflow for SNP markers. The workflow displayed represents the selection criteria and filters applied to the SNP dataset for the set of 95x *Aedes albopictus* specimens.

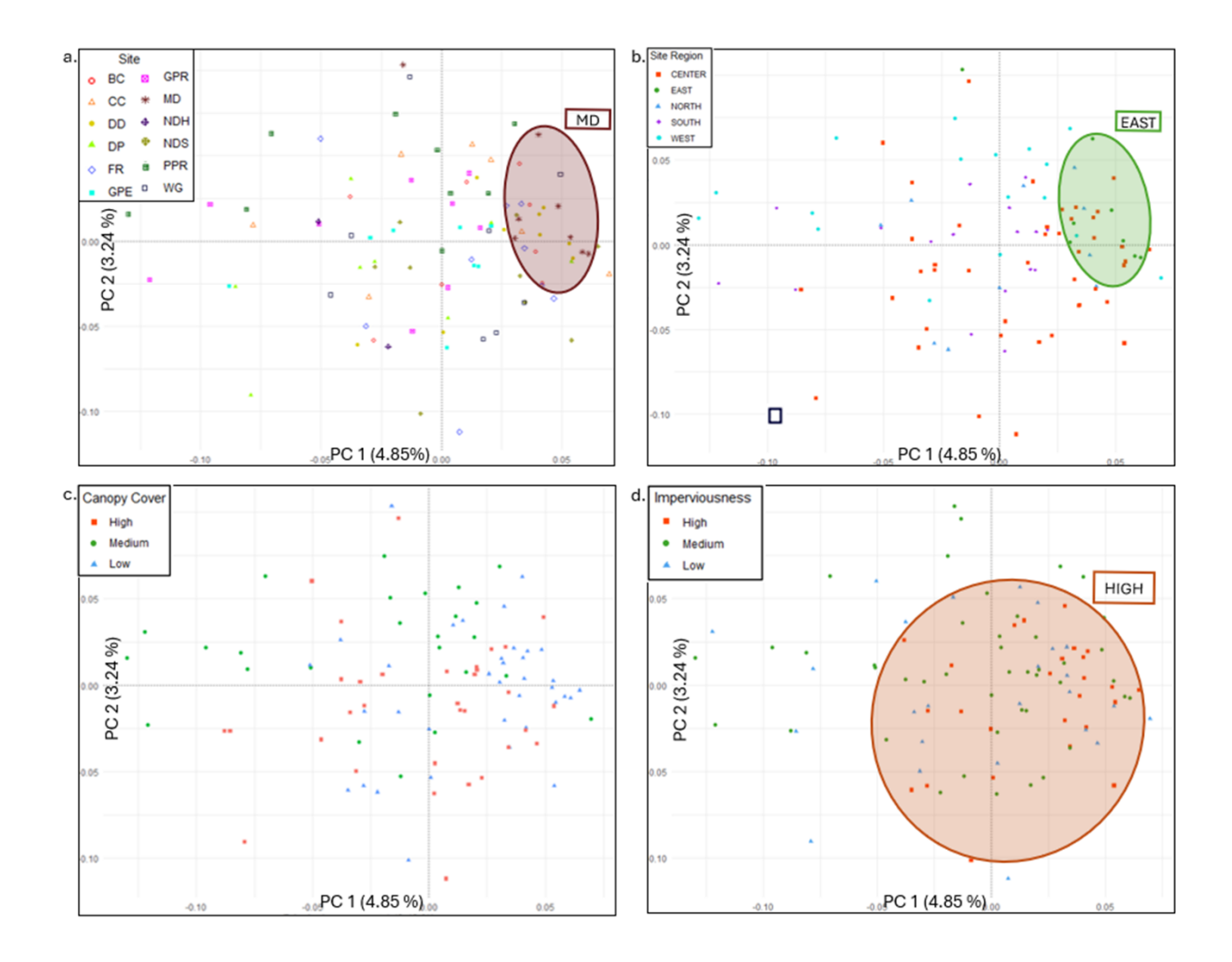
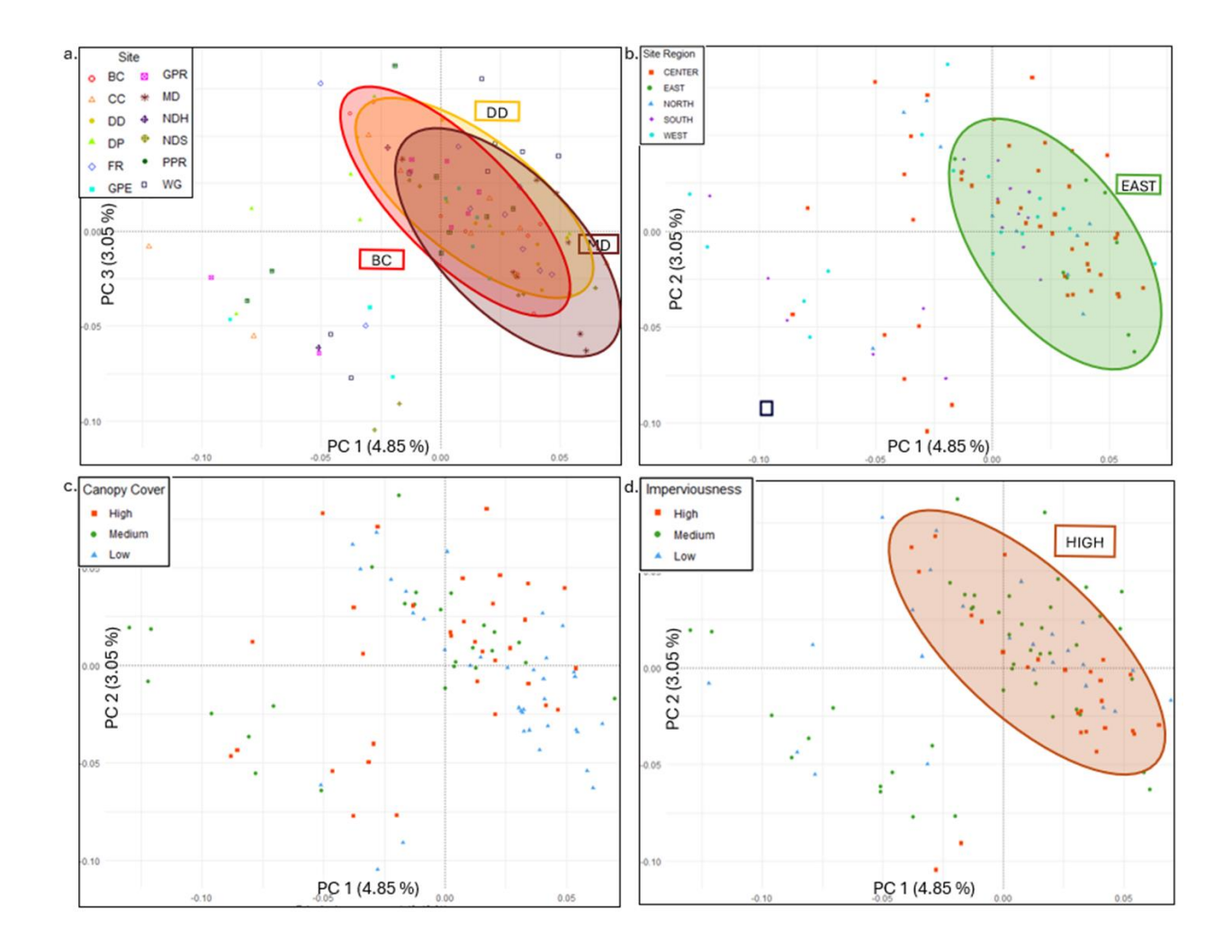
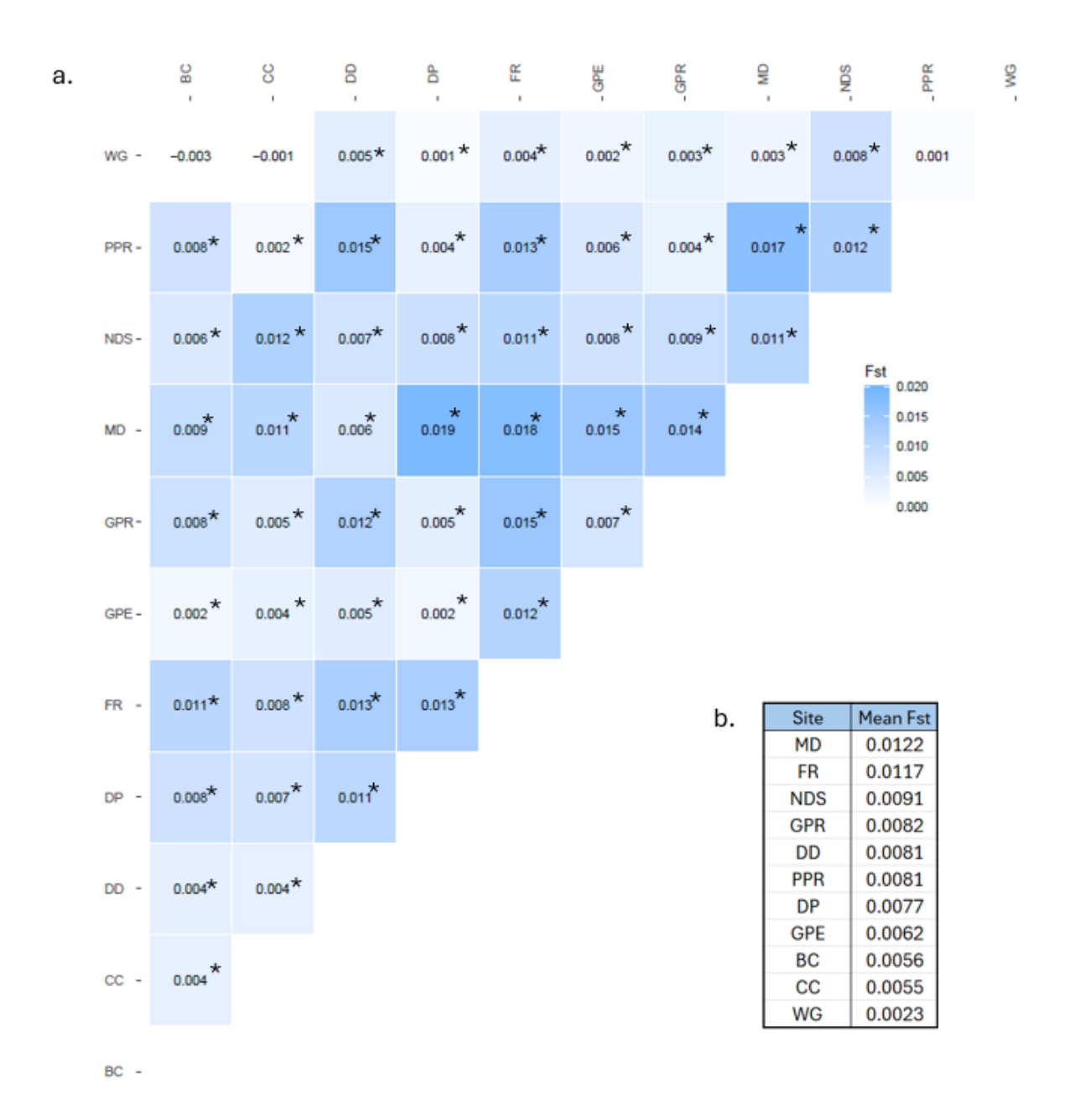


Figure 4.3. Principal components 1 and 2 loading plots for sampled mosquitoes color coded by (a) site, (b) geographic region, (c) canopy cover, and (d) impervious surface cover. Very clustering was evident with these loadings and for these variables (site, region, canopy cover, and imperviousness. a) The site MD cluster is marked with a maroon oval. (b) The East region cluster is designated with a green oval. (c) No distinct cluster was identified by canopy cover. (d) the High Imperviousness cluster is marked with an orange oval.



**Figure 4.4.** Principal components 1 and 3 loading plots for sampled mosquitoes color coded by (a) site, (b) geographic region, (c) canopy cover, and (d) impervious surface cover. These loadings produced very little distinct clustering, which also occurred with high overlap. (a) The cluster containing sites BC, DD and MD are marked red, gold, and maroon, respectively. (b) The East region cluster is designated with a green oval. (c) No distinct cluster was identified by canopy cover. (d) The High imperviousness cluster is marked with an orange oval. .



**Figure 4.5.** Pairwise  $F_{ST}$  values by site. Values represent  $F_{ST}$  values between study sites with 8-9x individual *Aedes albopictus* per site, with \* denoting significant variation (p = 0.05) measured by  $F_{st}$  between sites using results from n = 1000 bootstraps).

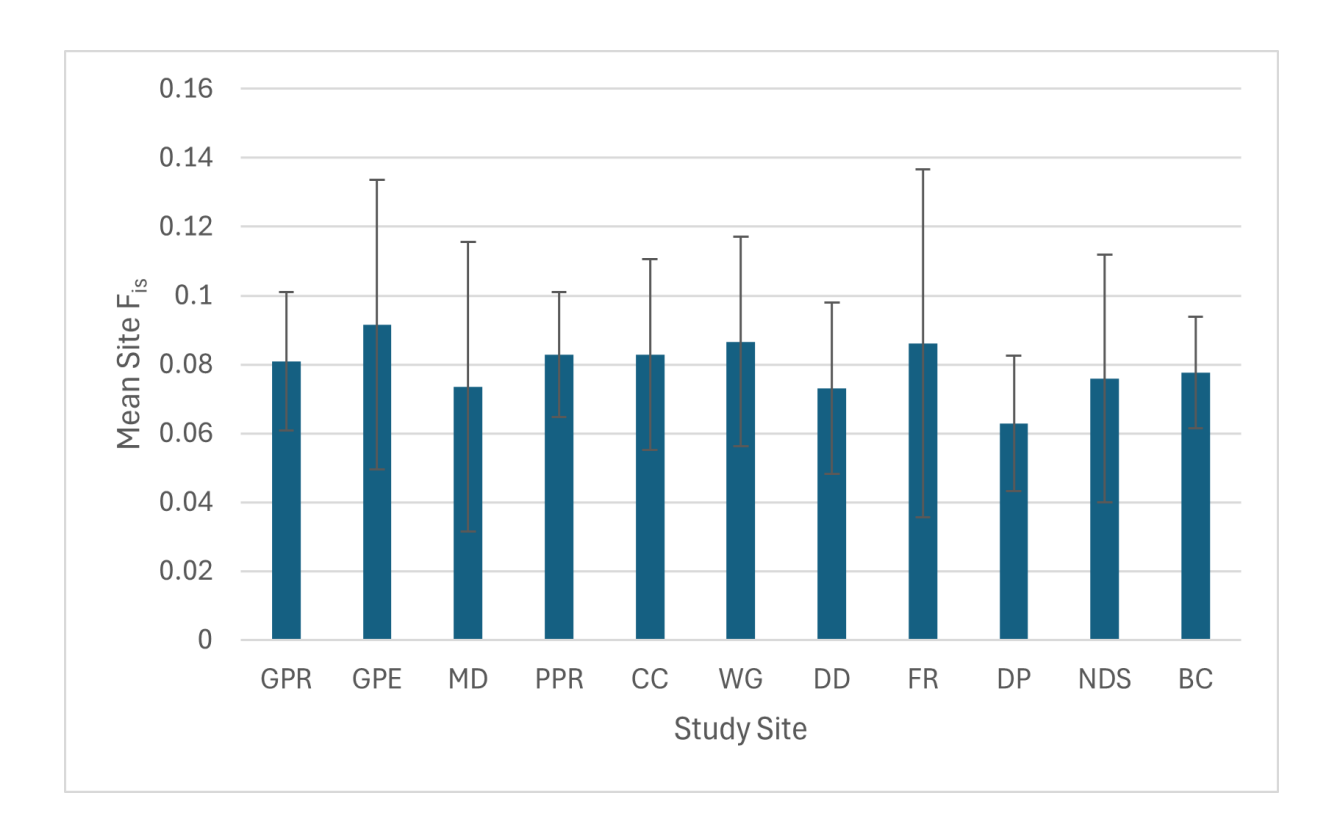


**Figure 4.6.** Average F<sub>IS</sub> inbreeding coefficient for the individual *Aedes albopictus* sampled at each study site. Error bars represent the standard deviation for each site's average inbreeding coefficient.

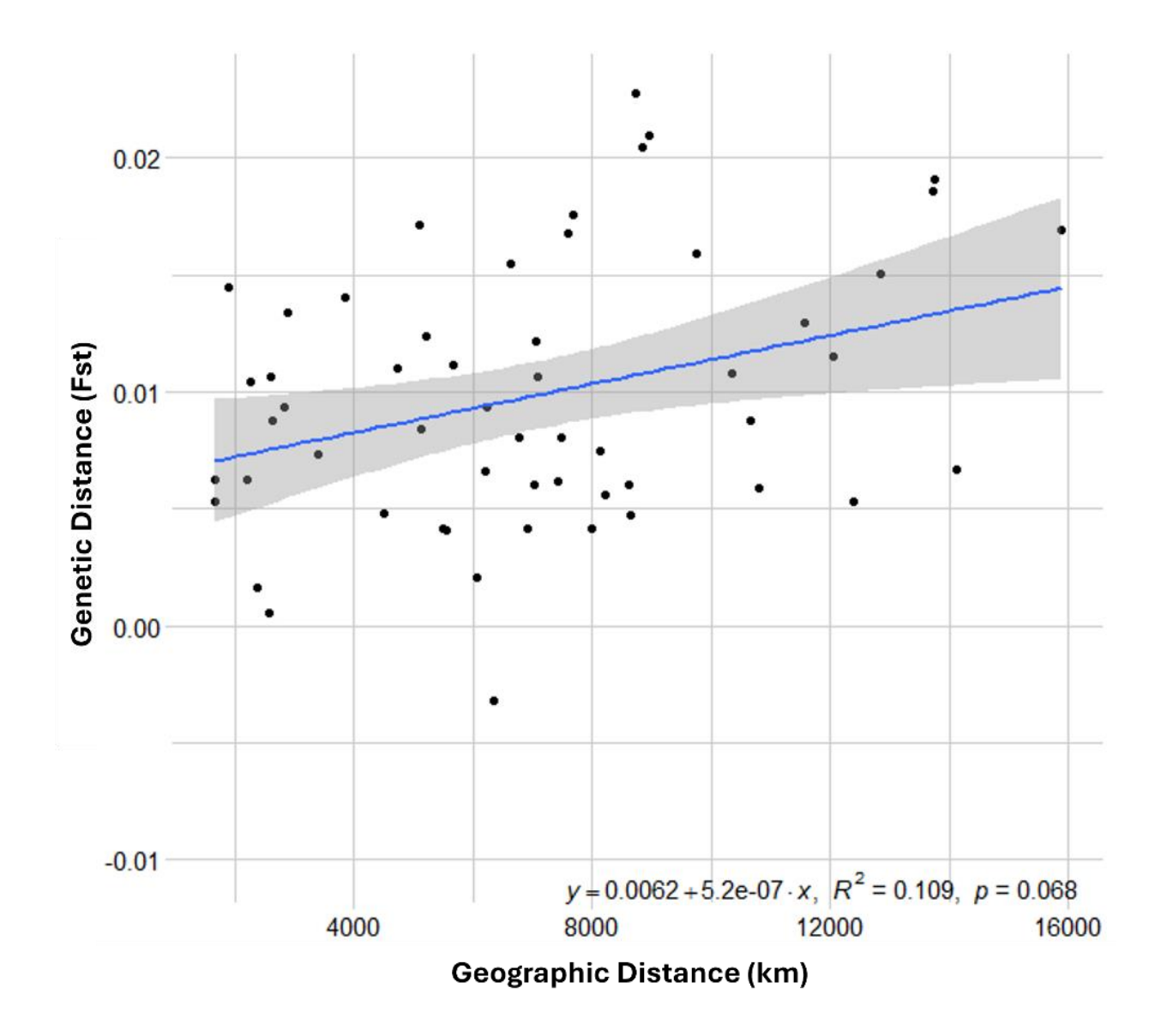


**Figure 4.7.** Genetic distance (Site-Site pairwise  $F_{ST}$ ) vs geographic distance (km). Best fit line represented in blue and variance in the Mantel Test permutations are represented in grey.

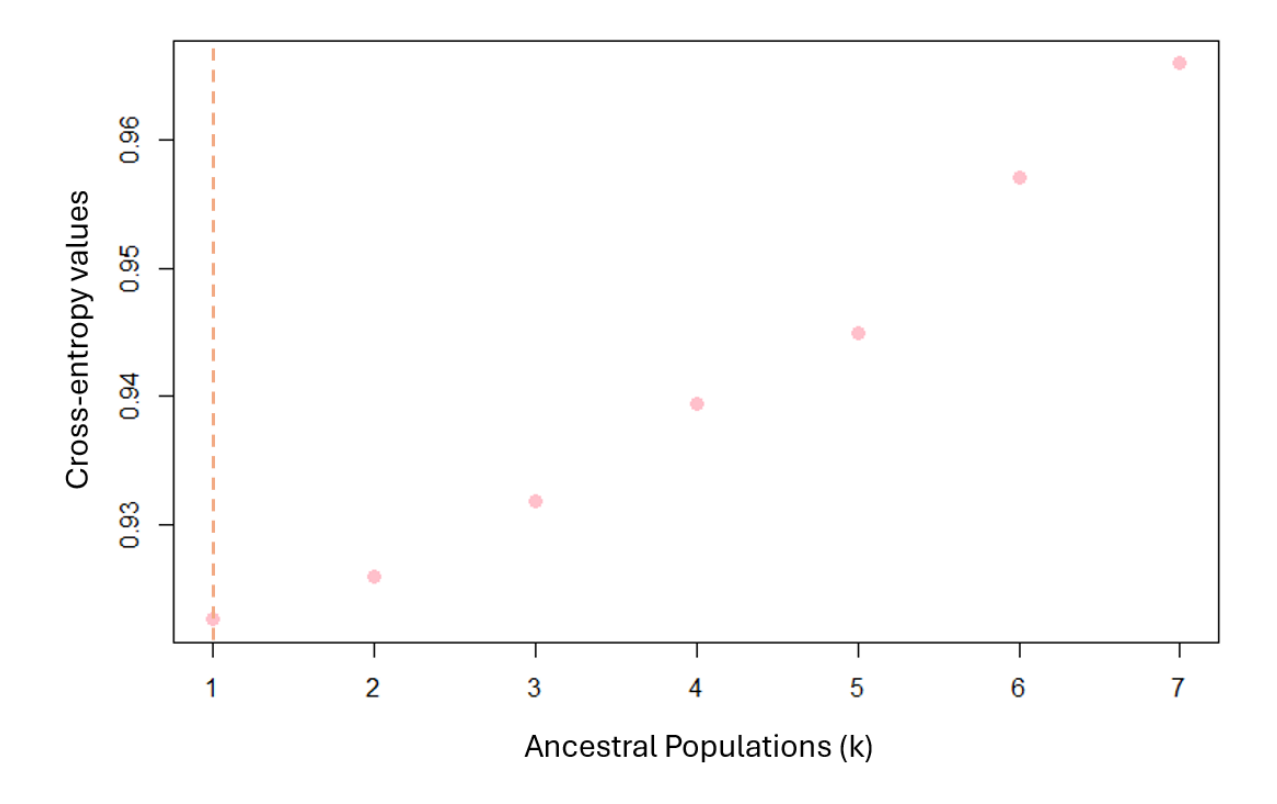


**Figure 4.8.** Potential ancestral populations (k) and corresponding cross-entropy values. Lowest error values at k=1 ancestral populations (indicated by orange line).

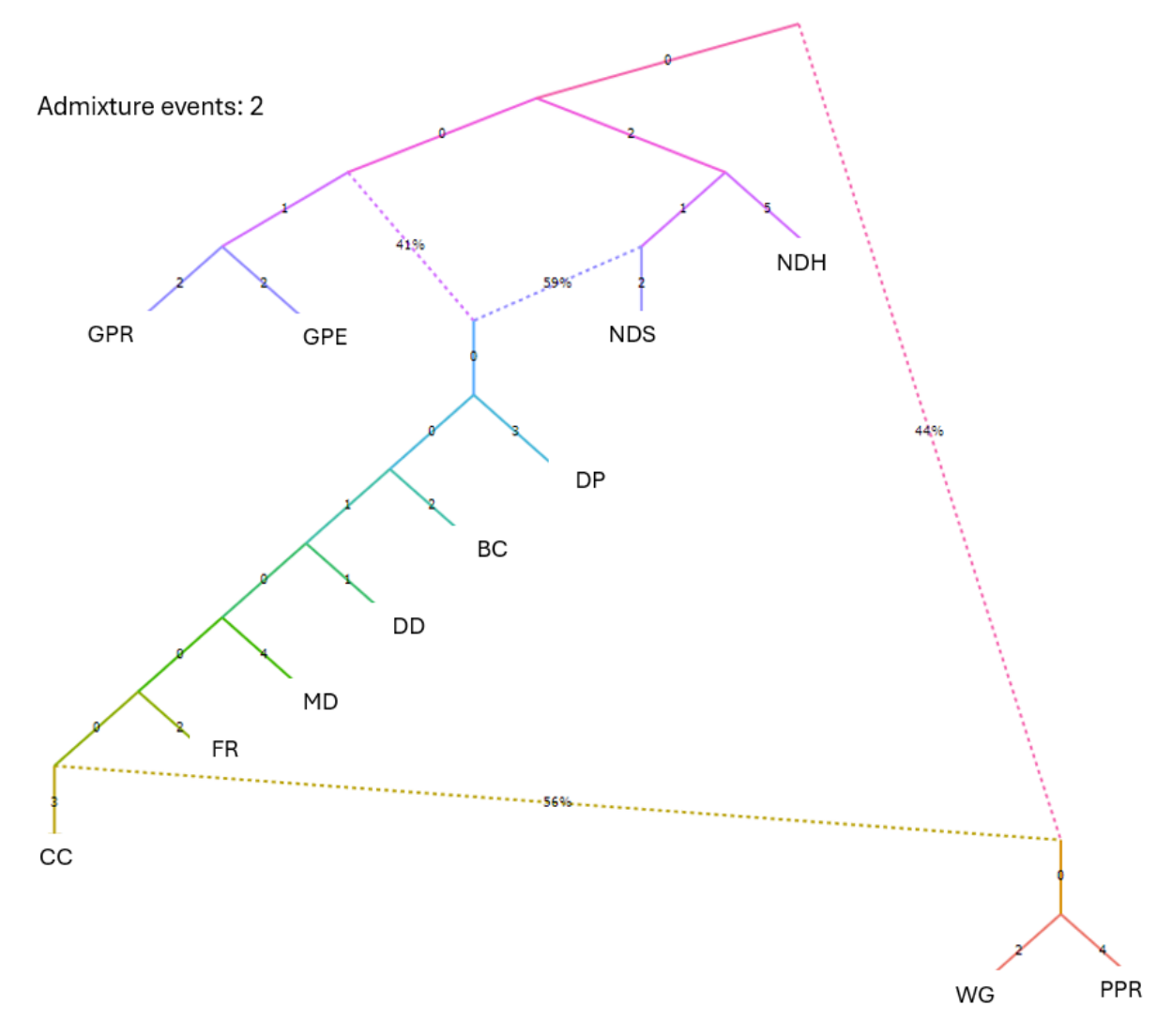


**Figure 4.9.** Potential admixture history of *Aedes albopictus* populations across study sites. Simulated 300 generations since introduction, *F*-statistic residual score was 969.68. Two admixture events shown here.

#### CHAPTER 5

### **CONCLUSIONS**

Synthesis of Key Findings

The guiding motivation of this dissertation was to conceptualize vector-borne disease (VBD) dynamics and vector ecology in the context of human-altered landscapes using *Aedes albopictus* populations across an urban areas as the system of interest. This was accomplished by critically reviewing modelling approaches to describing VBD systems and determining the most informative spatial scales at which to describe the ecology of this vector species. A review of empirical studies as well as previous empirical work in *Ae. albopictus* in the southeastern US helped determine the spatial scale of this vector's biology and informed the spatial distances at which microclimate variables were measured. I also recommend the integration of different modelling approaches with empirical investigation to fully employ the relative strengths of different approaches. This additionally led to selecting the appropriate modelling tools with which to determine the most important environmental and land cover effects and to develop vector control insights. Through the use of statistical modelling and the field collection of fine scale microclimate data, my research identified significant relationships between environmental variables associated with urbanization and the *Ae. albopictus* populations of Atlanta, GA.

Generalized linear mixed effects models of the field derived adult abundance data identified significant positive effects of impervious surfaces and daily temperature range (DTR) on adult *Ae. albopictus* abundance and significant negative effects of minimum relative humidity

(RH<sub>Min</sub>). Mixed effects models describing larval habitat density identified a significant positive effect of canopy cover. Larval habitat density was not a significant predictor in the adult abundance model, but it was a significantly positive predictor of larval abundance. Beyond the abundance of refugia for adult mosquitoes and potentially greater persistence of aquatic larval habitats under canopy cover, I argue that the connection of canopy cover to the human curated environments associated with residential areas also leads to more larval habitats. Even sites in my study not economically stressed yielded large larval populations and high larval habitat density, mostly due to human provisioned container habitats like flowerpots. This research highlights the importance of RH, temperature, and land cover in predicting *Ae. albopictus* population characteristics. I connect these variables to increasing urbanization, further supporting the characterization of *Ae. albopictus* as an urban adapted anthropophilic vector species.

The significant but limited genetic structure of the *Ae. albopictus* populations across this study area portrays a landscape with few barriers to gene flow. While highways and other human structures have been seen to create isolation by distance and by barrier in mosquito populations, any impedance posed by urban architecture and roads is eventually overcome either by gradual natural dispersal or perhaps more rapid human mediated spread of eggs. Rapid and stochastic establishment of populations may arise from a single productive larval habitat, with some larval habitats like used tires or buckets being easily moved and reconstituted with rainfall. Overall, these findings demonstrate the impact of both unimpeded natural dispersal and stochastic human events in facilitating the establishment and continued gene flow of vector populations. The ancestral models of this population show a single source population, suggesting a highly successful single invasion event near the onset of *Ae. albopictus's* colonization of North America, followed by admixtures and population movement between sites.

Novelty and Added Benefit of Research

While other studies have measured the effects of microclimate variables on mosquito vector ecology, this is the first study to apply this methodology of collecting detailed fine-scale temperature and relative humidity data using large numbers of data loggers in the field in Atlanta, GA. The large size of this urban area provides a valuable data point in characterizing sizable municipal regions with likely increased heat island effects. This genetic component of this research was novel both in the use of a newly developed SNP-chip offering high polymorphism coverage and improved genetic variation measurement resolution. While this SNP chip has been used and validated in one other study (Cosme et al. 2024), this is the first application of this specific SNP microarray tool in measuring population structure within a relatively small spatial scale inside one urban region. The viewpoint of synthesizing different approaches to modelling and choosing appropriate scales of measurement and analysis is a perspective that has been employed in other forms, but this approach is useful in its novel application to the Atlanta vector ecology system.

Recognizing the Effect of Urbanization in Exposure to VBD

The modelling of microclimate variables impacting adult *Ae. albopictus* abundance provides insights into how urbanization may contribute to larger populations of arbovirus vectors. As urbanization traditionally increases paved areas and thus urban heat island effects (Mohajerani et al. 2017), alternate approaches to urban planning could include more water-permeable green spaces like parks, which would likely also reduce the daily temperature swings (Yan et al. 2023). More broadly, outreach campaigns communicating risks of VBD as urban areas expand globally in the coming decades (Population Division United Nations 2018). Additionally, the negative effect of minimum RH on *Ae. albopictus* populations in this research

indicates a surface tension alteration increasing larval and pupal survival. Reducing surface tension is already a modality of larval control (Dawood et al. 2020), but this effect could be applied widely in urban parks where water features like fountains may be common as they were in some sites in this study.

Implications of human provisioning of larval habitat

This characterization of *Ae. albopictus* in Atlanta, GA is consistent with the conventional understanding of this species' ecology. While treeholes, the ancestral larval habitat for many container breeding mosquitoes, were identified in this study, no *Ae. albopictus* were found in these arboreal larval habitats. During the invasion and establishment of *Ae. albopictus* in North America, competition experiments predicted that the endemic *Aedes triseriatus* populations would persist in treehole larval environments due to competitive nutritional advantages over *Ae. albopictus* (Livdahl and Willey 1991). In my research, *Ae. triseriatus* was indeed found in treeholes, meaning that undeveloped landscapes may reduce the competitive edge of *Ae. albopictus* and be less vulnerable to the invasion and establishment by this urban adapted mosquito.

As most larval habitats I found were artificial, accounting for the cultural practices of the community is important for understanding larval habitat provisioning. The suburban residential sites in my study provided an abundance of larval habitats for *Ae. albopictus* largely from decorative planters and gardening water storage containers. There is a body of research indicating an association with depressed socioeconomic areas with an increased burden of mosquitoes and VBD, tied to factors like limited plumbing creating a reliance on household water containers (Ali et al. 2017) or the increased presence of discarded tires, disused containers, or abandoned swimming pools resulting from economic distress (Harrigan et al. 2010, LaDeau et

al. 2013, Dowling et al. 2013). Financial crises have actually shown acute increases of human West Nile Virus cases linked to vacant homes (Reisen et al. 2008). However, of the sites in this research, only one qualitatively showed signs of economic distress as indicated by multiple abandoned residences and persistent discarded containers serving as larval habitats. Other sites with less signs of economic distress were just as or even more abundant in adult Ae. albopictus and larval habitat density. A similar dynamic in a US city was seen in a study of *Culex* breeding sites in Los Angeles, CA. This mosquito survey also demonstrated a counterintuitive result with affluent neighborhoods provisioning more larval habitat due to widespread landscaping irrigation (Reisen et al. 1990). This effect of landscaping practices providing larval habitats matches what we saw in my research with positive larval habitat density being highest at some residential neighborhood sites with well-maintained single-family homes and landscaping. These insights regarding both the canopy influences on larval habitat density and the importance of social practices tell us that larval source management efforts in Atlanta should focus on education of communities regarding the risk landscaping and garden containers present in Ae. albopictus exposure.

Findings in context of the phylogeography of Aedes albopictus

Tracking the invasion dynamics of *Ae. albopictus* often relies on genetic tools, and reconstructing the genetic phylogeography of this species reveals many interesting phenomena regarding human mediated invasions and VBD spread. Recent investigations into the phylogenetic past of this species shows a slow dispersal from Asia in the Pleistocene to islands in the Indian Ocean through medieval trade routes (Delatte et al. 2011, Porretta et al. 2012). The last several decades illustrate a rapid dispersal worldwide from the Indo-Pacific region across Africa and into temperate zones in North America and Europe (Mousson et al. 2005,

Raharimalala et al. 2012, Maynard et al. 2017). The significance of identifying genetically distinct subpopulations is due to different interactions of vector genotype and environment leading to local variations in vectoral competence in mosquito species (Lambrechts 2011, Dickson et al. 2014, Severson and Behura 2016, Kristan et al. 2018). Mosquito lineages can differ biologically in ways important for pathogen transmission dynamics and may reflect different degrees of urban adaptation (Paupy et al. 2004, 2008, Costa-da-Silva et al. 2005). Vectorial capacity can be influenced by genetic variations between the vector and the pathogen with multiple gene pathways determining transmission potential (Beerntsen et al. 2000), while different permethrin resistant genotypes have been seen to respond differently to temperature and relative humidity conditions (Kristan et al. 2018). In the context of the research in this dissertation, which found very little variation between Ae. albopictus subpopulations in Atlanta, identifying the parent lineage and any genetic traits such as insecticide resistance or degrees of temperate tolerance would be meaningful for control efforts. Perhaps more worryingly, the rapid gene flow between these populations suggests that the introduction of insecticide resistant Ae. albopictus would likely result in rapid spread of this trait under the right selection pressures.

### Future research directions

The mismatch between larval habitat density and adult abundance within the sites of this research should be a future avenue of investigation. This disparity indicates that some sites are functioning as ecological sources. *Ae. albopictus* has been observed moving distances exceeding the typical dispersal range, up to several hundreds of meters, in the sech for adequate hosts (Maciel-de-freitas et al. 2006). A similar variation in resources may be driving movement from larval habitat dense areas hundreds of meters to sites with better host access or refuge spaces. Identifying potential corridors of population movement, and if landscape characteristics shape

movement patterns, would be valuable for ecological understanding of this species as well as advancing vector control knowledge. Regarding population structure, limited resources only allowed for one time point (August 2022) in the study to be sequenced. Future research could examine specimens from another field season (2021) to identify any temporal shifts in genotypes or site subpopulation dynamics. Shifts in genetic characteristics or even identification of different orders of relatives between sites may reveal some dispersal paths in this system.

Finally, a further research effort will include the creation of VBD risk map for Atlanta showing varying levels of exposure according to microclimate and landscape characteristics using the abundance model developed in this study and a mechanistic model of vectorial capacity. This would follow the general methodology of a similar risk map created of Athens, GA (Wimberly et al. 2020).

The landscape and the microclimates of heterogenous urban environments result in varying abundances of *Ae. albopictus* and larval habitat density. This dissertation demonstrates the key human element in creating the urban environments this vector species is so well adapted to, including the facilitation of invasion and further gene flow once *Ae. albopictus* is established in a new location. Modeling approaches and cross-scale discernment informed these research efforts, and ideally this multi-discipline approach will help inform predictions of VBD risk. The research in this dissertation advances our knowledge of this globally destructive and invasive mosquito vector while informing policy makers on how to reduce the risk of VBD in the face of increasing urbanization.

### REFERENCES

- Ahumada, J. A., D. Laoointe, and M. D. Samuel. 2004. Modeling the Population Dynamics of Culex quinquefasciatus (Diptera: Culicidae), along an Elevational Gradient in Hawaii.

  Journal of Medical Entomology 41:1157–1170.
- Akhtar, R., P. T. Gupta, and A. K. Srivastava. 2016. Urbanization, Urban Heat Island Effects and Dengue Outbreak in Delhi. Pages 99–111 *in* R. Akhtar, editor. Climate Change and Human Health Scenario in South and Southeast Asia. Springer International Publishing, Cham.
- Ali, S., O. Gugliemini, S. Harber, A. Harrison, L. Houle, J. Ivory, S. Kersten, R. Khan, J. Kim, C. LeBoa, E. Nez-Whitfield, J. O'Marr, E. Rothenberg, R. M. Segnitz, S. Sila, A. Verwillow, M. Vogt, A. Yang, and E. A. Mordecai. 2017. Environmental and Social Change Drive the Explosive Emergence of Zika Virus in the Americas. PLOS Neglected Tropical Diseases 11:e0005135.
- Alto, B. W., and D. Bettinardi. 2013. Temperature and Dengue Virus Infection in Mosquitoes:

  Independent Effects on the Immature and Adult Stages.
- Alto, B. W., and S. A. Juliano. 2001. Temperature Effects on the Dynamics of Aedes albopictus (Diptera: Culicidae) Populations in the Laboratory. Journal of medical entomology 38:548–556.
- Araujo, R. V., M. R. Albertini, A. L. Costa-da-Silva, L. Suesdek, N. C. S. Franceschi, N. M. Bastos, G. Katz, V. A. Cardoso, B. C. Castro, M. L. Capurro, and V. L. A. C. Allegro.

- 2015. São Paulo urban heat islands have a higher incidence of dengue than other urban areas. The Brazilian Journal of Infectious Diseases 19:146–155.
- Armistead, J. S., J. R. Arias, N. Nishimura, and L. P. Lounibos. 2008. Interspecific Larval Competition Between Aedes albopictus and Aedes japonicus (Diptera: Culicidae) in Northern Virginia. Journal of medical entomology 45:629–637.
- Arnfield, A. J. 2003. Two decades of urban climate research: a review of turbulence, exchanges of energy and water, and the urban heat island. International Journal of Climatology 23:1–26.
- Asigau, S., and P. G. Parker. 2018. The influence of ecological factors on mosquito abundance and occurrence in Galápagos. Journal of Vector Ecology 43:125–137.
- Auger, P., E. Kouokam, G. Sallet, M. Tchuente, and B. Tsanou. 2008. The Ross–Macdonald model in a patchy environment. Mathematical Biosciences 216:123–131.
- Barker, J. R., and H. J. MacIsaac. 2022. Species distribution models applied to mosquitoes: Use, quality assessment, and recommendations for best practice. Ecological Modelling 472:110073.
- Barrios, E., S. Lee, and O. Vasilieva. 2018. Assessing the effects of daily commuting in two-patch dengue dynamics: A case study of Cali, Colombia. Journal of Theoretical Biology 453:14–39.
- Baruah, K., and R. Rai. 2000. The impact of housing structures on filarial infection. Japanese journal of infectious diseases.
- Becker, B., P. T. Leisnham, and S. L. LaDeau. 2014. A tale of two city blocks: differences in immature and adult mosquito abundances between socioeconomically different urban

- blocks in Baltimore (Maryland, USA). International Journal of Environmental Research and Public Health 11:3256–3270.
- Beebe, N. W., L. Ambrose, L. A. Hill, J. B. Davis, G. Hapgood, R. D. Cooper, R. C. Russell, S.
  A. Ritchie, L. J. Reimer, N. F. Lobo, D. Syafruddin, and A. F. van den Hurk. 2013.
  Tracing the Tiger: Population Genetics Provides Valuable Insights into the Aedes
  (Stegomyia) albopictus Invasion of the Australasian Region. PLOS Neglected Tropical
  Diseases 7:e2361.
- Beerntsen, B. T., A. A. James, and B. M. Christensen. 2000. Genetics of Mosquito Vector Competence. Microbiology and Molecular Biology Reviews 64:115–137.
- Bellini, R., A. Albieri, F. Balestrino, M. Carrieri, D. Porretta, S. Urbanelli, M. Calvitti, R.
   Moretti, and S. Maini. 2010. Dispersal and Survival of Aedes albopictus (Diptera:
   Culicidae) Males in Italian Urban Areas and Significance for Sterile Insect Technique
   Application. Journal of Medical Entomology 47:1082–1091.
- Birungi, J., and L. E. Munstermann. 2002. Genetic Structure of Aedes albopictus (Diptera: Culicidae) Populations Based on Mitochondrial ND5 Sequences: Evidence for an Independent Invasion into Brazil and United States. Annals of the Entomological Society of America 95:125–132.
- Black, W. C., J. A. Ferrari, K. S. Rai, and D. Sprenger. 1988. Breeding structure of a colonising species: Aedes albopictus (Skuse) in the United States. Heredity 60:173–181.
- Blanco-Sierra, L., S. Mariani, S. Escartin, R. Eritja, J. R. B. Palmer, and F. Bartumeus. 2023.

  Drivers of longevity of wild-caught Aedes albopictus populations. Parasites & Vectors 16:328.

- Bohers, C., M. Vazeille, L. Bernaoui, L. Pascalin, K. Meignan, L. Mousson, G. Jakerian, A. Karch, X. de Lamballerie, and A.-B. Failloux. 2024. Aedes albopictus is a competent vector of five arboviruses affecting human health, greater Paris, France, 2023.

  Eurosurveillance 29:2400271.
- Bondo, K. J., D. Montecino-Latorre, L. Williams, M. Helwig, K. Duren, M. L. Hutchinson, and W. D. Walter. 2023. Spatial modeling of two mosquito vectors of West Nile virus using integrated nested Laplace approximations. Ecosphere 14:e4346.
- Bonizzoni, M., G. Gasperi, X. Chen, and A. A. James. 2013. The invasive mosquito species Aedes albopictus: current knowledge and future perspectives. Trends in Parasitology 29:460–468.
- Bosio, C. F., L. C. Harrington, D. E. Norris, T. W. Scott, J. W. Jones, and R. Sithiprasasna. 2005.

  Genetic structure of Aedes aegypti populations in Thailand using mitochondrial DNA.

  The American Journal of Tropical Medicine and Hygiene 72:434–442.
- Boukraa, S., F. N. Raharimalala, J.-Y. Zimmer, F. Schaffner, T. Bawin, E. Haubruge, and F. Francis. 2013. Reintroduction of the invasive mosquito species Aedes albopictus in Belgium in July 2013. Parasite 20:54.
- Brady, O. J., M. A. Johansson, C. A. Guerra, S. Bhatt, N. Golding, D. M. Pigott, H. Delatte, M. G. Grech, P. T. Leisnham, R. Maciel-de-Freitas, L. M. Styer, D. L. Smith, T. W. Scott, P. W. Gething, and S. I. Hay. 2013. Modelling adult Aedes aegypti and Aedes albopictus survival at different temperatures in laboratory and field settings. Parasites & Vectors 6:351.
- Briegel, H., and S. E. Timmermann. 2001. Aedes albopictus (Diptera: Culicidae): Physiological Aspects of Development and Reproduction. Journal of Medical Entomology 38:566–571.

- Brown, J. J., M. Pascual, M. C. Wimberly, L. R. Johnson, and C. C. Murdock. 2023. Humidity The overlooked variable in the thermal biology of mosquito-borne disease. Ecology letters 26:1029–1049.
- Brownstein, J. S., H. Rosen, D. Purdy, J. R. Miller, M. Merlino, F. Mostashari, and D. Fish. 2002. Spatial Analysis of West Nile Virus: Rapid Risk Assessment of an Introduced Vector-Borne Zoonosis. Vector-Borne and Zoonotic Diseases 2:157–164.
- Buckner, E. A., M. S. Blackmore, S. W. Golladay, and A. P. Covich. 2011. Weather and landscape factors associated with adult mosquito abundance in southwestern Georgia, U.S.A. Journal of Vector Ecology 36:269–278.
- Caprara, A., J. W. de O. Lima, A. C. P. Marinho, P. G. Calvasina, L. P. Landim, and J. Sommerfeld. 2009. Irregular water supply, household usage and dengue: a bio-social study in the Brazilian Northeast. Cadernos de Saúde Pública 25:S125–S136.
- Carrington, L. B., S. N. Seifert, M. V. Armijos, L. Lambrechts, and T. W. Scott. 2013a. Reduction of Aedes aegypti Vector Competence for Dengue Virus under Large Temperature Fluctuations. The American Journal of Tropical Medicine and Hygiene 88:689–697.
- Carrington, L. B., S. N. Seifert, N. H. Willits, L. Lambrechts, and T. W. Scott. 2013b. Large
  Diurnal Temperature Fluctuations Negatively Influence Aedes aegypti (Diptera:
  Culicidae) Life-History Traits. Journal of Medical Entomology 50:43–51.
- Carter, R. 2002. Spatial simulation of malaria transmission and its control by malaria transmission blocking vaccination. International Journal for Parasitology 32:1617–1624.
- Carvajal, T. M., K. Ogishi, S. Yaegeshi, L. F. T. Hernandez, K. M. Viacrusis, H. T. Ho, D. M. Amalin, and K. Watanabe. 2020. Fine-scale population genetic structure of dengue

- mosquito vector, Aedes aegypti, in Metropolitan Manila, Philippines. PLOS Neglected Tropical Diseases 14:e0008279.
- Cator, L. J., L. R. Johnson, E. A. Mordecai, F. El Moustaid, T. R. C. Smallwood, S. L. LaDeau,
  M. A. Johansson, P. J. Hudson, M. Boots, M. B. Thomas, A. G. Power, and S. Pawar.
  2020. The Role of Vector Trait Variation in Vector-Borne Disease Dynamics. Frontiers in Ecology and Evolution 8.
- Cator, L. J., S. Thomas, K. P. Paaijmans, S. Ravishankaran, J. A. Justin, M. T. Mathai, A. F. Read, M. B. Thomas, and A. Eapen. 2013. Characterizing microclimate in urban malaria transmission settings: a case study from Chennai, India. Malaria Journal 12:84.
- CDC. 2024, November 21. Current Dengue Outbreak.

  https://www.cdc.gov/dengue/outbreaks/2024/index.html.
- Chang, Y., J. Xiao, X. Li, S. Frolking, D. Zhou, A. Schneider, Q. Weng, P. Yu, X. Wang, X. Li, S. Liu, and Y. Wu. 2021. Exploring diurnal cycles of surface urban heat island intensity in Boston with land surface temperature data derived from GOES-R geostationary satellites. Science of The Total Environment 763:144224.
- Chareonviriyaphap, T., P. Akratanakul, S. Huntamai, S. Nettanomsak, and A. Prabaripai. 2004.

  Allozyme Patterns of Aedes albopictus, a Vector of Dengue in Thailand. Journal of

  Medical Entomology 41:657–663.
- Chaves, L. F., G. L. Hamer, E. D. Walker, W. M. Brown, M. O. Ruiz, and U. D. Kitron. 2011.

  Climatic variability and landscape heterogeneity impact urban mosquito diversity and vector abundance and infection. Ecosphere 2:art70.
- Chen, X.-G., X. Jiang, J. Gu, M. Xu, Y. Wu, Y. Deng, C. Zhang, M. Bonizzoni, W. Dermauw, J. Vontas, P. Armbruster, X. Huang, Y. Yang, H. Zhang, W. He, H. Peng, Y. Liu, K. Wu, J.

- Chen, M. Lirakis, P. Topalis, T. V. Leeuwen, A. B. Hall, X. Jiang, C. Thorpe, R. L. Mueller, C. Sun, R. M. Waterhouse, G. Yan, Z. J. Tu, X. Fang, and A. A. James. 2015. Genome sequence of the Asian Tiger mosquito, Aedes albopictus, reveals insights into its biology, genetics, and evolution. Proceedings of the National Academy of Sciences 112:E5907–E5915.
- Chikungunya | CDC Yellow Book 2024. (n.d.). .

  https://wwwnc.cdc.gov/travel/yellowbook/2024/infections-diseases/chikungunya.
- Christiansen-Jucht, C. D., P. E. Parham, A. Saddler, J. C. Koella, and M.-G. Basáñez. 2015.

  Larval and adult environmental temperatures influence the adult reproductive traits of Anopheles gambiae s.s. Parasites & Vectors 8:456.
- Cianci, D., N. Hartemink, and A. Ibáñez-Justicia. 2015. Modelling the potential spatial distribution of mosquito species using three different techniques. International Journal of Health Geographics 14:10.
- Cleveland, C., T. Dallas, S. Vigil, D. Mead, J. Corn, and A. Park. 2023. Vector communities under global change may exacerbate and redistribute infectious disease risk. Parasitology Research 122.
- Cohen, J. M., D. J. Civitello, A. J. Brace, E. M. Feichtinger, C. N. Ortega, J. C. Richardson, E. L. Sauer, X. Liu, and J. R. Rohr. 2016. Spatial scale modulates the strength of ecological processes driving disease distributions. Proceedings of the National Academy of Sciences 113:E3359–E3364.
- Colón-González, F. J., I. Harris, T. J. Osborn, C. Steiner São Bernardo, C. A. Peres, P. R. Hunter, and I. R. Lake. 2018. Limiting global-mean temperature increase to 1.5-2 °C could

- reduce the incidence and spatial spread of dengue fever in Latin America. Proceedings of the National Academy of Sciences of the United States of America 115:6243–6248.
- Colón-González, F. J., M. O. Sewe, A. M. Tompkins, H. Sjödin, A. Casallas, J. Rocklöv, C. Caminade, and R. Lowe. 2021. Projecting the risk of mosquito-borne diseases in a warmer and more populated world: a multi-model, multi-scenario intercomparison modelling study. The Lancet Planetary Health 5:e404–e414.
- Cosme, L. V., M. Corley, T. Johnson, D. W. Severson, G. Yan, X. Wang, N. Beebe, A. Maynard, M. Bonizzoni, A. Khorramnejad, A. J. Martins, J. B. P. Lima, L. E. Munstermann, S. N. Surendran, C.-H. Chen, K. Maringer, I. Wahid, S. Mukherjee, J. Xu, M. C. Fontaine, E. L. Estallo, M. Stein, T. Livdahl, P. Y. Scaraffia, B. H. Carter, M. Mogi, N. Tuno, J. W. Mains, K. A. Medley, D. E. Bowles, R. J. Gill, R. Eritja, R. González-Obando, H. T. T. Trang, S. Boyer, A.-M. Abunyewa, K. Hackett, T. Wu, J. Nguyễn, J. Shen, H. Zhao, J. E. Crawford, P. Armbruster, and A. Caccone. 2024. A genotyping array for the globally invasive vector mosquito, Aedes albopictus. Parasites & Vectors 17:106.
- Costa-da-Silva, A. L. da, M. L. Capurro, and J. E. Bracco. 2005. Genetic lineages in the yellow fever mosquito Aedes (Stegomyia) aegypti (Diptera: Culicidae) from Peru. Memórias do Instituto Oswaldo Cruz 100:539–544.
- Cui, G., S. Zhong, T. Zheng, Z. Li, X. Zhang, C. Li, E. Hemming-Schroeder, G. Zhou, and Y. Li. 2021. Aedes albopictus life table: environment, food, and age dependence survivorship and reproduction in a tropical area. Parasites & Vectors 14:568.
- Darsie, R., and R. Ward. 2005. Identification and geographical distribution of the mosquitoes of North America, North of Mexico. University Press of Florida.

- Dawood, A.-F. D., M. M. Baz, and M. I. Ibrahim. 2020. Influence of Aquatain<sup>TM</sup>, a monomolecular surface film on surface tension for controlling the filarial vector *Culex pipiens* (Diptera: Culicidae). Heliyon 6:e05314.
- Dee, L. E., D. Okamtoto, A. Gårdmark, J. M. Montoya, and S. J. Miller. 2020. Temperature variability alters the stability and thresholds for collapse of interacting species.Philosophical Transactions of the Royal Society B: Biological Sciences 375:20190457.
- DeGaetano, A. T. 2005. Meteorological effects on adult mosquito (Culex) populations in metropolitan New Jersey. International Journal of Biometeorology 49:345–353.
- Delatte, H., L. Bagny, C. Brengue, A. Bouetard, C. Paupy, and D. Fontenille. 2011. The invaders: Phylogeography of dengue and chikungunya viruses Aedes vectors, on the South West islands of the Indian Ocean. Infection, Genetics and Evolution 11:1769–1781.
- Delatte, H., G. Gimonneau, A. Triboire, and D. Fontenille. 2009. Influence of temperature on immature development, survival, longevity, fecundity, and gonotrophic cycles of Aedes albopictus, vector of chikungunya and dengue in the Indian Ocean. Journal of Medical Entomology 46:33–41.
- Delatte, H., C. Toty, S. Boyer, A. Bouetard, F. Bastien, and D. Fontenille. 2013. Evidence of Habitat Structuring Aedes albopictus Populations in Réunion Island. PLOS Neglected Tropical Diseases 7:e2111.
- Demers, J., S. Bewick, F. Agusto, K. A. Caillouët, W. F. Fagan, and S. L. Robertson. 2020.

  Managing disease outbreaks: The importance of vector mobility and spatially heterogeneous control. PLOS Computational Biology 16:e1008136.

- Demok, S., N. Endersby-Harshman, R. Vinit, L. Timinao, L. J. Robinson, M. Susapu, L. Makita,M. Laman, A. Hoffmann, and S. Karl. 2019. Insecticide resistance status of Aedes aegyptiand Aedes albopictus mosquitoes in Papua New Guinea. Parasites & Vectors 12:333.
- Dickson, L. B., I. Sanchez-Vargas, M. Sylla, K. Fleming, and W. C. B. Iv. 2014. Vector Competence in West African Aedes aegypti Is Flavivirus Species and Genotype Dependent. PLOS Neglected Tropical Diseases 8:e3153.
- Dieng, H., G. M. S. Rahman, A. Abu Hassan, M. R. Che Salmah, T. Satho, F. Miake, M. Boots, and A. Sazaly. 2012. The effects of simulated rainfall on immature population dynamics of Aedes albopictus and female oviposition. International Journal of Biometeorology 56:113–120.
- Dowling, Z., S. L. Ladeau, P. Armbruster, D. Biehler, and P. T. Leisnham. 2013. Socioeconomic Status Affects Mosquito (Diptera: Culicidae) Larval Habitat Type Availability and Infestation Level. Journal of Medical Entomology 50:764–772.
- Dritsou, V., P. Topalis, N. Windbichler, A. Simoni, A. Hall, D. Lawson, M. Hinsley, D. Hughes,
  V. Napolioni, F. Crucianelli, E. Deligianni, G. Gasperi, L. M. Gomulski, G. Savini, M.
  Manni, F. Scolari, A. R. Malacrida, B. Arcà, J. M. Ribeiro, F. Lombardo, G. Saccone, M.
  Salvemini, R. Moretti, G. Aprea, M. Calvitti, M. Picciolini, P. A. Papathanos, R.
  Spaccapelo, G. Favia, A. Crisanti, and C. Louis. 2015. A draft genome sequence of an invasive mosquito: an Italian Aedes albopictus. Pathogens and Global Health 109:207.
- Eckhoff, P. A., C. A. Bever, J. Gerardin, E. A. Wenger, and D. L. Smith. 2015. From puddles to planet: modeling approaches to vector-borne diseases at varying resolution and scale.

  Current Opinion in Insect Science 10:118–123.

- Eritja, R., J. R. B. Palmer, D. Roiz, I. Sanpera-Calbet, and F. Bartumeus. 2017. Direct Evidence of Adult Aedes albopictus Dispersal by Car. Scientific Reports 7:14399.
- Eskildsen, G. A., J. R. Rovira, O. Smith, M. J. Miller, K. L. Bennett, W. O. McMillan, and J. Loaiza. 2018. Maternal invasion history of Aedes aegypti and Aedes albopictus into the Isthmus of Panama: Implications for the control of emergent viral disease agents. PLoS ONE 13:e0194874.
- Evans, M. V., C. W. Hintz, L. Jones, J. Shiau, N. Solano, J. M. Drake, and C. C. Murdock. 2019.

  Microclimate and Larval Habitat Density Predict Adult Aedes albopictus Abundance in

  Urban Areas. The American Journal of Tropical Medicine and Hygiene 101:362–370.
- Evans, M. V., P. M. Newberry, and C. C. Murdock. 2020. Carry-over effects of the larval environment in mosquito-borne disease systems. Page 304 *in* J. M. Drake, M. Bonsall, and M. R. Strand, editors. Population Biology of Vector-Borne Diseases. Oxford University Press.
- Evans, M. V., J. C. Shiau, N. Solano, M. A. Brindley, J. M. Drake, and C. C. Murdock. 2018.

  Carry-over effects of urban larval environments on the transmission potential of dengue-2 virus. Parasites & Vectors 11.
- Ezanno, P., M. Andraud, G. Beaunée, T. Hoch, S. Krebs, A. Rault, S. Touzeau, E. Vergu, and S. Widgren. 2020. How mechanistic modelling supports decision making for the control of enzootic infectious diseases. Epidemics 32:100398.
- Ezeakacha, N. F., and D. A. Yee. 2019. The role of temperature in affecting carry-over effects and larval competition in the globally invasive mosquito Aedes albopictus. Parasites & Vectors 12:123.

- Failloux, A.-B., M. Vazeille, and F. Rodhain. 2002. Geographic Genetic Variation in Populations of the Dengue Virus Vector Aedes aegypti. Journal of Molecular Evolution 55:653–663.
- Fairbanks, E. L., M. Saeung, A. Pongsiri, E. Vajda, Y. Wang, D. J. McIver, J. H. Richardson, A. Tatarsky, N. F. Lobo, S. J. Moore, A. Ponlawat, T. Chareonviriyaphap, A. Ross, and N. Chitnis. 2024. Inference for entomological semi-field experiments: Fitting a mathematical model assessing personal and community protection of vector-control interventions. Computers in Biology and Medicine 168:107716.
- Faraji, A., A. Egizi, D. M. Fonseca, I. Unlu, T. Crepeau, S. P. Healy, and R. Gaugler. 2014.
   Comparative Host Feeding Patterns of the Asian Tiger Mosquito, Aedes albopictus, in
   Urban and Suburban Northeastern USA and Implications for Disease Transmission.
   PLOS Neglected Tropical Diseases 8:e3037.
- Fukui, S., Y. Kuwano, K. Ueno, K. Atsumi, and S. Ohta. 2022. Modeling the effect of rainfall changes to predict population dynamics of the Asian tiger mosquito Aedes albopictus under future climate conditions. PLoS ONE 17.
- Gao, D., Y. Lou, and S. Ruan. 2014. A periodic Ross-Macdonald model in a patchy environment.

  Discrete and continuous dynamical systems. Series B 19:3133–3145.
- Garcia-Rejon, J. E., J.-C. Navarro, N. Cigarroa-Toledo, and C. M. Baak-Baak. 2021. An Updated Review of the Invasive Aedes albopictus in the Americas; Geographical Distribution, Host Feeding Patterns, Arbovirus Infection, and the Potential for Vertical Transmission of Dengue Virus. Insects 12:967.
- Gimonneau, G., J. Bouyer, S. Morand, N. J. Besansky, A. Diabate, and F. Simard. 2010. A behavioral mechanism underlying ecological divergence in the malaria mosquito

  Anopheles gambiae. Behavioral Ecology 21:1087–1092.

- Gloria-Soria, A., A. F. Payne, S. M. Bialosuknia, J. Stout, N. Mathias, G. Eastwood, A. T. Ciota,
  L. D. Kramer, and P. M. Armstrong. 2021. Vector Competence of Aedes albopictus
  Populations from the Northeastern United States for Chikungunya, Dengue, and Zika
  Viruses. The American Journal of Tropical Medicine and Hygiene 104:1123–1130.
- Gloria-Soria, A., T. Shragai, A. T. Ciota, T. B. Duval, B. W. Alto, A. J. Martins, K. M. Westby, K.
  A. Medley, I. Unlu, S. R. Campbell, M. Kawalkowski, Y. Tsuda, Y. Higa, N. Indelicato, P.
  T. Leisnham, A. Caccone, and P. M. Armstrong. 2022. Population genetics of an invasive mosquito vector, Aedes albopictus in the Northeastern USA. NeoBiota: advancing research on alien species and biological invasions 78:99.
- Goodman, H., A. Egizi, D. M. Fonseca, P. T. Leisnham, and S. L. LaDeau. 2018. Primary bloodhosts of mosquitoes are influenced by social and ecological conditions in a complex urban landscape. Parasites & Vectors 11:218.
- Gotelli, N. J., and A. M. Ellison. 2006. Food-Web Models Predict Species Abundances in Response to Habitat Change. PLoS Biology 4.
- Gouagna, L. C., D. Damiens, C. F. Oliva, S. Boyer, G. Le Goff, C. Brengues, J.-S. Dehecq, J. Raude, F. Simard, and D. Fontenille. 2020. Strategic Approach, Advances, and Challenges in the Development and Application of the SIT for Area-Wide Control of Aedes albopictus Mosquitoes in Reunion Island. Insects 11:770.
- Goubert, C., G. Minard, C. Vieira, and M. Boulesteix. 2016. Population genetics of the Asian tiger mosquito Aedes albopictus, an invasive vector of human diseases. Heredity 117:125–134.
- Gu, W., and R. J. Novak. 2009. Predicting the impact of insecticide-treated bed nets on malaria transmission: the devil is in the detail. Malaria Journal 8:256.

- Gunathilaka, N., H. Upulika, L. Udayanga, and D. Amarasinghe. 2019. Effect of Larval Nutritional Regimes on Morphometry and Vectorial Capacity of Aedes aegypti for Dengue Transmission. BioMed Research International 2019:e3607342.
- Guo, Y., Z. Song, L. Luo, Q. Wang, G. Zhou, D. Yang, D. Zhong, and X. Zheng. 2018. Molecular evidence for new sympatric cryptic species of Aedes albopictus (Diptera: Culicidae) in China: A new threat from Aedes albopictus subgroup? Parasites & Vectors 11:228.
- Gutiérrez-López, R., S. M. Bialosuknia, A. T. Ciota, T. Montalvo, J. Martínez-de la Puente, L. Gangoso, J. Figuerola, and L. D. Kramer. 2019. Vector Competence of Aedes caspius and Ae. albopictus Mosquitoes for Zika Virus, Spain. Emerging Infectious Diseases 25:346–348.
- Halstead, S. B. 2007. Dengue. The Lancet 370:1644–1652.
- Hanley, K. A., H. Cecilia, S. R. Azar, B. A. Moehn, J. T. Gass, N. I. Oliveira da Silva, W. Yu, R. Yun, B. M. Althouse, N. Vasilakis, and S. L. Rossi. 2024. Trade-offs shaping transmission of sylvatic dengue and Zika viruses in monkey hosts. Nature Communications 15:2682.
- Harrigan, R. J., H. A. Thomassen, W. Buermann, R. F. Cummings, M. E. Kahn, and T. B. Smith. 2010. Economic Conditions Predict Prevalence of West Nile Virus. PLOS ONE 5:e15437.
- Harrington, L. C., T. W. Scott, K. Lerdthusnee, R. C. Coleman, A. Costero, G. G. Clark, J. J. Jones, S. Kitthawee, P. Kittayapong, R. Sithiprasasna, and J. D. Edman. 2005. Dispersal of the dengue vector Aedes aegypti within and between rural communities. Am. J. Trop. Med. Hyg. 72(2):12.
- Hartig, F. 2024. "DHARMa: Residual Diagnostics for Hierarchical (Multi-Level / Mixed)

  Regression Models" R package.

- Hay, S. I., C. A. Guerra, P. W. Gething, A. P. Patil, A. J. Tatem, A. M. Noor, C. W. Kabaria, B. H. Manh, I. R. F. Elyazar, S. Brooker, D. L. Smith, R. A. Moyeed, and R. W. Snow. 2009. A World Malaria Map: Plasmodium falciparum Endemicity in 2007. PLOS Medicine 6:e1000048.
- Heersink, D. K., J. Meyers, P. Caley, G. Barnett, B. Trewin, T. Hurst, and C. Jansen. 2016. Statistical modeling of a larval mosquito population distribution and abundance in residential Brisbane. Journal of Pest Science 89:267–279.
- Hemme, R. R., C. L. Thomas, D. D. Chadee, and D. W. Severson. 2010. Influence of Urban Landscapes on Population Dynamics in a Short-Distance Migrant Mosquito: Evidence for the Dengue Vector Aedes aegypti. PLOS Neglected Tropical Diseases 4:e634.
- Hlaing, T., W. Tun-Lin, P. Somboon, D. Socheat, T. Setha, S. Min, S. Thaung, O. Anyaele, B. De Silva, M. S. Chang, A. Prakash, Y. Linton, and C. Walton. 2010. Spatial genetic structure of Aedes aegypti mosquitoes in mainland Southeast Asia. Evolutionary Applications 3:319–339.
- Hopperstad, K. A., M. H. Reiskind, P. E. Labadie, and M. O. Burford Reiskind. 2019. Patterns of genetic divergence among populations of Aedes aegypti L. (Diptera: Culicidae) in the southeastern USA. Parasites & Vectors 12:511.
- Howe, D. A., J. M. Hathaway, K. N. Ellis, and L. R. Mason. 2017. Spatial and temporal variability of air temperature across urban neighborhoods with varying amounts of tree canopy. Urban Forestry & Urban Greening 27:109–116.
- Huber, J. H., M. L. Childs, J. M. Caldwell, and E. A. Mordecai. 2018. Seasonal temperature variation influences climate suitability for dengue, chikungunya, and Zika transmission. PLOS Neglected Tropical Diseases 12:e0006451.

- Huber, K., L. L. Loan, N. Chantha, and A.-B. Failloux. 2004. Human transportation influences

  Aedes aegypti gene flow in Southeast Asia. Acta Tropica 90:23–29.
- IPCC. 2023. AR6 Synthesis Report: Climate Change 2023. https://www.ipcc.ch/report/ar6/syr/.
- Irvine, M. A., J. W. Kazura, T. D. Hollingsworth, and L. J. Reimer. 2018. Understanding heterogeneities in mosquito-bite exposure and infection distributions for the elimination of lymphatic filariasis. Proceedings of the Royal Society B: Biological Sciences 285:20172253.
- Ismail, N.-A., N. C. Dom, R. Ismail, A. H. Ahmad, A. Zaki, and S. N. Camalxaman. 2015.

  Mitochondrial Cytochrome Oxidase I Gene Sequence Analysis of Aedes Albopictus in

  Malaysia. Journal of the American Mosquito Control Association 31:305–312.
- Iyaloo, D. P., K. B. Elahee, A. Bheecarry, and R. S. Lees. 2014. Guidelines to site selection for population surveillance and mosquito control trials: A case study from Mauritius. Acta Tropica 132:S140–S149.
- Johnson, C. A., R. M. Coutinho, E. Berlin, K. E. Dolphin, J. Heyer, B. Kim, A. Leung, J. L. Sabellon, and P. Amarasekare. 2016. Effects of temperature and resource variation on insect population dynamics: the bordered plant bug as a case study. Functional Ecology 30:1122–1131.
- Johnson, L. R., R. B. Gramacy, J. Cohen, E. Mordecai, C. Murdock, J. Rohr, S. J. Ryan, A. M. Stewart-Ibarra, and D. Weikel. 2018. Phenomenological forecasting of disease incidence using heteroskedastic Gaussian processes: A dengue case study. The Annals of Applied Statistics 12:27–66.
- Jones, C. M., A. L. Wilson, M. C. Stanton, J. R. Stothard, F. Guglielmo, J. Chirombo, L. Mafuleka, R. Oronje, and T. Mzilahowa. 2023. Integrating vector control within an

- emerging agricultural system in a region of climate vulnerability in southern Malawi: A focus on malaria, schistosomiasis, and arboviral diseases. Current Research in Parasitology & Vector-borne Diseases 4:100133.
- Joyce, A. L., M. M. Torres, R. Torres, and M. Moreno. 2018. Genetic variability of the Aedes aegypti (Diptera: Culicidae) mosquito in El Salvador, vector of dengue, yellow fever, chikungunya and Zika. Parasites & Vectors 11:637.
- Kambhampati, S., W. C. Black, and K. S. Rai. 1991. Geographic origin of the US and Brazilian Aedes albopictus inferred from allozyme analysis. Heredity 67:85–94.
- Kamgang, B., C. Brengues, D. Fontenille, F. Njiokou, F. Simard, and C. Paupy. 2011. Genetic Structure of the Tiger Mosquito, Aedes albopictus, in Cameroon (Central Africa). PLoS ONE 6.
- Kamgang, B., C. Ngoagouni, A. Manirakiza, E. Nakouné, C. Paupy, and M. Kazanji. 2013.
   Temporal Patterns of Abundance of Aedes aegypti and Aedes albopictus (Diptera:
   Culicidae) and Mitochondrial DNA Analysis of Ae. albopictus in the Central African
   Republic. PLOS Neglected Tropical Diseases 7:e2590.
- Kamgang, B., T. A. Wilson-Bahun, H. Irving, M. O. Kusimo, A. Lenga, and C. S. Wondji. 2018.

  Geographical distribution of Aedes aegypti and Aedes albopictus (Diptera: Culicidae) and genetic diversity of invading population of Ae. albopictus in the Republic of the Congo.

  Wellcome Open Research 3:79.
- Kearney, M., and W. Porter. 2009. Mechanistic niche modelling: combining physiological and spatial data to predict species' ranges. Ecology Letters 12:334–350.

- Khan, S. U., N. H. Ogden, A. A. Fazil, P. H. Gachon, G. U. Dueymes, A. L. Greer, and V. Ng. 2020. Current and Projected Distributions of Aedes aegypti and Ae. albopictus in Canada and the U.S. Environmental Health Perspectives 128:057007.
- Kotsakiozi, P., J. B. Richardson, V. Pichler, G. Favia, A. J. Martins, S. Urbanelli, P. A.Armbruster, and A. Caccone. 2017. Population genomics of the Asian tiger mosquito,Aedes albopictus: insights into the recent worldwide invasion. Ecology and Evolution 7:10143.
- Kraemer, M. U., M. E. Sinka, K. A. Duda, A. Q. Mylne, F. M. Shearer, C. M. Barker, C. G.
  Moore, R. G. Carvalho, G. E. Coelho, W. Van Bortel, G. Hendrickx, F. Schaffner, I. R.
  Elyazar, H.-J. Teng, O. J. Brady, J. P. Messina, D. M. Pigott, T. W. Scott, D. L. Smith, G.
  W. Wint, N. Golding, and S. I. Hay. 2015. The global distribution of the arbovirus vectors
  Aedes aegypti and Ae. albopictus. eLife 4:e08347.
- Kristan, M., T. A. Abeku, and J. Lines. 2018. Effect of environmental variables and kdr resistance genotype on survival probability and infection rates in Anopheles gambiae (s.s.). Parasites & Vectors 11:560.
- Lacroix, R., H. Delatte, T. Hue, and P. Reiter. 2009. Dispersal and Survival of Male and Female Aedes albopictus (Diptera: Culicidae) on Réunion Island. Journal of Medical Entomology 46:1117–1124.
- LaDeau, S. L., C. A. Calder, P. J. Doran, and P. P. Marra. 2011. West Nile virus impacts in American crow populations are associated with human land use and climate. Ecological Research 26:909–916.
- LaDeau, S. L., P. T. Leisnham, D. Biehler, and D. Bodner. 2013. Higher Mosquito Production in Low-Income Neighborhoods of Baltimore and Washington, DC: Understanding

- Ecological Drivers and Mosquito-Borne Disease Risk in Temperate Cities. International Journal of Environmental Research and Public Health 10:1505–1526.
- Lambin, E. F., A. Tran, S. O. Vanwambeke, C. Linard, and V. Soti. 2010. Pathogenic landscapes:

  Interactions between land, people, disease vectors, and their animal hosts. International

  Journal of Health Geographics 9:54.
- Lambrechts, L. 2011. Quantitative genetics of Aedes aegypti vector competence for dengue viruses: towards a new paradigm? Trends in Parasitology 27:111–114.
- Lambrechts, L., K. P. Paaijmans, T. Fansiri, L. B. Carrington, L. D. Kramer, M. B. Thomas, and T. W. Scott. 2011. Impact of daily temperature fluctuations on dengue virus transmission by Aedes aegypti. Proceedings of the National Academy of Sciences 108:7460–7465.
- Laporta, G. Z., A. M. Potter, J. F. A. Oliveira, B. P. Bourke, D. B. Pecor, and Y.-M. Linton. 2023.

  Global Distribution of Aedes aegypti and Aedes albopictus in a Climate Change Scenario of Regional Rivalry. Insects 14:49.
- Laureano-Rosario, A. E., A. P. Duncan, P. A. Mendez-Lazaro, J. E. Garcia-Rejon, S. Gomez-Carro, J. Farfan-Ale, D. A. Savic, and F. E. Muller-Karger. 2018. Application of Artificial Neural Networks for Dengue Fever Outbreak Predictions in the Northwest Coast of Yucatan, Mexico and San Juan, Puerto Rico. Tropical Medicine and Infectious Disease 3:5.
- Lee, S., and C. Castillo-Chavez. 2015. The role of residence times in two-patch dengue transmission dynamics and optimal strategies. Journal of Theoretical Biology 374:152–164.

- Lees, R. S., J. R. Gilles, J. Hendrichs, M. J. Vreysen, and K. Bourtzis. 2015. Back to the future: the sterile insect technique against mosquito disease vectors. Current Opinion in Insect Science 10:156–162.
- Leisnham, P. T., and S. A. Juliano. 2009. Spatial and temporal patterns of coexistence between competing Aedes mosquitoes in urban Florida. Oecologia 160:343–352.
- Leisnham, P. T., S. L. LaDeau, and S. A. Juliano. 2014. Spatial and Temporal Habitat Segregation of Mosquitoes in Urban Florida. PLOS ONE 9:e91655.
- Lessler, J., and D. A. T. Cummings. 2016. Mechanistic Models of Infectious Disease and Their Impact on Public Health. American Journal of Epidemiology 183:415–422.
- Leta, S., T. J. Beyene, E. M. D. Clercq, K. Amenu, M. U. G. Kraemer, and C. W. Revie. 2018.

  Global risk mapping for major diseases transmitted by Aedes aegypti and Aedes albopictus. International Journal of Infectious Diseases 67:25–35.
- Li, Y., F. Kamara, G. Zhou, S. Puthiyakunnon, C. Li, Y. Liu, Y. Zhou, L. Yao, G. Yan, and X.-G.Chen. 2014. Urbanization Increases Aedes albopictus Larval Habitats and AcceleratesMosquito Development and Survivorship. PLOS Neglected Tropical Diseases 8:e3301.
- Li, Y., G. Zhou, D. Zhong, X. Wang, E. Hemming-Schroeder, R. E. David, M.-C. Lee, S. Zhong,
  G. Yi, Z. Liu, G. Cui, and G. Yan. 2021. Widespread multiple insecticide resistance in the
  major dengue vector Aedes albopictus in Hainan Province, China. Pest Management
  Science 77:1945–1953.
- Liew, C., and C. F. Curtis. 2004. Horizontal and vertical dispersal of dengue vector mosquitoes, Aedes aegypti and Aedes albopictus, in Singapore. Medical and Veterinary Entomology 18:351–360.

- Lipson, M. 2020. Applying f4-statistics and admixture graphs: Theory and examples. Molecular Ecology Resources 20:1658–1667.
- Little, E., D. Biehler, P. T. Leisnham, R. Jordan, S. Wilson, and S. L. LaDeau. 2017. Socio-Ecological Mechanisms Supporting High Densities of Aedes albopictus (Diptera: Culicidae) in Baltimore, MD. Journal of Medical Entomology 54:1183–1192.
- Livdahl, T. P., and M. S. Willey. 1991. Prospects for an Invasion: Competition Between Aedes albopictus and Native Aedes triseriatus. Science 253:189–191.
- Louise, C., P. O. Vidal, and L. Suesdek. 2015. Microevolution of Aedes aegypti. PLOS ONE 10:e0137851.
- Lucati, F., S. Delacour, J. R. B. Palmer, J. Caner, A. Oltra, C. Paredes-Esquivel, S. Mariani, S.
  Escartin, D. Roiz, F. Collantes, M. Bengoa, T. Montalvo, J. A. Delgado, R. Eritja, J.
  Lucientes, A. Albó Timor, F. Bartumeus, and M. Ventura. 2022. Multiple invasions,
  Wolbachia and human-aided transport drive the genetic variability of Aedes albopictus in
  the Iberian Peninsula. Scientific Reports 12:20682.
- Ma, Z., D. Xing, Q. Liu, G. Wang, and T. Zhao. 2023. Population genetic characterization of (Aedes albopictus) mosquitoes (Diptera: Culicidae) from the Yangtze River Basin of China based on rDNA-ITS2. Infection, Genetics and Evolution 113:105485.
- Maciel-de-freitas, R., R. B. Neto, J. M. Gonçalves, C. T. Codeço, and R. Lourenço-de-oliveira.

  2006. Movement of Dengue Vectors Between the Human Modified Environment and an
  Urban Forest in Rio de Janeiro. Journal of Medical Entomology 43:1112–1120.
- Madzokere, E. T., W. Hallgren, O. Sahin, J. A. Webster, C. E. Webb, B. Mackey, and L. J. Herrero. 2020. Integrating statistical and mechanistic approaches with biotic and environmental variables improves model predictions of the impact of climate and land-

- use changes on future mosquito-vector abundance, diversity and distributions in Australia. Parasites & Vectors 13:484.
- Maia, R. T., V. M. Scarpassa, L. H. Maciel-Litaiff, and W. P. Tadei. 2009. Reduced levels of genetic variation in Aedes albopictus (Diptera: Culicidae) from Manaus, Amazonas State, Brazil, based on analysis of the mitochondrial DNA ND5 gene. Genetics and molecular research: GMR 8:998–1007.
- Maier, R., P. Flegontov, O. Flegontova, U. Işıldak, P. Changmai, and D. Reich. 2023. On the limits of fitting complex models of population history to f-statistics. eLife 12:e85492.
- Maimusa, H. A., A. H. Ahmad, N. F. A. Kassim, and J. Rahim. 2016. Age-Stage, Two-Sex Life

  Table Characteristics of Aedes albopictus and Aedes Aegypti in Penang Island, Malaysia.

  Journal of the American Mosquito Control Association 32:1–11.
- Manni, M., L. M. Gomulski, N. Aketarawong, G. Tait, F. Scolari, P. Somboon, C. R. Guglielmino, A. R. Malacrida, and G. Gasperi. 2015. Molecular markers for analyses of intraspecific genetic diversity in the Asian Tiger mosquito, Aedes albopictus. Parasites & Vectors 8:188.
- Manni, M., C. R. Guglielmino, F. Scolari, A. Vega-Rúa, A.-B. Failloux, P. Somboon, A. Lisa, G. Savini, M. Bonizzoni, L. M. Gomulski, A. R. Malacrida, and G. Gasperi. 2017. Genetic evidence for a worldwide chaotic dispersion pattern of the arbovirus vector, Aedes albopictus. PLoS Neglected Tropical Diseases 11:e0005332.
- Marini, F., B. Caputo, M. Pombi, G. Tarsitani, and A. della Torre. 2010. Study of Aedes albopictus dispersal in Rome, Italy, using sticky traps in mark-release-recapture experiments. Medical and Veterinary Entomology 24:361–368.

- Marshall, J. M., A. Bennett, S. S. Kiware, and H. J. W. Sturrock. 2016. The Hitchhiking Parasite: Why Human Movement Matters to Malaria Transmission and What We Can Do About It. Trends in Parasitology 32:752–755.
- Maynard, A. J., L. Ambrose, R. D. Cooper, W. K. Chow, J. B. Davis, M. O. Muzari, A. F. van den Hurk, S. Hall-Mendelin, J. M. Hasty, T. R. Burkot, M. J. Bangs, L. J. Reimer, C. Butafa, N. F. Lobo, D. Syafruddin, Y. N. M. Maung, R. Ahmad, and N. W. Beebe. 2017. Tiger on the prowl: Invasion history and spatio-temporal genetic structure of the Asian tiger mosquito Aedes albopictus (Skuse 1894) in the Indo-Pacific. PLOS Neglected Tropical Diseases 11:e0005546.
- McClure, K. M., C. Lawrence, and A. M. Kilpatrick. 2018. Land Use and Larval Habitat

  Increase Aedes albopictus (Diptera: Culicidae) and Culex quinquefasciatus (Diptera:

  Culicidae) Abundance in Lowland Hawaii. Journal of Medical Entomology 55:1509–

  1516.
- Md. Naim, D., N. Z. M. Kamal, and S. Mahboob. 2020. Population structure and genetic diversity of *Aedes aegypti* and *Aedes albopictus* in Penang as revealed by mitochondrial DNA cytochrome oxidase I. Saudi Journal of Biological Sciences 27:953–967.
- Medley, K. A., D. G. Jenkins, and E. A. Hoffman. 2015. Human-aided and natural dispersal drive gene flow across the range of an invasive mosquito. Molecular Ecology 24:284–295.
- Menach, A. L., F. E. McKenzie, A. Flahault, and D. L. Smith. 2005. The unexpected importance of mosquito oviposition behaviour for malaria: non-productive larval habitats can be sources for malaria transmission. Malaria Journal 4:23.
- Merkin, R. 2004. The Urban Heat Island's Effect on the diurnal temperature range. Thesis, Massachusetts Institute of Technology.

- Messina, J. P., M. U. Kraemer, O. J. Brady, D. M. Pigott, F. M. Shearer, D. J. Weiss, N. Golding,
  C. W. Ruktanonchai, P. W. Gething, E. Cohn, J. S. Brownstein, K. Khan, A. J. Tatem, T.
  Jaenisch, C. J. Murray, F. Marinho, T. W. Scott, and S. I. Hay. 2016. Mapping global
  environmental suitability for Zika virus. eLife 5:e15272.
- Miazgowicz, K. L., M. S. Shocket, S. J. Ryan, O. C. Villena, R. J. Hall, J. Owen, T. Adanlawo, K. Balaji, L. R. Johnson, E. A. Mordecai, and C. C. Murdock. 2020. Age influences the thermal suitability of Plasmodium falciparum transmission in the Asian malaria vector Anopheles stephensi. Proceedings of the Royal Society B: Biological Sciences 287:20201093.
- Miller, J. R., S. Koren, K. A. Dilley, V. Puri, D. M. Brown, D. M. Harkins, F. Thibaud-Nissen, B. Rosen, X.-G. Chen, Z. Tu, I. V. Sharakhov, M. V. Sharakhova, R. Sebra, T. B. Stockwell, N. H. Bergman, G. G. Sutton, A. M. Phillippy, P. M. Piermarini, and R. S. Shabman.
  2018. Analysis of the Aedes albopictus C6/36 genome provides insight into cell line utility for viral propagation. GigaScience 7:gix135.
- Misslin, R., O. Telle, E. Daudé, A. Vaguet, and R. E. Paul. 2016. Urban climate versus global climate change—what makes the difference for dengue? Annals of the New York Academy of Sciences 1382:56–72.
- Mohajerani, A., J. Bakaric, and T. Jeffrey-Bailey. 2017. The urban heat island effect, its causes, and mitigation, with reference to the thermal properties of asphalt concrete. Journal of Environmental Management 197:522–538.
- Moller-Jacobs, L. L., C. C. Murdock, and M. B. Thomas. 2014. Capacity of mosquitoes to transmit malaria depends on larval environment. Parasites & Vectors 7:593.

- Monteiro, L. C. C., J. R. B. de Souza, and C. M. R. de Albuquerque. 2007. Eclosion rate, development and survivorship of Aedes albopictus (Skuse)(Diptera: Culicidae) under different water temperatures. Neotropical Entomology 36:966–971.
- Moore, C. G., and C. J. Mitchell. 1997. Aedes albopictus in the United States: Ten-Year Presence and Public Health Implications Volume 3, Number 3—September 1997 Emerging Infectious Diseases journal CDC.
- Mordecai, E. A., J. M. Caldwell, M. K. Grossman, C. A. Lippi, L. R. Johnson, M. Neira, J. R. Rohr, S. J. Ryan, V. Savage, M. S. Shocket, R. Sippy, A. M. Stewart Ibarra, M. B. Thomas, and O. Villena. 2019. Thermal biology of mosquito-borne disease. Ecology Letters 22:1690–1708.
- Mordecai, E. A., J. M. Cohen, M. V. Evans, P. Gudapati, L. R. Johnson, C. A. Lippi, K.
  Miazgowicz, C. C. Murdock, J. R. Rohr, S. J. Ryan, V. Savage, M. S. Shocket, A. S.
  Ibarra, M. B. Thomas, and D. P. Weikel. 2017a. Detecting the impact of temperature on transmission of Zika, dengue, and chikungunya using mechanistic models. PLOS
  Neglected Tropical Diseases 11:e0005568.
- Mordecai, E. A., J. M. Cohen, M. V. Evans, P. Gudapati, L. R. Johnson, C. A. Lippi, K.
  Miazgowicz, C. C. Murdock, J. R. Rohr, S. J. Ryan, V. Savage, M. S. Shocket, A. S.
  Ibarra, M. B. Thomas, and D. P. Weikel. 2017b. Detecting the impact of temperature on transmission of Zika, dengue, and chikungunya using mechanistic models. PLOS
  Neglected Tropical Diseases 11:e0005568.
- Morgan, J., C. Strode, and J. E. Salcedo-Sora. 2021. Climatic and socio-economic factors supporting the co-circulation of dengue, Zika and chikungunya in three different ecosystems in Colombia. PLoS Neglected Tropical Diseases 15:e0009259.

- Motoki, M. T., D. M. Fonseca, E. F. Miot, B. Demari-Silva, P. Thammavong, S.

  Chonephetsarath, N. Phommavanh, J. C. Hertz, P. Kittayapong, P. T. Brey, and S.

  Marcombe. 2019. Population genetics of Aedes albopictus (Diptera: Culicidae) in its native range in Lao People's Democratic Republic. Parasites & Vectors 12:477.
- Mousson, L., C. Dauga, T. Garrigues, F. Schaffner, M. Vazeille, and A.-B. Failloux. 2005.

  Phylogeography of Aedes (Stegomyia) aegypti (L.) and Aedes (Stegomyia) albopictus

  (Skuse) (Diptera: Culicidae) based on mitochondrial DNA variations. Genetical Research

  86:1–11.
- Mousson, L., K. Zouache, C. Arias-Goeta, V. Raquin, P. Mavingui, and A.-B. Failloux. 2012. The Native Wolbachia Symbionts Limit Transmission of Dengue Virus in Aedes albopictus.

  PLOS Neglected Tropical Diseases 6:e1989.
- Multini, L. C., A. L. da S. de Souza, M. T. Marrelli, and A. B. B. Wilke. 2019. Population structuring of the invasive mosquito Aedes albopictus (Diptera: Culicidae) on a microgeographic scale. PLoS ONE 14.
- Murdock, C. C., S. Blanford, S. Luckhart, and M. B. Thomas. 2014a. Ambient temperature and dietary supplementation interact to shape mosquito vector competence for malaria.

  Journal of insect physiology 67:37–44.
- Murdock, C. C., S. Blanford, S. Luckhart, and M. B. Thomas. 2014b. Ambient temperature and dietary supplementation interact to shape mosquito vector competence for malaria.

  Journal of insect physiology 67:37–44.
- Murdock, C. C., M. V. Evans, T. D. McClanahan, K. L. Miazgowicz, and B. Tesla. 2017. Fine-scale variation in microclimate across an urban landscape shapes variation in mosquito

- population dynamics and the potential of Aedes albopictus to transmit arboviral disease. PLOS Neglected Tropical Diseases 11:e0005640.
- Murdock, C. C., K. P. Paaijmans, A. S. Bell, J. G. King, J. F. Hillyer, A. F. Read, and M. B. Thomas. 2012. Complex effects of temperature on mosquito immune function.

  Proceedings of the Royal Society B: Biological Sciences 279:3357–3366.
- Nagao, Y., U. Thavara, P. Chitnumsup, A. Tawatsin, C. Chansang, and D. Campbell-Lendrum. 2003. Climatic and social risk factors for Aedes infestation in rural Thailand. Tropical Medicine & International Health 8:650–659.
- Nayar, J. K., and A. Ali. 2003. A review of monomolecular surface films as larvicides and pupicides of mosquitoes. Journal of Vector Ecology: Journal of the Society for Vector Ecology 28:190–199.
- Nipa, K. F., and L. J. S. Allen. 2020. Disease Emergence in Multi-Patch Stochastic Epidemic Models with Demographic and Seasonal Variability. Bulletin of Mathematical Biology 82:152.
- Ohm, J. R., F. Baldini, P. Barreaux, T. Lefevre, P. A. Lynch, E. Suh, S. A. Whitehead, and M. B. Thomas. 2018. Rethinking the extrinsic incubation period of malaria parasites. Parasites & Vectors 11.
- Olanratmanee, P., P. Kittayapong, C. Chansang, A. A. Hoffmann, A. R. Weeks, and N. M. Endersby. 2013. Population Genetic Structure of Aedes (Stegomyia) aegypti (L.) at a Micro-Spatial Scale in Thailand: Implications for a Dengue Suppression Strategy. PLoS Neglected Tropical Diseases 7.
- Oliva, C. F., M. Q. Benedict, C. M. Collins, T. Baldet, R. Bellini, H. Bossin, J. Bouyer, V. Corbel, L. Facchinelli, F. Fouque, M. Geier, A. Michaelakis, D. Roiz, F. Simard, C. Tur,

- and L.-C. Gouagna. 2021. Sterile Insect Technique (SIT) against Aedes Species

  Mosquitoes: A Roadmap and Good Practice Framework for Designing, Implementing and

  Evaluating Pilot Field Trials. Insects 12:191.
- Oliveira, R. L. de, M. Vazeille, A. M. B. de Filippis, and A.-B. Failloux. 2003. Large genetic differentiation and low variation in vector competence for dengue and yellow fever viruses of Aedes albopictus from Brazil, the United States, and the Cayman Islands.

  American Journal of Tropical Medicine and Hygiene 69:105.
- Paaijmans, K. P., J. I. Blanford, R. G. Crane, M. E. Mann, L. Ning, K. V. Schreiber, and M. B. Thomas. 2014. Downscaling reveals diverse effects of anthropogenic climate warming on the potential for local environments to support malaria transmission. Climatic Change 125:479–488.
- Packierisamy, P. R., C.-W. Ng, M. Dahlui, J. Inbaraj, V. K. Balan, Y. A. Halasa, and D. S. Shepard. 2015. Cost of Dengue Vector Control Activities in Malaysia. The American Journal of Tropical Medicine and Hygiene 93:1020–1027.
- Palatini, U., R. A. Masri, L. V. Cosme, S. Koren, F. Thibaud-Nissen, J. K. Biedler, F. Krsticevic,
  J. S. Johnston, R. Halbach, J. E. Crawford, I. Antoshechkin, A. Failloux, E. Pischedda, M. Marconcini, J. Ghurye, A. Rhie, A. Sharma, D. A. Karagodin, J. Jenrette, S. Gamez, P. Miesen, A. Caccone, M. V. Sharakhova, Z. Tu, P. A. Papathanos, R. P. V. Rij, O. S. Akbari, J. Powell, A. M. Phillippy, and B. M. 2020. Improved reference genome of the arboviral vector Aedes albopictus. bioRxiv:2020.02.28.969527.
- Park, A. W., C. A. Cleveland, T. A. Dallas, and J. L. Corn. 2016. Vector species richness increases haemorrhagic disease prevalence through functional diversity modulating the duration of seasonal transmission. Parasitology 143:874–879.

- Paupy, C., C. Brengues, B. Kamgang, J.-P. Hervé, D. Fontenille, and F. Simard. 2008. Gene flow between domestic and sylvan populations of Aedes aegypti (Diptera: Culicidae) in North Cameroon. Journal of Medical Entomology 45:391–400.
- Paupy, C., N. Chantha, K. Huber, N. Lecoz, J.-M. Reynes, F. Rodhain, and A. B. Failloux. 2004.

  INFLUENCE OF BREEDING SITES FEATURES ON GENETIC DIFFERENTIATION

  OF AEDES AEGYPTI POPULATIONS ANALYZED ON A LOCAL SCALE IN

  PHNOM PENH MUNICIPALITY OF CAMBODIA. The American Journal of Tropical

  Medicine and Hygiene 71:73–81.
- Paupy, C., R. Girod, M. Salvan, F. Rodhain, and A.-B. Failloux. 2001. Population structure of Aedes albopictus from La Réunion Island (Indian Ocean) with respect to susceptibility to a dengue virus. Heredity 87:273–283.
- Paupy, C., G. Le Goff, C. Brengues, M. Guerra, J. Revollo, Z. Barja Simon, J.-P. Hervé, and D. Fontenille. 2012. Genetic structure and phylogeography of Aedes aegypti, the dengue and yellow-fever mosquito vector in Bolivia. Infection, Genetics and Evolution 12:1260–1269.
- Pérez-Díaz, J. L., M. A. Álvarez-Valenzuela, and J. C. García-Prada. 2012. The effect of the partial pressure of water vapor on the surface tension of the liquid water–air interface.

  Journal of Colloid and Interface Science 381:180–182.
- Perkins, T. A., T. W. Scott, A. Le Menach, and D. L. Smith. 2013. Heterogeneity, Mixing, and the Spatial Scales of Mosquito-Borne Pathogen Transmission. PLoS Computational Biology 9.
- Poelchau, M. F., J. A. Reynolds, C. G. Elsik, D. L. Denlinger, and P. A. Armbruster. 2013. Deep sequencing reveals complex mechanisms of diapause preparation in the invasive

- mosquito, Aedes albopictus. Proceedings of the Royal Society B: Biological Sciences 280:20130143.
- Population Division United Nations. 2018. World Urbanization Prospects. https://www.un.org/development/desa/pd/content/urbanization-0.
- Porretta, D., V. Mastrantonio, R. Bellini, P. Somboon, and S. Urbanelli. 2012. Glacial History of a Modern Invader: Phylogeography and Species Distribution Modelling of the Asian Tiger Mosquito Aedes albopictus. PLOS ONE 7:e44515.
- Potter, K. A., H. Arthur Woods, and S. Pincebourde. 2013. Microclimatic challenges in global change biology. Global Change Biology 19:2932–2939.
- R Core Team. 2024. "splines" R package.
- Raharimalala, F. N., L. H. Ravaomanarivo, P. Ravelonandro, L. S. Rafarasoa, K. Zouache, V. Tran-Van, L. Mousson, A.-B. Failloux, E. Hellard, C. V. Moro, B. O. Ralisoa, and P. Mavingui. 2012. Biogeography of the two major arbovirus mosquito vectors, Aedes aegypti and Aedes albopictus (Diptera, Culicidae), in Madagascar. Parasites & Vectors 5:56.
- Rašić, G., N. Endersby-Harshman, W. Tantowijoyo, A. Goundar, V. White, Q. Yang, I. Filipović,
  P. Johnson, A. A. Hoffmann, and E. Arguni. 2015. Aedes aegypti has spatially structured
  and seasonally stable populations in Yogyakarta, Indonesia. Parasites & Vectors 8:610.
- Regilme, M. A. F., T. M. Carvajal, A.-C. Honnen, D. M. Amalin, and K. Watanabe. 2021. The influence of roads on the fine-scale population genetic structure of the dengue vector Aedes aegypti (Linnaeus). PLOS Neglected Tropical Diseases 15:e0009139.
- Reiner, R. C., T. A. Perkins, C. M. Barker, T. Niu, L. F. Chaves, A. M. Ellis, D. B. George, A. L. Menach, J. R. C. Pulliam, D. Bisanzio, C. Buckee, C. Chiyaka, D. A. T. Cummings, A. J.

- Garcia, M. L. Gatton, P. W. Gething, D. M. Hartley, G. Johnston, E. Y. Klein, E. Michael, S. W. Lindsay, A. L. Lloyd, D. M. Pigott, W. K. Reisen, N. Ruktanonchai, B. K. Singh, A. J. Tatem, U. Kitron, S. I. Hay, T. W. Scott, and D. L. Smith. 2013. A systematic review of mathematical models of mosquito-borne pathogen transmission: 1970–2010. Journal of The Royal Society Interface 10:20120921.
- Reiner, R. C., S. T. Stoddard, and T. W. Scott. 2014. Socially structured human movement shapes dengue transmission despite the diffusive effect of mosquito dispersal. Epidemics 6:30–36.
- Reisen, W. K., R. P. Meyer, C. H. Tempelis, and J. J. Spoehel. 1990. Mosquito abundance and bionomics in residential communities in Orange and Los Angeles Counties, California. Journal of Medical Entomology 27:356–367.
- Reisen, W. K., R. M. Takahashi, B. D. Carroll, and R. Quiring. 2008. Delinquent mortgages, neglected swimming pools, and West Nile virus, California. Emerging Infectious Diseases 14:1747–1749.
- Reiter, P. 1998. Aedes albopictus and the world trade in used tires, 1988-1995: the shape of things to come? Journal of the American Mosquito Control Association 14:83–94.
- Richards, S. L., L. Ponnusasmy, T. R. Unnasch, K. Hassan, and C. S. Apperson. 2006. Host-Feeding Patterns of Aedes albopictus (Diptera: Culicidae) in Relation to Availability of Human and Domestic Animals in Suburban Landscapes of Central North Carolina. Journal of medical entomology 43:543–551.
- Richardson, J. L., M. C. Urban, D. I. Bolnick, and D. K. Skelly. 2014. Microgeographic adaptation and the spatial scale of evolution. Trends in Ecology & Evolution 29:165–176.

- Richardson, K., A. A. Hoffmann, P. Johnson, S. Ritchie, and M. R. Kearney. 2011. Thermal Sensitivity of Aedes aegypti From Australia: Empirical Data and Prediction of Effects on Distribution. Journal of Medical Entomology 48:914–923.
- Rochlin, I., D. V. Ninivaggi, M. L. Hutchinson, and A. Farajollahi. 2013. Climate Change and Range Expansion of the Asian Tiger Mosquito (Aedes albopictus) in Northeastern USA: Implications for Public Health Practitioners. PLOS ONE 8:e60874.
- Rochlin, I., G. White, N. Reissen, T. Martheswaran, and A. Faraji. 2022. Effects of aerial adulticiding for mosquito management on nontarget insects: A Bayesian and community ecology approach. Ecosphere 13:e3896.
- Rogers, D. J., J. E. Suk, and J. C. Semenza. 2014. Using global maps to predict the risk of dengue in Europe. Acta Tropica 129:1–14.
- Romeo-Aznar, V., L. Picinini Freitas, O. Gonçalves Cruz, A. A. King, and M. Pascual. 2022. Fine-scale heterogeneity in population density predicts wave dynamics in dengue epidemics. Nature Communications 13:996.
- Romeo-Aznar, V., O. Telle, M. Santos-Vega, R. Paul, and M. Pascual. 2024. Crowded and warmer: Unequal dengue risk at high spatial resolution across a megacity of India. PLOS Climate 3:e0000240.
- Ruan, S., D. Xiao, and J. C. Beier. 2008. On the Delayed Ross–Macdonald Model for Malaria

  Transmission. Bulletin of mathematical biology 70:1098–1114.
- Ruktanonchai, N. W., D. L. Smith, and P. De Leenheer. 2016. Parasite sources and sinks in a patched Ross–Macdonald malaria model with human and mosquito movement:

  Implications for control. Mathematical Biosciences 279:90–101.

- Russell, M. C., C. M. Herzog, Z. Gajewski, C. Ramsay, F. El Moustaid, M. V. Evans, T. Desai, N. L. Gottdenker, S. L. Hermann, A. G. Power, and A. C. McCall. 2022. Both consumptive and non-consumptive effects of predators impact mosquito populations and have implications for disease transmission. eLife 11:e71503.
- Ryan, S. J., C. J. Carlson, B. Tesla, M. H. Bonds, C. N. Ngonghala, E. A. Mordecai, L. R. Johnson, and C. C. Murdock. 2021. Warming temperatures could expose more than 1.3 billion new people to Zika virus risk by 2050. Global Change Biology 27:84–93.
- Salim, M., M. Kamran, I. Khan, A. U. R. Saljoqi, S. Ahmad, M. H. Almutairi, A. A. Sayed, L. Aleya, M. M. Abdel-Daim, and M. Shah. 2023. Effect of larval diets on the life table parameters of dengue mosquito, Aedes aegypti (L.) (Diptera: Culicidae) using age-stage two sex life table theory. Scientific Reports 13:11969.
- Salje, H., J. Lessler, I. Maljkovic Berry, M. C. Melendrez, T. Endy, S. Kalayanarooj, A. A-Nuegoonpipat, S. Chanama, S. Sangkijporn, C. Klungthong, B. Thaisomboonsuk, A.
  Nisalak, R. V. Gibbons, S. Iamsirithaworn, L. R. Macareo, I.-K. Yoon, A. Sangarsang, R.
  G. Jarman, and D. A. T. Cummings. 2017. Dengue diversity across spatial and temporal scales: Local structure and the effect of host population size. Science 355:1302–1306.
- Samuel, M. D., B. L. Woodworth, C. T. Atkinson, P. J. Hart, and D. A. LaPointe. 2015. Avian malaria in Hawaiian forest birds: infection and population impacts across species and elevations. Ecosphere 6:art104.
- Santos-Vega, M., R. Lowe, L. Anselin, V. Desai, K. G. Vaishnav, A. Naik, and M. Pascual. 2023.

  Quantifying climatic and socioeconomic drivers of urban malaria in Surat, India: a

  statistical spatiotemporal modelling study. The Lancet. Planetary Health 7:e985–e998.

- Saucedo, O., and J. H. Tien. 2022. Host movement, transmission hot spots, and vector-borne disease dynamics on spatial networks. Infectious Disease Modelling 7:742–760.
- Schmidt, C. A., G. Comeau, A. J. Monaghan, D. J. Williamson, and K. C. Ernst. 2018. Effects of desiccation stress on adult female longevity in Aedes aegypti and Ae. albopictus (Diptera: Culicidae): results of a systematic review and pooled survival analysis. Parasites & Vectors 11:267.
- Schmidt, T. L., J. Chung, A.-C. Honnen, A. R. Weeks, and A. A. Hoffmann. 2020. Population genomics of two invasive mosquitoes (Aedes aegypti and Aedes albopictus) from the Indo-Pacific. PLOS Neglected Tropical Diseases 14:e0008463.
- Schmidt, T. L., G. Rašić, D. Zhang, X. Zheng, Z. Xi, and A. A. Hoffmann. 2017. Genome-wide SNPs reveal the drivers of gene flow in an urban population of the Asian Tiger Mosquito, Aedes albopictus. PLOS Neglected Tropical Diseases 11:e0006009.
- van Schoor, T., E. T. Kelly, N. Tam, and G. M. Attardo. 2020. Impacts of Dietary Nutritional

  Composition on Larval Development and Adult Body Composition in the Yellow Fever

  Mosquito (Aedes aegypti). Insects 11:535.
- Severson, D. W., and S. K. Behura. 2016. Genome Investigations of Vector Competence in Aedes aegypti to Inform Novel Arbovirus Disease Control Approaches. Insects 7.
- Shah, M. M., A. R. Krystosik, B. A. Ndenga, F. M. Mutuku, J. M. Caldwell, V. Otuka, P. K. Chebii, P. W. Maina, Z. Jembe, C. Ronga, D. Bisanzio, A. Anyamba, R. Damoah, K. Ripp, P. Jagannathan, E. A. Mordecai, and A. D. LaBeaud. 2019. Malaria smear positivity among Kenyan children peaks at intermediate temperatures as predicted by ecological models. Parasites & Vectors 12:288.

- Shepard, D. S., E. A. Undurraga, Y. A. Halasa, and J. D. Stanaway. 2016. The global economic burden of dengue: a systematic analysis. The Lancet Infectious Diseases 16:935–941.
- Sherpa, S., D. Rioux, C. Pougnet-Lagarde, and L. Després. 2018. Genetic diversity and distribution differ between long-established and recently introduced populations in the invasive mosquito *Aedes albopictus*. Infection, Genetics and Evolution 58:145–156.
- Sherpa, S., J. Tutagata, T. Gaude, F. Laporte, S. Kasai, I. H. Ishak, X. Guo, J. Shin, S. Boyer, S.
  Marcombe, T. Chareonviriyaphap, J.-P. David, X.-G. Chen, X. Zhou, and L. Després.
  2022. Genomic Shifts, Phenotypic Clines, and Fitness Costs Associated With Cold
  Tolerance in the Asian Tiger Mosquito. Molecular Biology and Evolution 39:msac104.
- Shocket, M. S., A. B. Verwillow, M. G. Numazu, H. Slamani, J. M. Cohen, F. El Moustaid, J. Rohr, L. R. Johnson, and E. A. Mordecai. 2020. Transmission of West Nile and five other temperate mosquito-borne viruses peaks at temperatures between 23°C and 26°C. eLife 9:e58511.
- Shutt, D. P., D. W. Goodsman, K. Martinez, Z. J. L. Hemez, J. R. Conrad, C. Xu, D. Osthus, C. Russell, J. M. Hyman, and C. A. Manore. 2022. A Process-based Model with Temperature, Water, and Lab-derived Data Improves Predictions of Daily Culex pipiens/restuans Mosquito Density. Journal of Medical Entomology 59:1947–1959.
- Smith, D. L., K. E. Battle, S. I. Hay, C. M. Barker, T. W. Scott, and F. E. McKenzie. 2012. Ross, Macdonald, and a Theory for the Dynamics and Control of Mosquito-Transmitted Pathogens. PLoS Pathogens 8.
- Smith, D. L., A. K. Musiime, K. Maxwell, S. W. Lindsay, and S. Kiware. 2021. A New Test of a Theory about Old Mosquitoes. Trends in parasitology 37:185–194.

- Smith, D. L., T. A. Perkins, L. S. Tusting, T. W. Scott, and S. W. Lindsay. 2013. Mosquito

  Population Regulation and Larval Source Management in Heterogeneous Environments.

  PLOS ONE 8:e71247.
- Smith, N. R., J. M. Trauer, M. Gambhir, J. S. Richards, R. J. Maude, J. M. Keith, and J. A. Flegg. 2018. Agent-based models of malaria transmission: a systematic review. Malaria Journal 17:299.
- Soltani, A., and E. Sharifi. 2017. Daily variation of urban heat island effect and its correlations to urban greenery: A case study of Adelaide. Frontiers of Architectural Research 6:529–538.
- Stein, A., K. Gerstner, and H. Kreft. 2014. Environmental heterogeneity as a universal driver of species richness across taxa, biomes and spatial scales. Ecology Letters 17:866–880.
- Swan, T., T. L. Russell, K. M. Staunton, M. A. Field, S. A. Ritchie, and T. R. Burkot. 2022. A literature review of dispersal pathways of Aedes albopictus across different spatial scales: implications for vector surveillance. Parasites & Vectors 15:303.
- Tan, P. Y., N. H. Wong, C. L. Tan, S. K. Jusuf, M. F. Chang, and Z. Q. Chiam. 2018. A method to partition the relative effects of evaporative cooling and shading on air temperature within vegetation canopy. Journal of Urban Ecology 4.
- Tene Fossog, B., C. Antonio-Nkondjio, P. Kengne, F. Njiokou, N. J. Besansky, and C. Costantini. 2013. Physiological correlates of ecological divergence along an urbanization gradient: differential tolerance to ammonia among molecular forms of the malaria mosquito Anopheles gambiae. BMC Ecology 13:1.
- Tesla, B., L. R. Demakovsky, E. A. Mordecai, S. J. Ryan, M. H. Bonds, C. N. Ngonghala, M. A. Brindley, and C. C. Murdock. 2018. Temperature drives Zika virus transmission:

- evidence from empirical and mathematical models. Proceedings. Biological Sciences 285.
- Tippelt, L., D. Werner, and H. Kampen. 2020. Low temperature tolerance of three Aedes albopictus strains (Diptera: Culicidae) under constant and fluctuating temperature scenarios. Parasites & Vectors 13:587.
- Tjaden, N. B., S. M. Thomas, D. Fischer, and C. Beierkuhnlein. 2013. Extrinsic Incubation

  Period of Dengue: Knowledge, Backlog, and Applications of Temperature Dependence.

  PLoS Neglected Tropical Diseases 7.
- Tokarz, R., and R. J. Novak. 2018. Spatial-temporal distribution of Anopheles larval habitats in Uganda using GIS/remote sensing technologies. Malaria Journal 17:420.
- Urbanelli, S., R. Bellini, M. Carrieri, P. Sallicandro, and G. Celli. 2000. Population structure of Aedes albopictus (Skuse): the mosquito which is colonizing Mediterranean countries.

  Heredity 84:331–337.
- Urbanski, J., M. Mogi, D. O'Donnell, M. DeCotiis, T. Toma, and P. Armbruster. 2012. Rapid Adaptive Evolution of Photoperiodic Response during Invasion and Range Expansion across a Climatic Gradient. The American Naturalist 179:490–500.
- US Department of Commerce, N. 2025. Discussion on Humidity. NOAA's National Weather Service. https://www.weather.gov/lmk/humidity.
- Usmani-Brown, S., L. Cohnstaedt, and L. E. Munstermann. 2009. Population Genetics of Aedes albopictus (Diptera: Culicidae) Invading Populations, Using Mitochondrial nicotinamide Adenine Dinucleotide Dehydrogenase Subunit 5 Sequences. Annals of the Entomological Society of America 102:144–150.

- Vadivalagan, C., P. Karthika, K. Murugan, C. Panneerselvam, M. Paulpandi, P. Madhiyazhagan,
  H. Wei, A. T. Aziz, M. S. Alsalhi, S. Devanesan, M. Nicoletti, R. Paramasivan, D. Dinesh,
  and G. Benelli. 2016. Genetic deviation in geographically close populations of the
  dengue vector Aedes aegypti (Diptera: Culicidae): influence of environmental barriers in
  South India. Parasitology Research 115:1149–1160.
- Valentine, M. J., B. Ciraola, M. T. Aliota, M. Vandenplas, S. Marchi, B. Tenebray, I. Leparc-Goffart, C. A. Gallagher, A. Beierschmitt, T. Corey, K. M. Dore, X. de Lamballerie, C. Wang, C. C. Murdock, and P. J. Kelly. 2020a. No evidence for sylvatic cycles of chikungunya, dengue and Zika viruses in African green monkeys (Chlorocebus aethiops sabaeus) on St. Kitts, West Indies. Parasites & Vectors 13:540.
- Valentine, M. J., B. Ciraola, G. R. Jacobs, C. Arnot, P. J. Kelly, and C. C. Murdock. 2020b.

  Effects of seasonality and land use on the diversity, relative abundance, and distribution of mosquitoes on St. Kitts, West Indies. Parasites & Vectors 13:543.
- Valentine, M. J., C. C. Murdock, and P. J. Kelly. 2019. Sylvatic cycles of arboviruses in non-human primates. Parasites & Vectors 12:463.
- Valerio, L., F. Marini, G. Bongiorno, L. Facchinelli, M. Pombi, B. Caputo, M. Maroli, and A. Della Torre. 2010. Host-feeding patterns of Aedes albopictus (Diptera: Culicidae) in urban and rural contexts within Rome province, Italy. Vector Borne and Zoonotic Diseases (Larchmont, N.Y.) 10:291–294.
- Vavassori, L., A. Saddler, and P. Müller. 2019. Active dispersal of Aedes albopictus: a mark-release-recapture study using self-marking units. Parasites & Vectors 12:583.
- Vazeille, M., L. Mousson, I. Rakatoarivony, R. Villeret, F. Rodhain, J. B. Duchemin, and A. B. Failloux. 2001. Population genetic structure and competence as a vector for dengue type

- 2 virus of Aedes aegypti and Aedes albopictus from Madagascar. The American Journal of Tropical Medicine and Hygiene 65:491–497.
- Vega-Rúa, A., M. Marconcini, Y. Madec, M. Manni, D. Carraretto, L. M. Gomulski, G. Gasperi, A.-B. Failloux, and A. R. Malacrida. 2020. Vector competence of Aedes albopictus populations for chikungunya virus is shaped by their demographic history.
  Communications Biology 3:1–13.
- Verdonschot, P. F. M., and A. A. Besse-Lototskaya. 2014. Flight distance of mosquitoes (Culicidae): A metadata analysis to support the management of barrier zones around rewetted and newly constructed wetlands. Limnologica 45:69–79.
- Vontas, J., E. Kioulos, N. Pavlidi, E. Morou, A. della Torre, and H. Ranson. 2012. Insecticide resistance in the major dengue vectors *Aedes albopictus* and *Aedes aegypti*. Pesticide Biochemistry and Physiology 104:126–131.
- Vyhmeister, E., G. Provan, B. Doyle, and B. Bourke. 2020. Multi-cluster and environmental dependant vector born disease models. Heliyon 6:e04090.
- Wang, B.-G., L. Qiang, and Z.-C. Wang. 2019. An almost periodic Ross–Macdonald model with structured vector population in a patchy environment. Journal of Mathematical Biology.
- Wang, G.-H., J. Du, C. Y. Chu, M. Madhav, G. L. Hughes, and J. Champer. 2022. Symbionts and gene drive: two strategies to combat vector-borne disease. Trends in Genetics 38:708–723.
- Wei, Y., S. He, J. Wang, P. Fan, Y. He, K. Hu, Y. Chen, G. Zhou, D. Zhong, and X. Zheng. 2022. .

  Frontiers in Public Health 10:1028026.

- Wei, Y., J. Wang, Z. Song, Y. He, Z. Zheng, P. Fan, D. Yang, G. Zhou, D. Zhong, and X. Zheng. 2019. Patterns of spatial genetic structures in Aedes albopictus (Diptera: Culicidae) populations in China. Parasites & Vectors 12:552.
- Westbrook, C. J., M. H. Reiskind, K. N. Pesko, K. E. Greene, and L. P. Lounibos. 2010. Larval environmental temperature and the susceptibility of Aedes albopictus Skuse (Diptera: Culicidae) to chikungunya virus. Vector-Borne and Zoonotic Diseases 10:241–247.
- Whitlock, M. C., and K. E. Lotterhos. 2015. Reliable Detection of Loci Responsible for Local Adaptation: Inference of a Null Model through Trimming the Distribution of F(ST). The American Naturalist 186 Suppl 1:S24-36.
- Whittaker, C., P. Winskill, M. Sinka, S. Pironon, C. Massey, D. J. Weiss, M. Nguyen, P. W. Gething, A. Kumar, A. Ghani, and S. Bhatt. (n.d.). A novel statistical framework for exploring the population dynamics and seasonality of mosquito populations. Proceedings of the Royal Society B: Biological Sciences 289:20220089.
- Wilke, A. B. B., C. Chase, C. Vasquez, A. Carvajal, J. Medina, W. D. Petrie, and J. C. Beier. 2019. Urbanization creates diverse aquatic habitats for immature mosquitoes in urban areas. Scientific Reports 9.
- Wilke, A. B. B., C. Vasquez, W. Petrie, A. J. Caban-Martinez, and J. C. Beier. 2018. Construction sites in Miami-Dade County, Florida are highly favorable environments for vector mosquitoes. PLOS ONE 13:e0209625.
- Wilke, A. B. B., R. Wilk-da-Silva, and M. T. Marrelli. 2017. Microgeographic population structuring of Aedes aegypti (Diptera: Culicidae). PLOS ONE 12:e0185150.
- Williams, C. R., P. H. Johnson, S. A. Long, L. P. Rapley, and S. A. Ritchie. 2008. Rapid estimation of Aedes aegypti population size using simulation modeling, with a novel

- approach to calibration and field validation. Journal of Medical Entomology 45:1173–1179.
- Willoughby, J. R., B. A. McKenzie, J. Ahn, T. D. Steury, C. A. Lepzcyk, and S. Zohdy. 2024.

  Assessing and managing the risk of Aedes mosquito introductions via the global maritime trade network. PLOS Neglected Tropical Diseases 18:e0012110.
- Wimberly, M. C., J. K. Davis, M. V. Evans, A. Hess, P. M. Newberry, N. Solano-Asamoah, and C. C. Murdock. 2020. Land cover affects microclimate and temperature suitability for arbovirus transmission in an urban landscape. PLOS Neglected Tropical Diseases 14:e0008614.
- Womack, M. L., T. S. Thuma, and B. R. Evans. 1995. Distribution of Aedes albopictus in Georgia, USA. Journal of the American Mosquito Control Association 11:237.
- World Health Organization. (n.d.). Current state: The malaria situation worldwide. https://worldmalariareport2024.org.
- World Health Organization and UNICEF/UNDP/World Bank/WHO Special Programme for Research and Training in Tropical Diseases. 2017. Global vector control response 2017-2030. World Health Organization, Geneva.
- Wu, S. L., J. M. Henry, D. T. Citron, D. M. Ssebuliba, J. N. Nsumba, H. M. S. C, O. J. Brady, C. A. Guerra, G. A. García, A. R. Carter, H. M. Ferguson, B. E. Afolabi, S. I. Hay, R. C. R. Jr, S. Kiware, and D. L. Smith. 2023. Spatial dynamics of malaria transmission. PLOS Computational Biology 19:e1010684.
- Wu, S. L., H. M. Sánchez C., J. M. Henry, D. T. Citron, Q. Zhang, K. Compton, B. Liang, A. Verma, D. A. T. Cummings, A. Le Menach, T. W. Scott, A. L. Wilson, S. W. Lindsay, C. L. Moyes, P. A. Hancock, T. L. Russell, T. R. Burkot, J. M. Marshall, S. Kiware, R. C.

- Reiner, and D. L. Smith. 2020. Vector bionomics and vectorial capacity as emergent properties of mosquito behaviors and ecology. PLoS Computational Biology 16:e1007446.
- Yan, M., L. Chen, S. Leng, and R. Sun. 2023. Effects of local background climate on urban vegetation cooling and humidification: Variations and thresholds. Urban Forestry & Urban Greening 80:127840.
- Yang, D., Y. He, W. Ni, Q. Lai, Y. Yang, J. Xie, T. Zhu, G. Zhou, and X. Zheng. 2020. Semi-field life-table studies of Aedes albopictus (Diptera: Culicidae) in Guangzhou, China. PLOS ONE 15:e0229829.
- Yeo, H., H. Z. Tan, Q. Tang, T. R. H. Tan, N. Puniamoorthy, and F. E. Rheindt. 2023. Dense residential areas promote gene flow in dengue vector mosquito *Aedes albopictus*. iScience 26:107577.
- Yoon, I.-K., A. Getis, J. Aldstadt, A. L. Rothman, D. Tannitisupawong, C. J. M. Koenraadt, T. Fansiri, J. W. Jones, A. C. Morrison, R. G. Jarman, A. Nisalak, M. P. Mammen, S. Thammapalo, A. Srikiatkhachorn, S. Green, D. H. Libraty, R. V. Gibbons, T. Endy, C. Pimgate, and T. W. Scott. 2012. Fine Scale Spatiotemporal Clustering of Dengue Virus Transmission in Children and Aedes aegypti in Rural Thai Villages. PLoS Neglected Tropical Diseases 6:e1730.
- Zhang, H.-D., J. Gao, C.-X. Li, Z. Ma, Y. Liu, G. Wang, Q. Liu, D. Xing, X.-X. Guo, T. Zhao, Y.-T. Jiang, Y.-D. Dong, and T.-Y. Zhao. 2022a. Genetic Diversity and Population Genetic Structure of Aedes albopictus in the Yangtze River Basin, China. Genes 13:1950.
- Zhang, H.-D., J. Gao, D. Xing, X.-X. Guo, C.-X. Li, Y.-D. Dong, Z. Zheng, Z. Ma, Z.-M. Wu, X.-J. Zhu, M.-H. Zhao, Q.-M. Liu, T. Yan, H.-L. Chu, and T.-Y. Zhao. 2022b. Fine-scale

- genetic structure and wolbachia infection of aedes albopictus (Diptera: Culicidae) in Nanjing city, China. Frontiers in Genetics 13.
- Zhao, M., X. Ran, D. Xing, W. Liu, Z. Ma, Y. Liao, Q. Zhang, Y. Bai, L. Liu, K. Chen, M. Wu, J. Gao, H. Zhang, and T. Zhao. 2024. Population genetics of *Aedes albopictus* in the port cities of Hainan Island and Leizhou Peninsula, China. Infection, Genetics and Evolution 117:105539.
- Zhao, N., K. Charland, M. Carabali, E. O. Nsoesie, M. Maheu-Giroux, E. Rees, M. Yuan, C. G. Balaguera, G. J. Ramirez, and K. Zinszer. 2020. Machine learning and dengue forecasting: Comparing random forests and artificial neural networks for predicting dengue burden at national and sub-national scales in Colombia. PLoS Neglected Tropical Diseases 14:e0008056.
- Zhong, D., E. Lo, R. Hu, M. E. Metzger, R. Cummings, M. Bonizzoni, K. K. Fujioka, T. E. Sorvillo, S. Kluh, S. P. Healy, C. Fredregill, V. L. Kramer, X. Chen, and G. Yan. 2013. Genetic Analysis of Invasive Aedes albopictus Populations in Los Angeles County, California and Its Potential Public Health Impact. PLOS ONE 8:e68586.
- Zimmerman, S. J., C. L. Aldridge, and S. J. Oyler-McCance. 2020. An empirical comparison of population genetic analyses using microsatellite and SNP data for a species of conservation concern. BMC Genomics 21:382.

## APPENDIX A

## CHAPTER 3 SUPPLEMENTARY INFORMATION

**Supplementary Table A.1.** All study site variable correlations for both 7-day lags and 14-day lags with positive larval habitat characteristics and land cover traits.

	Larval Habitats	Temp14Min	Temp14Max	Temp14DTR	Temp14Avg	RH14Min	RH14Max	RH14Flux	RH14Avg	Temp7Min	Тетр7Мах	Temp7DTR	Temp7Avg	RH7Min	RH7Мах	RH7Flux	RH7Avg	Imp500m	Can100m
LarvalHabitats	1.000	0.295	-0.033	-0.352	0.197	0.354	0.104	-0.324	0.308	0.285	-0.058	-0.327	0.188	0.329	0.066	-0.332	0.302	-0.336	0.341
Temp14Min	0.295	1.000	0.398	-0.464	0.819	0.418	0.108	-0.368	0.288	0.969	0.459	-0.446	0.895	0.402	0.059	-0.408	0.324	0.071	-0.040
Temp14Max	-0.033	0.398	1.000	0.093	0.701	-0.115	0.581	-0.027	0.217	0.395	0.826	0.464	0.553	-0.356	0.137	0.387	-0.165	0.226	-0.369
Temp14DTR	-0.352	-0.464	0.093	1.000	-0.441	-0.864	-0.505	0.900	-0.739	-0.440	0.343	0.760	-0.241	-0.618	-0.042	0.635	-0.468	0.462	-0.482
Temp14Avg	0.197	0.819	0.701	-0.441	1.000	0.298	0.429	-0.386	0.406	0.817	0.620	-0.141	0.860	0.086	0.033	-0.084	0.071	0.104	-0.182
RH14Min	0.354	0.418	-0.115	-0.864	0.298	1.000	0.445	-0.965	0.851	0.385	-0.316	-0.681	0.145	0.807	0.265	-0.801	0.730	-0.602	0.624
RH14Max	0.104	0.108	0.581	-0.505	0.429	0.445	1.000	-0.617	0.712	0.101	0.114	0.020	0.103	0.021	0.295	0.017	0.154	-0.320	0.172
RH14Flux	-0.324	-0.368	-0.027	0.900	-0.386	-0.965	-0.617	1.000	-0.909	-0.339	0.261	0.583	-0.136	-0.672	-0.185	0.671	-0.609	0.584	-0.573
RH14Avg	0.308	0.288	0.217	-0.739	0.406	0.851	0.712	-0.909	1.000	0.250	-0.111	-0.348	0.079	0.514	0.348	-0.486	0.628	-0.579	0.500
Temp7Min	0.285	0.969	0.395	-0.440	0.817	0.385	0.101	-0.339	0.250	1.000	0.477	-0.457	0.937	0.417	0.097	-0.420	0.336	0.072	-0.052
Temp7Max	-0.058	0.459	0.826	0.343	0.620	-0.316	0.114	0.261	-0.111	0.477	1.000	0.564	0.680	-0.434	0.028	0.454	-0.291	0.371	-0.451
Temp7DTR	-0.327	-0.446	0.464	0.760	-0.141	-0.681	0.020	0.583	-0.348	-0.457	0.564	1.000	-0.193	-0.832	-0.062	0.853	-0.610	0.307	-0.408
Temp7Avg	0.188	0.895	0.553	-0.241	0.860	0.145	0.103	-0.136	0.079	0.937	0.680	-0.193	1.000	0.126	0.043	-0.125	0.058	0.222	-0.254
RH7Min	0.329	0.402	-0.356	-0.618	0.086	0.807	0.021	-0.672	0.514	0.417	-0.434	-0.832	0.126	1.000	0.329	-0.992	0.888	-0.451	0.532
RH7Max	0.066	0.059	0.137	-0.042	0.033	0.265	0.295	-0.185	0.348	0.097	0.028	-0.062	0.043	0.329	1.000	-0.209	0.569	-0.301	0.182
RH7Flux	-0.332	-0.408	0.387	0.635	-0.084	-0.801	0.017	0.671	-0.486	-0.420	0.454	0.853	-0.125	-0.992	-0.209	1.000	-0.845	0.428	-0.527
RH7Avg	0.302	0.324	-0.165	-0.468	0.071	0.730	0.154	-0.609	0.628	0.336	-0.291	-0.610	0.058	0.888	0.569	-0.845	1.000	-0.493	0.503
lmp500m	-0.336	0.071	0.226	0.462	0.104	-0.602	-0.320	0.584	-0.579	0.072	0.371	0.307	0.222	-0.451	-0.301	0.428	-0.493	1.000	-0.848
Can100m	0.341	-0.040	-0.369	-0.482	-0.182	0.624	0.172	-0.573	0.500	-0.052	-0.451	-0.408	-0.254	0.532	0.182	-0.527	0.503	-0.848	1.000

**Supplementary Table A.2.** Average study site temperature and relative humidity variables during study period displayed with standard deviation (+/-).

Site	Temp14DTR	Temp14Min	Temp14Avg	Temp14Max	RH14Flux	RH14Min	RH14Avg	RH14Max
ВС	14.83+/-2.55	19.45+/-3.69	24.7+/-3.2	34.28+/-3.05	53.31+/-5.68	45.61+/-6.15	78.78+/-4.88	98.92+/-1.52
CC	12.86+/-2.18	18.31+/-3.94	22.87+/-3.12	31.17+/-2.9	43.81+/-6.47	55.75+/-6.98	85.14+/-5.31	99.56+/-0.65
DD	18.19+/-8.57	19.15+/-3.43	21.39+/-5.98	28.19+/-8.19	63+/-24.4	41.63+/-14.14	68.61+/-18.23	84.9+/-21.67
DP	8.91+/-2.63	18.24+/-3.43	21.73+/-2.64	27.15+/-1.23	29.2+/-8.67	70.58+/-8.84	92+/-4.97	99.78+/-0.35
FR	13.78+/-3.58	18.15+/-3.82	22.92+/-2.83	31.93+/-1.16	44.56+/-7.62	55.42+/-7.63	88.01+/-4.23	99.98+/-0.07
GPE	15.58+/-3.6	18.17+/-3.99	23.31+/-3.12	33.76+/-3.74	49.43+/-8.5	50.23+/-8.66	82.96+/-5.09	99.65+/-0.80
GPR	19.23+/-3.55	17.53+/-4.37	23.83+/-3.11	36.76+/-2.62	53.58+/-7.98	46.27+/-8.27	82.98+/-5.46	99.85+/-0.46
MD	17.42+/-2.88	18.65+/-3.83	24.93+/-3.28	36.07+/-4.26	56.17+/-7.72	43.33+/-7.67	78.79+/-5.18	99.5+/-1.27
NDH	16.61+/-3.22	18.26+/-3.94	23.94+/-3.11	34.86+/-1.54	51.18+/-7.49	48.59+/-7.69	82.66+/-4.45	99.77+/-0.40
NDS	18.93+/-3.30	18.18+/-3.66	24.31+/-3.05	37.12+/-3.76	55.18+/-7.29	44.73+/-7.37	80.91+/-4.81	99.9+/-0.19
PPR	13.85+/-2.83	18.39+/-4.23	23.7+/-3.23	32.24+/-2.36	49.38+/-6.73	49.56+/-7.59	79.85+/-4.99	98.94+/-1.51
WG	13.3+/-3.06	18.49+/-3.78	22.54+/-2.88	31.79+/-2.44	39.51+/-7.79	60.42+/-7.85	88.47+/-5.31	99.93+/-0.20

**Supplementary Table A.3.** Average monthly temperature and relative humidity variables across site displayed with standard deviation calculated with (a) 7-day and (b) 14-day lags.

a.	Month	Temp7DTR	Temp7Min	Temp7Avg	Temp7Max	RH7Min	RH7Avg	RH7Max
	June	15.63+/-3.44	19.61+/-1.38	25.76+/-1.99	35.24+/-3.73	45.35+/-9.31	76.2+/-6.45	98.16+/-2.39
	July	13.72+/-5	21.73+/-0.52	25.91+/-1.37	35.45+/-5.11	58.15+/-9.66	88.69+/-4.18	99.99+/-0.03
	August	12.23+/-3.82	20.69+/-0.62	24.86+/-1.32	32.92+/-4.14	61.72+/-12.2	89.24+/-5.38	99.97+/-0.09
	September	16.14+/-3.64	17.82+/-1.37	23.39+/-1.23	33.96+/-3.37	49.56+/-7.45	82.47+/-4.73	99.86+/-0.5
	October	18.84+/-3.75	10.23+/-0.76	17.1+/-0.74	29.07+/-3.32	42.89+/-8.07	79.07+/-4.63	99.14+/-1.74
b.	Month	Temp14DTR	Temp14Min	Temp14Avg	Temp14Max	RH14Min	RH14Avg	RH14Max
	June	14.69+/-3.17	19.56+/-0.68	25.12+/-1.24	34.25+/-3.14	47.7+/-7.84	78.42+/-4.97	98.59+/-1.66
	July	13.41+/-3.82	3.82+/-21.52	25.8+/-1.35	34.93+/-4.06	56.38+/-9.1	86.98+/-4.73	99.83+/-0.44
	August	13.78+/-4.93	4.93+/-20.5	24.22+/-3.14	32.98+/-4.15	56.71+/-12.8	85.73+/-11.96	98.51+/-7.23
	September	15.38+/-4.77	4.77+/-18.87	23.45+/-2.65	32.94+/-4.66	52.44+/-10.05	83.17+/-9.52	98.1+/-9.01
	October	19.2+/-4.26	4.26+/-11.62	18.15+/-1.14	29.62+/-5.07	41.82+/-9.57	77.84+/-7.43	96.93+/-11.52

**Supplementary Table A.4.** Adult Abundance Models Performance. Models are ranked by AIC performance. Models significantly different from the null model, passing uniformity/dispersion tests via DHARMa, and converging are marked in green. Models not significantly different from the null model or failing uniformity/dispersion tests via DHARMa are marked in orange. Models

Response Variable	Fixed Effects	Fixed Effect Interactions	Random Effects	AIC	DHARMa Problem?	Diff. Null?	df. resid	Significant Effects
alboTotalA	s(RH14Min) + s(Temp14DTR) + Imp500m		Site, Month/Year	946.2	N	Y	109	Imp500m: 0.007734 ** , RH14Min: 4.35e-06 ***, Temp14DTR: 0.000175 ***
alboTotalA	s(RH14Flux) + s(Temp14DTR) + Imp500m		Site, Month/Year	947.5	Y	Y	110	Imp500m: 0.01893 *, Temp14DTR: 0.00307 **
alboTotalA	s(RH14Min) + s(Temp14DTR) + Imp500m	RH14Min: Temp14DTR	Site, Month/Year	947.8	N	Y	109	Imp500m: 0.00912 **, RH14Min: 0.00106 **, Temp14DTR: 0.02188 *
alboTotalA	s(RH7Flux) + s(Temp7DTR) + Imp500m	RH7Flux: Temp7DTR	Site, Month/Year	948.6	N	Y	109	RH7Flux:Temp7DTR: 0.03674 *, Temp7DTR: 0.00652 **
alboTotalA	s(RH14Flux) + s(Temp14DTR) + Imp500m	RH14Flux: Temp14DTR	Site, Month/Year	949.5	Y	Y	109	Imp500m; 0.0207 *
alboTotalA	s(RH14Flux) + s(Temp14DTR) + Can100m		Site, Month/Year	950	Y	Y	110	Temp14DTR: 0.00557 **
alboTotalA	s(RH7Flux) + s(Temp7DTR) + Can100m	RH7Flux: Temp7DTR	Site, Month/Year	950.2	Y	Y	109	none
alboTotalA	s(RH14Min) + s(Temp14DTR) + Can100m		Site, Month/Year	950.2	N	Y	110	Temp14DTR: 0.000732 ***
alboTotalA	s(RH7Min) + s(Temp7DTR) + Imp500m	RH7Min: Temp7DTR	Site, Month/Year	950.3	Y	Y	109	none

Response Variable	Fixed Effects	Fixed Effect Interactions	Random Effects	AIC	DHARMa Problem?	Diff. Null?	df. resid	Significant Effects
alboTotalA	s(RH7Flux) + s(Temp7DTR) + Imp500m		Site, Month/Year	950.3	N	Y	110	RH7Flux: 0.01213 * , Temp7DTR: 0.01705 *
alboTotalA	s(RH7Min) + s(Temp7DTR) + Imp500m		Site, Month/Year	951	Y	N	110	RH7Min:0.000318 ***, Temp7DTR:0.023369 *
alboTotalA	s(RH14Min) + s(Temp14DTR) + Can100m	RH14Min: Temp14DTR	Site, Month/Year	951.2	N	Y	109	RH14Min: 0.00228 **, Temp14DTR: 0.03180 *
alboTotalA	s(RH7Min) + s(Temp7DTR) + Can100m	RH7Min: Temp7DTR	Site, Month/Year	951.9	Y	Y	109	RH7Min:Temp7DTR: 0.0469 *
alboTotalA	s(RH14Flux) + s(Temp14DTR) + Can100m	RH14Flux: Temp14DTR	Site, Month/Year	951.9	Y	Y	109	none
alboTotalA	s(RH7Flux) + s(Temp7DTR) +		Site, Month/Year	952.1	Υ	Y	110	RH7Flux: 0.0174 * , Temp7DTR:0.0183 *
alboTotalA	s(RH14Flux) + Imp500m		Site, Month/Year	953.4	Υ	N	112	none
alboTotalA	s(RH14Flux)		Site, Month/Year	953.5	Y	N	113	none
alboTotalA	s(RH7Flux)		Site, Month/Year	953.6	Y	N	113	none

Response Variable	Fixed Effects	Fixed Effect Interactions	Random Effects	AIC	DHARMa Problem?	Diff. Null?	df. resid	Significant Effects
alboTotalA	s(RH7Min) + s(Temp7DTR) +		Site, Month/Year	953.6	N	N	110	RH7Min: 0.00046 ***, Temp7DTR: 0.02832 *
alboTotalA	s(RH7Flux) + Imp500m		Site, Month/Year	953.8	N	N	112	RH7Flux: 0.00671 **
alboTotalA	s(RH7Min)		Site, Month/Year	953.9	N	N	113	RH7Min: 0.0153 *
alboTotalA	s(RH7Min) + Imp500m		Site, Month/Year	953.9	N	N	112	RH7Min: 0.00621 **
alboTotalA	s(RH14Flux) + Can100m		Site, Month/Year	954.5	Υ	N	112	
alboTotalA	s(RH7Flux) + Can100m		Site, Month/Year	955.1	N	N	112	none
alboTotalA	s(RH7Min) + Can100m		Site, Month/Year	955.3	N	N	112	RH7Min: 0.0101 *
alboTotalA	lmp500m + Can100m		Site, Month/Year	956.1	Y	N	113	none
alboTotalA	s(RH14Min)		Site, Month/Year	956.3	Y	N	113	none
alboTotalA	s(RH14Min) + Can100m		Site, Month/Year	957.9	na	na	na	**no convergence**

Response Variable	Fixed Effects	Fixed Effect Interactions	Random Effects	AIC	DHARMa Problem?	Diff. Null?	df. resid	Significant Effects
alboTotalA	s(Temp14DTR)		Site, Month/Year	957.9	Y	N	113	none
alboTotalA	Imp500m + Can100m	Imp500m: Can100m	Site, Month/Year	958	Υ	N	112	none
alboTotalA	s(Temp7DTR)		Site, Month/Year	958.1	Y	N	113	none
alboTotalA	s(RH14Min) + Imp500m		Site, Month/Year	no converg ence	na	na	na	**no convergence**
alboTotalA	Can100m		Site, Month/Year	956.1	Υ	N	114	none
alboTotalA	lmp500m		Site, Month/Year	955.4	Y	N	114	none

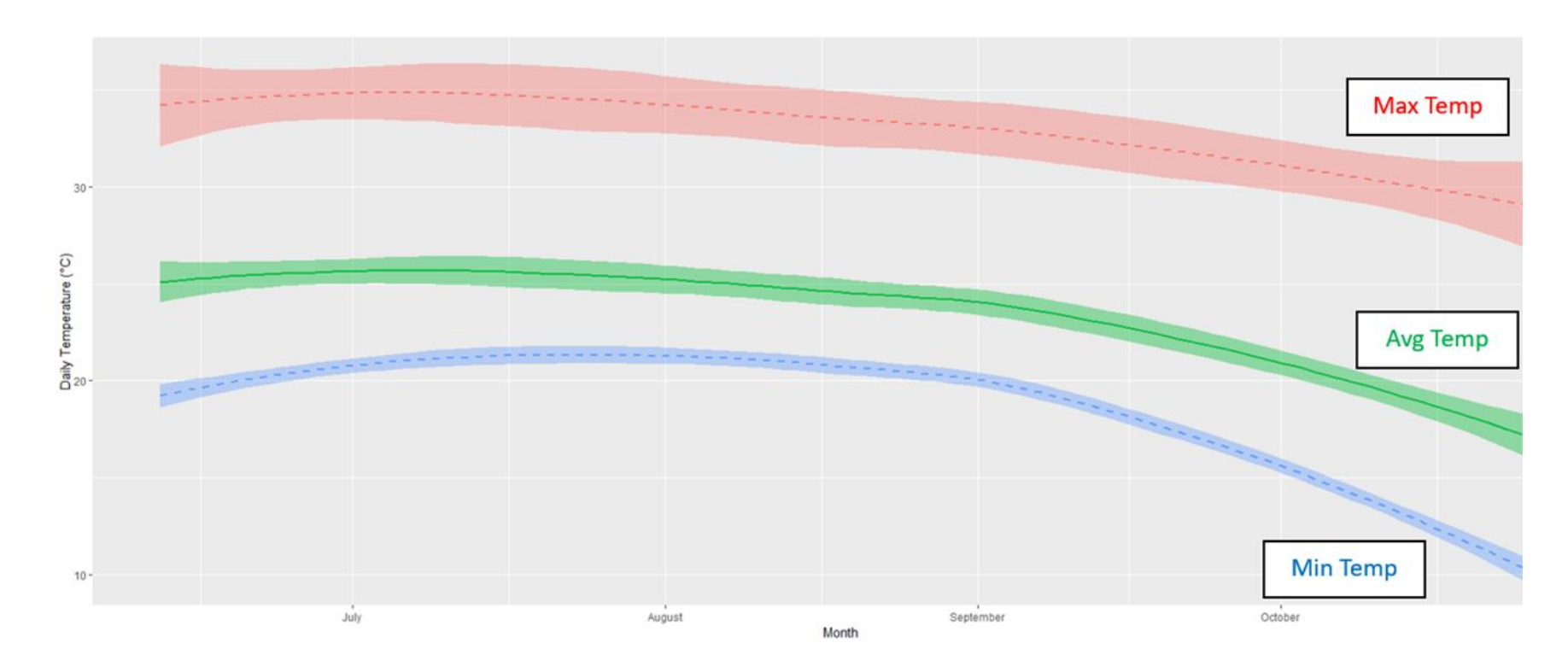
**Supplementary Table 5.** Larval Habitat Density Models Performance. Models are ranked by AIC performance. Models significantly different from the null model, passing uniformity/dispersion tests via DHARMa, and converging are marked in green. Models not significantly different from the null model or failing uniformity/dispersion tests via DHARMa are marked in orange. Models failing to converge are colored in grey.

Response	Fixed Effects	Fixed Effect Interactions	Random Effects	AIC	DHARMa Problem?	Different from Null Model?	df.resid	Significant Effects
LarvalHabitats	Can100m		Site, Month/Year	292.7	N	Y	113	Can100m: 0.0194 *
LarvalHabitats	s(RH14Min) + Imp500m		Site, Month/Year	293.1	N	N	112	RH14Min: 0.0152 *
LarvalHabitats	s(Temp7Min)		Site, Month/Year	293.6	N	N	113	Temp7Min: 9.89e-06***
LarvalHabitats	s(Temp14DTR)		Site, Month/Year	294.3	N	N	113	Temp14DTR: 0.0251 *
LarvalHabitats	s(RH14Flux) + Imp500m		Site, Month/Year	294.5		N	112	none
LarvalHabitats	Imp500m		Site, Month/Year	294.6	Y	N	114	Imp500m: 0.0476 *
LarvalHabitats	Imp500m+ Can100m		Site, Month/Year	294.7	Y	N	113	none
LarvalHabitats	Imp500m+ Can100m	Imp500m: Can100m	Site, Month/Year	294.7	Y	N	113	none
LarvalHabitats	s(RH14Min) + s(Temp14DTR) + Can100m		Site, Month/Year	295.4	N	N	110	none
LarvalHabitats	Temp7Avg		Site, Month/Year	295.9	N	N	114	Temp7Avg
LarvalHabitats	RH14Max		Site, Month/Year	295.9	N	N	114	none
LarvalHabitats	s(RH14Min) + s(Temp14DTR) + Imp500m		Site, Month/Year	296.5	Y	N	110	none
LarvalHabitats	s(RH14Min) + s(Temp14DTR) + Can100m	RH14Min: Temp14DTR	Site, Month/Year	297.4	Y	N	109	none

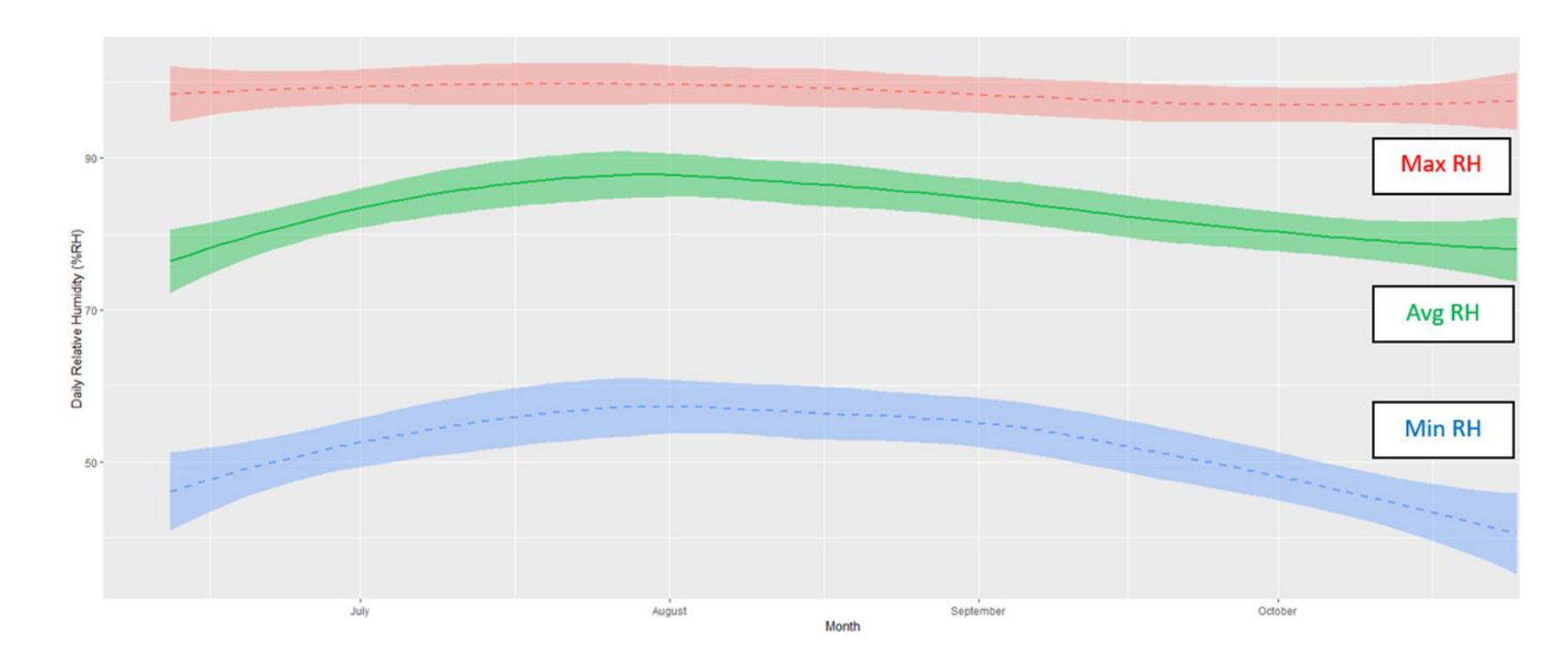
Response	Fixed Effects	Fixed Effect Interactions	Random Effects	AIC	DHARMa Problem?	Different from Null Model?	df.resid	Significant Effects
LarvalHabitats	s(RH7Max)		Site, Month/Year	298.1	N	N	114	none
LarvalHabitats	Temp14Avg		Site, Month/Year	298.3	N	N	114	none
LarvalHabitats	s(RH7Flux) + Imp500m		Site, Month/Year	298.5	Y	N	112	none
LarvalHabitats	s(RH14Min) + s(Temp14DTR) + Imp500m	RH14Min: Temp14DTR	Site, Month/Year	298.5	N	N	109	none
LarvalHabitats	s(RH14Flux) + s(Temp14DTR) +	RH14Flux: Temp14DTR	Site, Month/Year	299.2	N	N	109	none
LarvalHabitats	s(RH7Min)		Site, Month/Year	300	N	N	113	none
LarvalHabitats	s(RH7Flux)		Site, Month/Year	300.1	N	N	113	none
LarvalHabitats	s(Temp7Max)		Site, Month/Year	300.3	N	N	113	none
LarvalHabitats	s(RH7Min) + s(Temp7DTR) + Imp500m		Site, Month/Year	302.4	Y	N	110	none
LarvalHabitats	s(RH7Flux) + s(Temp7DTR) + Imp500m		Site, Month/Year	302.4	Y	N	110	none
LarvalHabitats	s(RH7Flux) + s(Temp7DTR) + Can100m	RH7Flux: Temp7DTR	Site, Month/Year	302.5	Y	N	109	Can100m: 0.025 *

Response	Fixed Effects	Fixed Effect Interactions	Random Effects	AIC	DHARMa Problem?	Different from Null Model?	df.resid	Significant Effects
LarvalHabitats	s(RH7Min) + s(Temp7DTR) +	RH7Min: Temp7DTR	Site, Month/Year	302.6	Y	N	109	Can100m: 0.0258 *
LarvalHabitats	s(RH7Flux) + s(Temp7DTR) + Imp500m	RH7Flux: Temp7DTR	Site, Month/Year	304.3	Y	N	109	none
LarvalHabitats	s(Temp7DTR)		Site, Month/Year	na	na	na	na	**no convergence**
LarvalHabitats	s(RH7Min) + s(Temp7DTR) + Imp500m	RH7Min:Temp 7DTR	Site, Month/Year	na	na	na	na	**no convergence**
LarvalHabitats	s(RH7Min) + s(Temp7DTR) +		Site, Month/Year	na	na	na	na	**no convergence**
LarvalHabitats	s(RH7Flux) + s(Temp7DTR) +		Site, Month/Year	na	na	na	na	**no convergence**
LarvalHabitats	s(RH7Min) + Can100m		Site, Month/Year	na	na	na	na	**no convergence**
LarvalHabitats	s(RH7Min) + Imp500m		Site, Month/Year	na	na	na	na	**no convergence**
LarvalHabitats	s(RH7Flux) + Can100m		Site, Month/Year	na	na	na	na	**no convergence**
LarvalHabitats	s(RH14Flux) + s(Temp14DTR) +		Site, Month/Year	na	na	na	na	**no convergence**
LarvalHabitats	s(RH14Flux) + s(Temp14DTR) +	RH14Flux: Temp14DTR	Site, Month/Year	na	na	na	na	**no convergence**

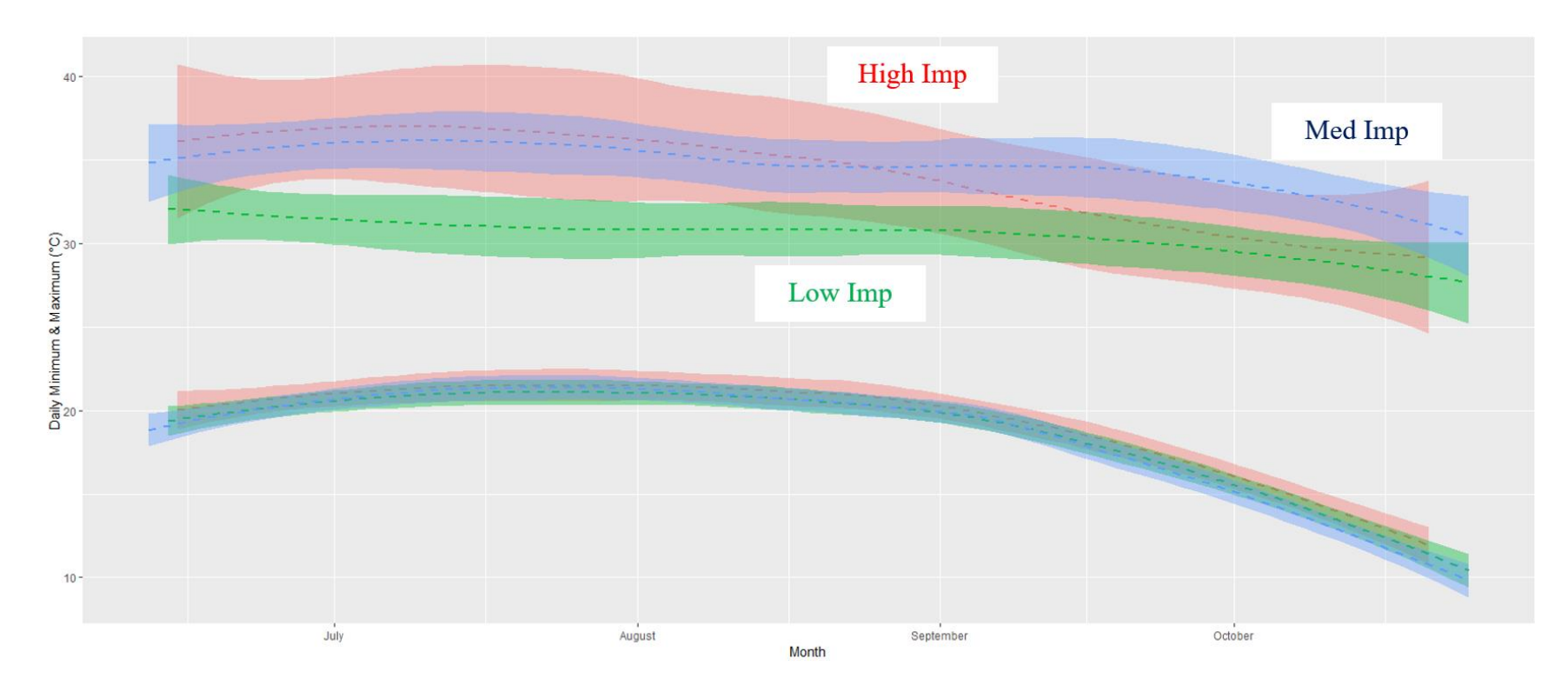
Response	Fixed Effects	Fixed Effect	Random	AIC	DHARMa	Different from	df.resid	Significant Effects
		Interactions	Effects		Problem?	Null Model?		
LarvalHabitats	s(RH14Flux) +		Site,	na	na	na	na	**no convergence**
	Can100m		Month/Year					
LarvalHabitats	s(RH14Min) +		Site,	na	na	na	na	**no convergence**
	Can100m		Month/Year					
LarvalHabitats	s(RH14Flux)		Site,	na			na	**no convergence**
			Month/Year		na	na		
LarvalHabitats	s(RH14Min)		Site,	i na	na	na	na	**no convergence**
			Month/Year					



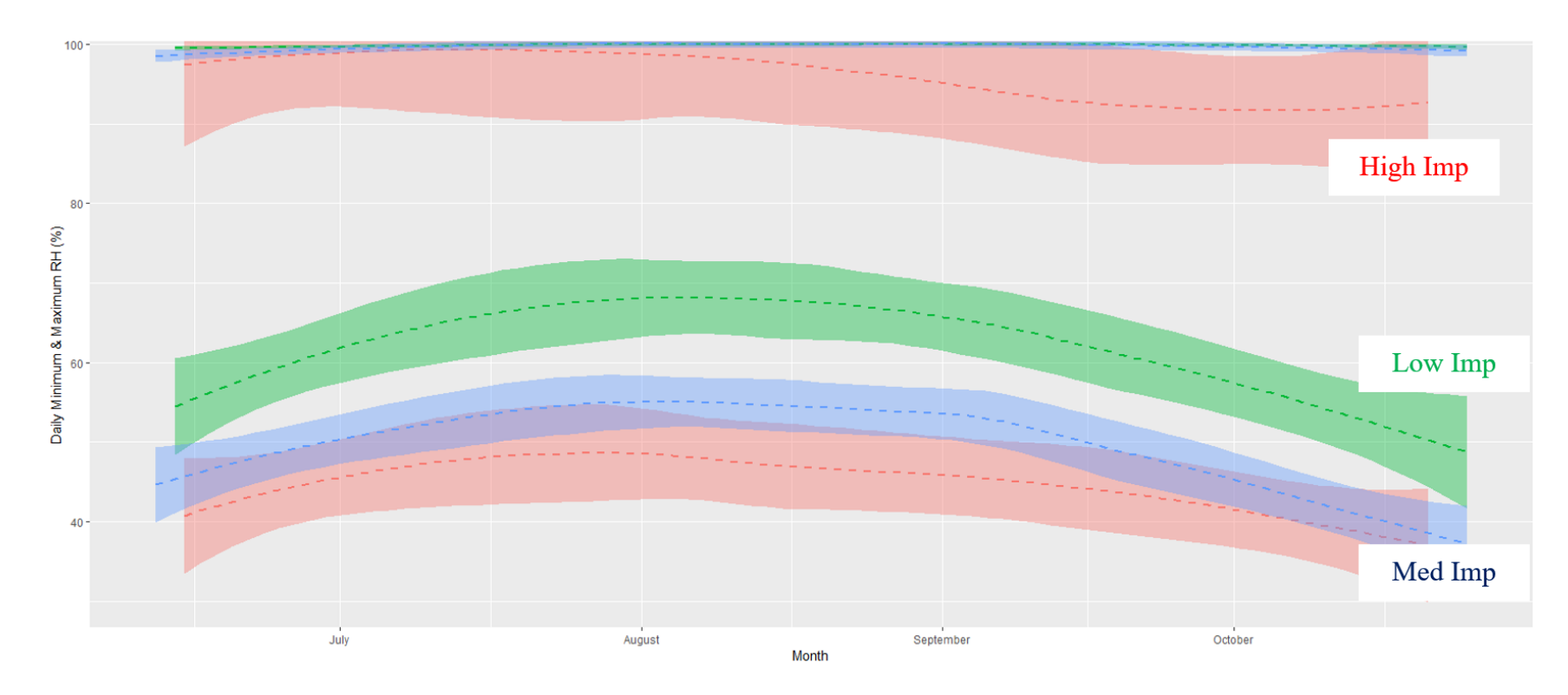
**Supplemental Figure A.1.** Daily temperature values across the study sites by month. Monthly values include both the 2021 and 2022 field season values. The red dashed line represents maximum temperatures, the green solid line represents average temperatures, and the blue dashed line represents minimum temperatures



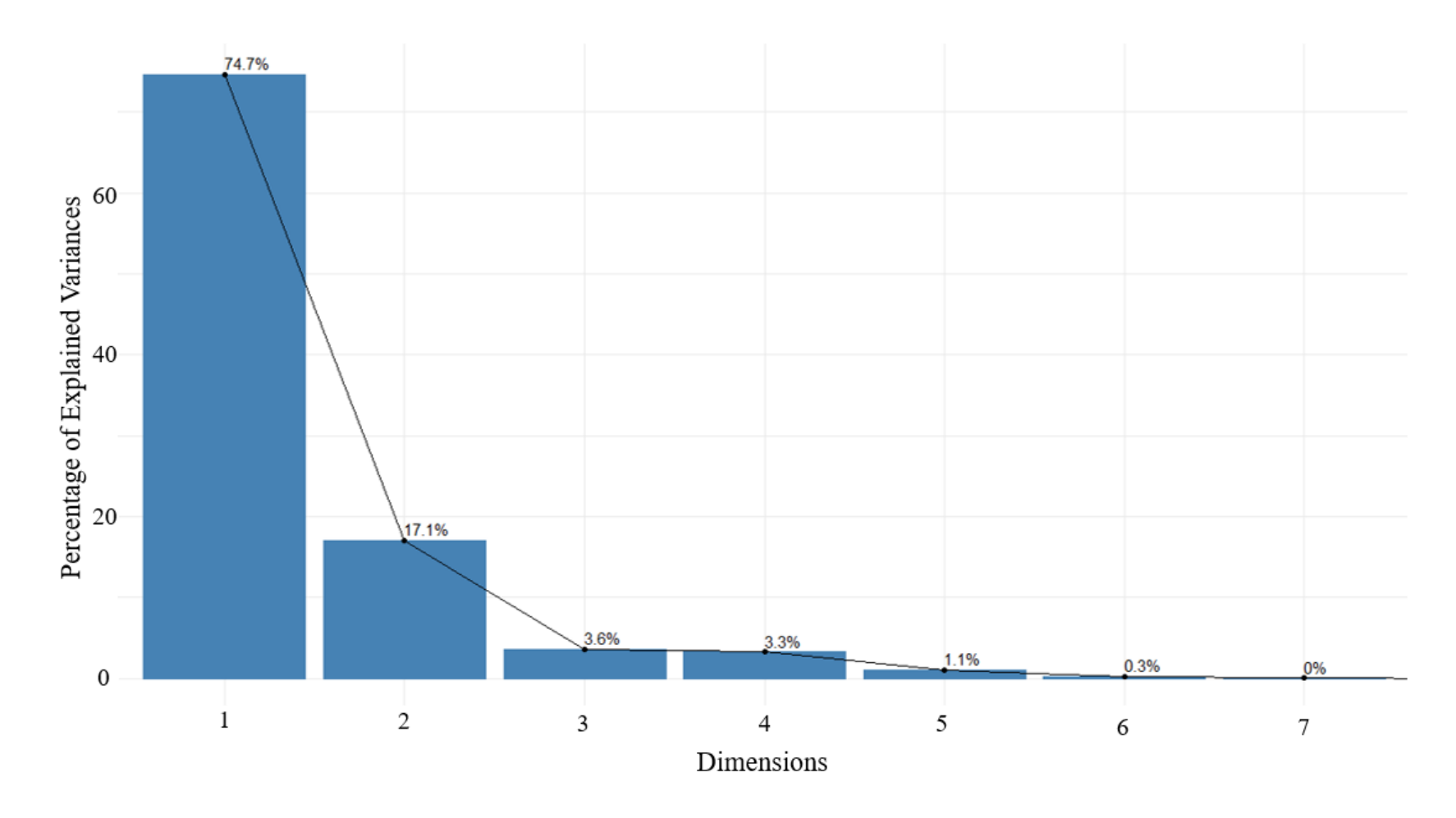
**Supplemental Figure A.2.** Daily relative humidity values across the study sites by month. Monthly values include both the 2021 and 2022 field season values averages. The red dashed line represents maximum RH values, the green solid line represents average RH values, and the blue dashed line represents minimum RH values.



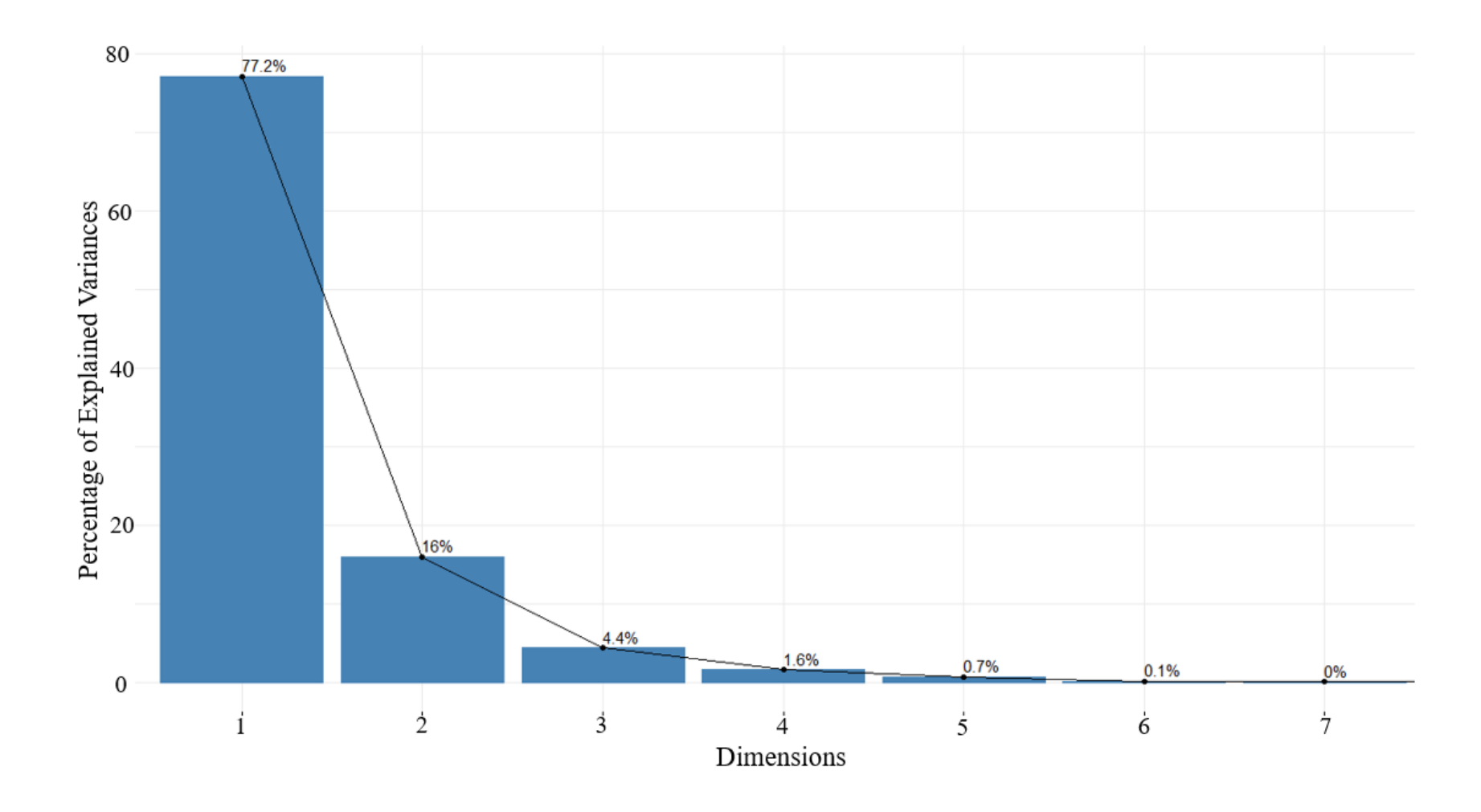
**Supplemental Figure A.3.** Average maximum and minimum temperature values by month and site imperviousness. Monthly values include both the 2021 and 2022 field season values averages. The red plot represents High Imperviousness Sites, the blue plot represents Medium Imperviousness Sites, and the green plot represents Low Imperviousness Sites.



**Supplemental Figure A.4.** Daily relative humidity values across the study sites by month. Monthly values include both the 2021 and 2022 field season values averages. The red plot represents High Imperviousness Sites, the green plot represents Medium Imperviousness Sites, and the blue plot represents Low Imperviousness Sites.



**Supplemental Figure A.5.** 7-day lag variables scree plot. Principal component analysis dimensions 1 through 7 represented with their respective percentage of explained variance.



**Supplemental Figure A.6.** 14-day lag variables scree plot. Principal component analysis dimensions 1 through 7 represented with their respective percentage of explained variance.

## APPENDIX B

## CHAPTER 4 SUPPLEMENTARY INFORMATION

## Supplemental B: DNA Extraction Checklist for Aedes albopictus.

Using DNeasy Kit (Qiage	en):
-------------------------	------

Take mosquito in 1.5 mL microcentrifuge tube, noting the sample ID #1-95 o Add 180ul ATL Buffer Grind with pestle for 1 min o Add 20 uL Proteinase K Vortex for 15 seconds Incubate in hot water bath at 56°C for 2 hours Remove from hot water bath and vortex for 15 seconds Add 4 uL RNAse A, vortex, incubate at room temperature for 2 minutes Add 200 uL Buffer AL, vortex Add **200 uL Ethanol** (100%), vortex Transfer to DNeasy spin column with 2 mL collection tube (#1) o Centrifuge at **8000 rpm for 1 min**, discard flow through and tube Transfer spin column to new 2 mL collection tube (#2) Add 500 uL Buffer AW1 o Centrifuge at **8000 rpm for 1 min**, discard flow through and tube Transfer spin column to new 2 mL collection tube (#3) o Add 500 uL Buffer AW2 Centrifuge at 14,000 rpm for 2 min, discard flow through and tube Transfer spin column to new 2 mL collection tube (#4) o Do not add more buffer (drying out last of the ethanol) Repeat centrifuge at 14,000 rpm for 1 min, discard tube

- ☐ Transfer spin column to new 1.5 mL microcentrifuge tube for DNA elution Add 100 uL TE buffer (1x if already low EDTA 0.1mM, 1/10x if regular EDTA) Let TE Buffer sit on spin filter for 5 min Centrifuge for 1 min at 8000 rpm, retaining 1.5 mL tube with the DNA Add another **100 uL TE Buffer** (low EDTA or 1/10x dilution) Let TE Buffer sit for 5 min Centrifuge for 1 min at 8000 rpm, retaining 1.5 mL tube with the DNA Test potentially high concentration DNA samples (female Ae. albopictus) with Qubit to see if minimum 10ng/uL concentration met after first elution. Set these aside for final pipetting without second elution or spin concentration. Other samples in 1.5 mL microcentrifuge tubes will have approximately 200 uL of eluted DNA. □ Pipette all of the ~200 uL of eluted DNA into an Amicon Ultra 0.5 mL -30k centrifugal unit with attached 2 mL collection tube below it to collect the flow through; discard the spin filter from the previous steps. o Spin the concentrator centrifugal unit at 14,000g or ~13,500 rpm (for 7 cm rotor radius average) for 10 min at 4°C o Discard the flow through and the 2 mL collection tube Place filter column, now with the 15k DNA caught within it, **flipped upside down** into a new 2 mL collection tube
  - o Spin at 1,000g or ~3,500 rpm (for 7 cm rotor radius average) for 2 min at 4°C
  - Approximately 26 uL of concentrated DNA will be at the bottom of the 2 mL
     collection tube.

- ☐ Prepare a 500 uL Qubit sample tube with 199 uL HS dsDNA working solution
  - o Add 1 uL DNA sample concentrate from the 2 mL spin tube to Qubit sample tube
  - O Vortex for 3 seconds and let rest at room temperature for 2 minutes
  - Read concentration 3x times with Qubit and record the average
- □ Calculate the volume of ddH2O and DNA concentrated solution that must be added to obtain 22 uL of 10ng/uL solution in a 500 uL microtube.
  - o Use spreadsheet formula and double check final values (220 ng of DNA)
  - Pipette needed volume of concentrated DNA solution and molecular grade ddH2O into a 500 uL microtube.
  - 22 uL is mixed so that 20 uL can be pipetted into the final deep well plate, allowing for a small amount of loss due to surface adhesion.
- □ Pipette the calculate volume of DNA solution and ddH20 into the well code corresponding to the sample ID #1-95
  - o Leave well H12 empty for the control run
  - Seal 96-well plate Beckman Coulter deep well plate with Thermo Scientific plate seals, store at -20°C until shipment to UNC Genomics Core.
  - Store any remaining sample DNA solutions at -20°C.

## **Preparation Notes:**

- Label initial sample tubes #1-95 with corresponding well ID's
- Label spin columns with corresponding well ID's
- Label final elution spin tube with corresponding well ID's
- Label Qubit sample tubes with corresponding well ID's

- Label both 2 mL spin tubes for samples undergoing Amicon Ultra spin concentration
- Can stop procedure after proteinase K digest/hot water bath for 6 months at room temperature.